DiSAA
DIPARTIMENTO
di SCIENZE
AGRARIE e
AMBIENTALI

UNIVERSITÀ
DEGLI STUDI
DI MILANO

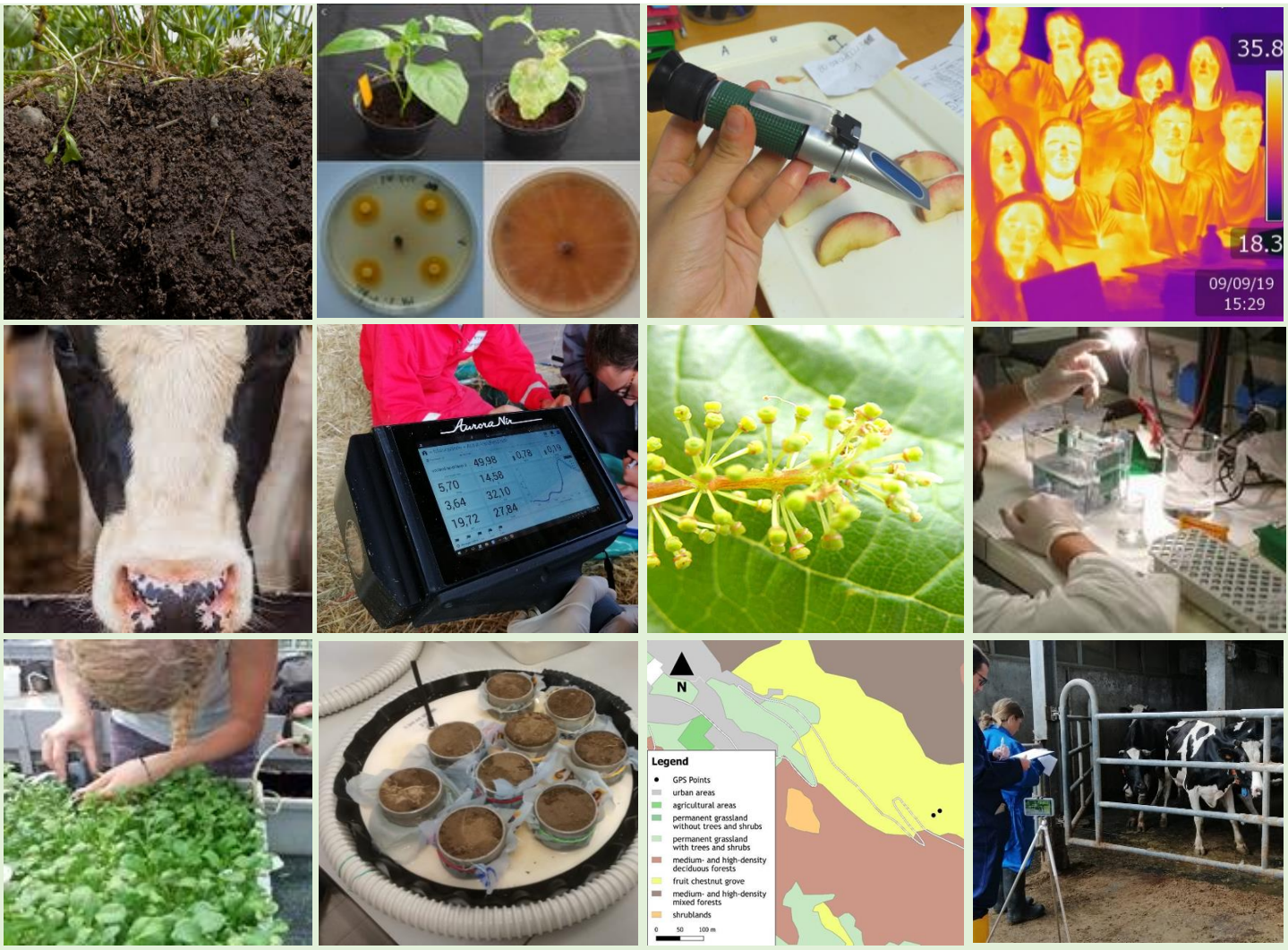

Research Enriched Education Labs

Final Report

2019

DiSAA
DIPARTIMENTO di SCIENZE AGRARIE e AMBIENTALI

UNIVERSITÀ DEGLI STUDI DI MILANO

Research Enriched Education Labs

Final Report

2019

Postfazione

Scrivere una postfazione è insolito. Abbiamo però pensato fosse più efficace scrivere una postfazione alla raccolta dei report, predisposti dagli studenti che hanno frequentato la prima edizione dei Laboratori REE (*Research Enriched Education*), organizzati dal dipartimento, per potere dare un quadro della sperimentazione didattica, anche alla luce dell'evento finale, ossia della presentazione orale dei report finali, che la presente pubblicazione riporta in forma scritta.

Anticipando il giudizio finale di piena soddisfazione per questa esperienza, è necessario sottolineare che per il Dipartimento essa ha rappresentato una scommessa impegnativa, per le ingenti risorse investite in termini di fondi dipartimentali e di impiego del personale (docenti, tecnici, amministrativi, assegnisti e dottorandi). Risorse impiegate per il percorso di progettazione e relativo finanziamento dei singoli laboratori, e successivamente per l'organizzazione operativa e la loro realizzazione pratica. Sfortunatamente la carenza di risorse finanziarie ci ha costretto a non attivare alcuni laboratori proposti e a finanziarne solo parzialmente altri.

Lo sforzo organizzativo è stato ripagato fin dall'inizio dalla significativa adesione all'iniziativa da parte degli studenti delle nostre magistrali, ai quali era indirizzata l'iniziativa.

La scommessa per questo progetto di attività didattiche innovative è stata rimarcata con il suo inserimento tra le azioni pianificate nel Piano triennale del dipartimento relativo al periodo 2018-2020, che tra gli altri obbiettivi annovera quello di "avviare progetti di sperimentazione di insegnamenti che adottino una didattica innovativa finalizzata all'integrazione didattica/ricerca". Questa azione è stata elaborata secondo quanto previsto dal piano strategico di Ateneo 2017-2019, che, nello specifico, identifica tra gli altri il seguente obbiettivo generale: "sviluppare un modello di Research Enriched Education e sviluppare un approccio culturale alla didattica in cui i docenti prendano parte al processo di innovazione delle metodologie didattiche focalizzato sullo studente e sull'utilizzo di nuove tecnologie".

Si tratta di un'azione in piena coerenza con quanto convenuto in ambito LERU, come anche riportato in un recente documento (LERU - League of European Universities - 2017 - Excellent education in research-rich universities, https://www.leru.org/files/Excellent-Education-in-Research-Rich-Universities-Full-paper.pdf), nel quale le università che fanno parte della LERU riconoscono la necessità di:

1. sviluppare strategie che migliorino le sinergie tra ricerca e istruzione degli studenti;
2. lavorare in collaborazione con studenti e altre parti interessate, laddove possibile, per attuare curricula arricchiti di ricerca;
3. considerare l'eccellenza nell'insegnamento e l'insegnamento stesso come attività alla pari di quelle di ricerca eccellente;

4. premiare e promuovere le eccellenze tra i docenti universitari e i coordinatori delle attività didattiche;
5. caratterizzare l'insegnamento con le più recenti scoperte e pratiche di ricerca e offrire un'esperienza di ricerca attiva a tutti gli studenti dalla laurea in poi;
6. riconoscere che le competenze, le conoscenze e le capacità necessarie per la ricerca sono vitali per molti cittadini nel mondo moderno, e dichiararlo chiaramente agli studenti e ai datori di lavoro;
7. promuovere una cultura della qualità e della valorizzazione, attraverso il dialogo e la collaborazione, in relazione alla formazione degli studenti e all'esperienza degli studenti;
8. dare consapevolezza agli studenti affinché diventino leader e agenti di cambiamento.

In particolare, il Dipartimento si era posto l'obiettivo di realizzare almeno 6 e 12 insegnamenti integrativi rispettivamente nel 2019 e nel 2020, presso i laboratori dipartimentali, secondo un approccio di Research Enriched Education, destinati agli studenti delle lauree magistrali.

A tale fine, nel Consiglio di Dipartimento del 21 giugno 2018, è stato deliberato di investire su tale progetto, nel triennio 2018-2020, circa 150.000 euro dei fondi dipartimentali, ai quali aggiungere una quota disponibile dei fondi Fondo unico dipartimentale 2019 e 2020. I fondi sono stati e saranno utilizzati per acquisire nuove strumentazioni, per realizzare eventuali interventi di manutenzione straordinaria e ordinaria alle attrezzature già disponibili, nonché per l'acquisto dei materiali di consumo e il compenso per gli esercitatori da impiegare per le attività didattiche.

Tra gli obiettivi che si intendevano perseguire vi era anche quello di incoraggiare la reciproca conoscenza tra gli studenti delle nostre diverse lauree magistrali, attraverso la realizzazione di laboratori di interesse trasversale rispetto ai singoli corsi di studio e mediante il lavoro di gruppo.

I laboratori sono stati realizzati tra luglio e settembre 2019; le attività si sono concluse con un seminario di presentazione dei risultati da parte di un rappresentante degli studenti per laboratorio, presso l'Azienda Agraria Didattico-sperimentale di Landriano (PV). La mattinata di lavoro è terminata con un momento di convivialità, nel corso del quale, con il prezioso supporto dei tecnici dell'azienda di Landriano e di Arcagna, discenti e docenti (professori, ricercatori, tecnici, assegnisti, dottorandi ed esercitatori) hanno condiviso una colazione campagnola.

In conclusione, dobbiamo esprimere la piena soddisfazione per l'iniziativa, testimoniata anche dai giudizi anonimi formulati dagli studenti. Soddisfazione che è andata ben oltre le nostre attese soprattutto per la maturità e interesse mostrato dagli studenti e la grande disponibilità ed entusiasmo dei colleghi, giovani e senior, che hanno organizzato e realizzato un'iniziativa così impegnativa.

Anna Sandrucci e Osvaldo Failla

Direzione DiSAA

Summary

BASIC

Innovative and low impact approaches for plant protection

Albè R., Burato A., Calastri E., Ceresa A., Errhahouly J., Golino M., Malaguzzi C., Motta D., Paganoni V., Panzetti C.

Abstract

In agriculture, the control of plant diseases is an important topic: while there is necessity to maintain and to increase the current crop production, there is also a strong drive towards the reduction of inputs in order to achieve more sustainability.
The REE project "BASIC" aims to provide knowledge on low-impact tools that can be employed in agriculture against biological stresses, exploiting specific plant-pathogen systems to perform efficacy tests on these tools. These low-impact tools include molecules and biocontrol agents, employed against different fungal, bacterial, and viral pathogens.
Silicates were employed against the fungus *Botrytis cinerea* on lettuce leaves and testing the possible phytotoxic effect of silicates on basil plants. The assays were carried out using 3 concentrations of silicates (0.5%, 1%, 2%) and non-treated controls, and resulted in 1% and 2% concentrations displaying phytotoxicity on basil, while the 1% treatment was effective in reducing *B. cinerea* infection on lettuce leaves. Two biocontrol bacterial strains (*Paenibacillus pasadenensis* R16 and *Pantoea agglomerans* 255-7), as well as one biocontrol fungal isolate (*Trichoderma* sp.) were used to reduce the damage caused by the fungal pathogen *Rhizoctonia solani* on lettuce seedlings. The effect of the pathogen was evaluated as a reduction in germination rate. Only the treatment with Trichoderma kept germination rate at a level similar to healthy control. Two biocontrol bacterial strains (*P. pasadenensis* R16 and *Pseudomonas syringae* 260-02) were used to reduce the damage caused by the foliar bacterial pathogen *P. syringae* DC3000 on *Nicotiana benthamiana* plants, although no appreciable difference was observed between the symptoms in treated and non-treated plants. Lastly, dsRNA molecules were synthesized and used against *Tomato Aspermy Virus*, inoculated on *N. benthamiana* plants. Also in this case, the symptoms caused by the virus had the same intensity with or without the treatment.

Key words: BCAs, biocontrol, IPM, dsRNA.

Introduction

Plant diseases are a widespread reality in agriculture, a serious threat to food security and safety, and some diseases could drastically reduce the production of crops.

It became possible to develop effective methods to control the diffusion of diseases, either by affecting the pathogen directly or by acting on pests that can act as vectors for diseases. During the previous century, the most effective strategies that were employed to reduce the incidence of diseases were based on the use of chemical compounds, synthetic or natural inorganic compounds, to interfere with the pathogen. While these strategies worked very well in controlling the diseases, they showed several drawbacks, both because of their characteristics and because of improper use, such as the development of resistance to the pesticides from the target organism, side effects on both the agroecosystem and surrounding areas as well as non-target organisms (benefic organism or people working in the field).

These problems became more evident and several regulations (such as directive 128/2009 of the European Community) were introduced with the aim to reduce the use of pesticides, and completely abolish the pesticides that could have a greater impact on health and the

environment. These laws also increased the pressure towards finding alternative strategies to control diseases which could be employed in agriculture to substitute these less environment-friendly practices.

Among the alternative solutions, biological control, often shortened as biocontrol, is a new strategy. It is generally defined as the use of a natural antagonist of a detrimental organism to reduce the population, and ability to cause damage, of the undesired organism. In plant pathology, it is possible to use beneficial microorganisms, or molecules they produce, to reduce the pathogens' ability to colonize the host or induce symptoms, effectively controlling the disease (Junaid *et al.*, 2013).

Biocontrol offers several advantages: (i) the specific interaction between the biocontrol agent (BCA) and pathogen which can guarantee a lesser or no effect against non-target organisms (ii) lesser environmental impact as well as (iii) reducing the possibilities of developing resistance in the pathogen (Copping and Menn, 2000). At the same time, the disadvantages of working with living organisms are (i) reduced shelf-life compared to conventional pesticides, (ii) unreliable results of their application (Copping and Menn, 2000).

As the ease of use and the success of the treatment are the most important characteristics for successful use in agriculture, research of new BCA, adapted to a different range of plant hosts, climatic conditions, or effective against different pathogens is very important to allow biocontrol to become more and more utilized in the future.

Aim

The aim of the REE BASIC is to test biocontrol activity of bacteria and fungi strains (BCA) and molecules on different model systems against different pathogens.

Materials and Methods

Materials

- Plates with Potato dextrose agar (PDA); 80
- Lysogeny Broth Agar; 500 mL
- Plate with King's agar; 50
- *Nicotiana benthamiana* plants:108
- Lettuce seeds: 900
- Lettuce leaves: 300
- Basil plants: 20 pots (4-5 plants/pot)
- Solution of silicate: 0,5%, 1%,2% [SI]
- Biocontrol agents: *Pseudomonas syringae* strain 260-02, *Paenibacillus pasadanensis* strain R16, *Pantoea agglomerans* strain 255-7, *Trichoderma* spp.
- Pathogens: *Pseudomonas syringae* pv *tomato* strain DC3000, *Tomato Aspermy Virus* (TAV), *Botrytis cinerea* strain MG53 (BC), *Rhizoctonia solani* strain RS1.

Methods

We organized the activities in Work Packages (WP):

WP1: Bioassay against Fungi

Task a: BCA's ability to contrast inhibition of lettuce seeds germination by *Rhizoctonia solani*. (Protocol is described in Fatouros *et al.*, 2018 and Fig.1)

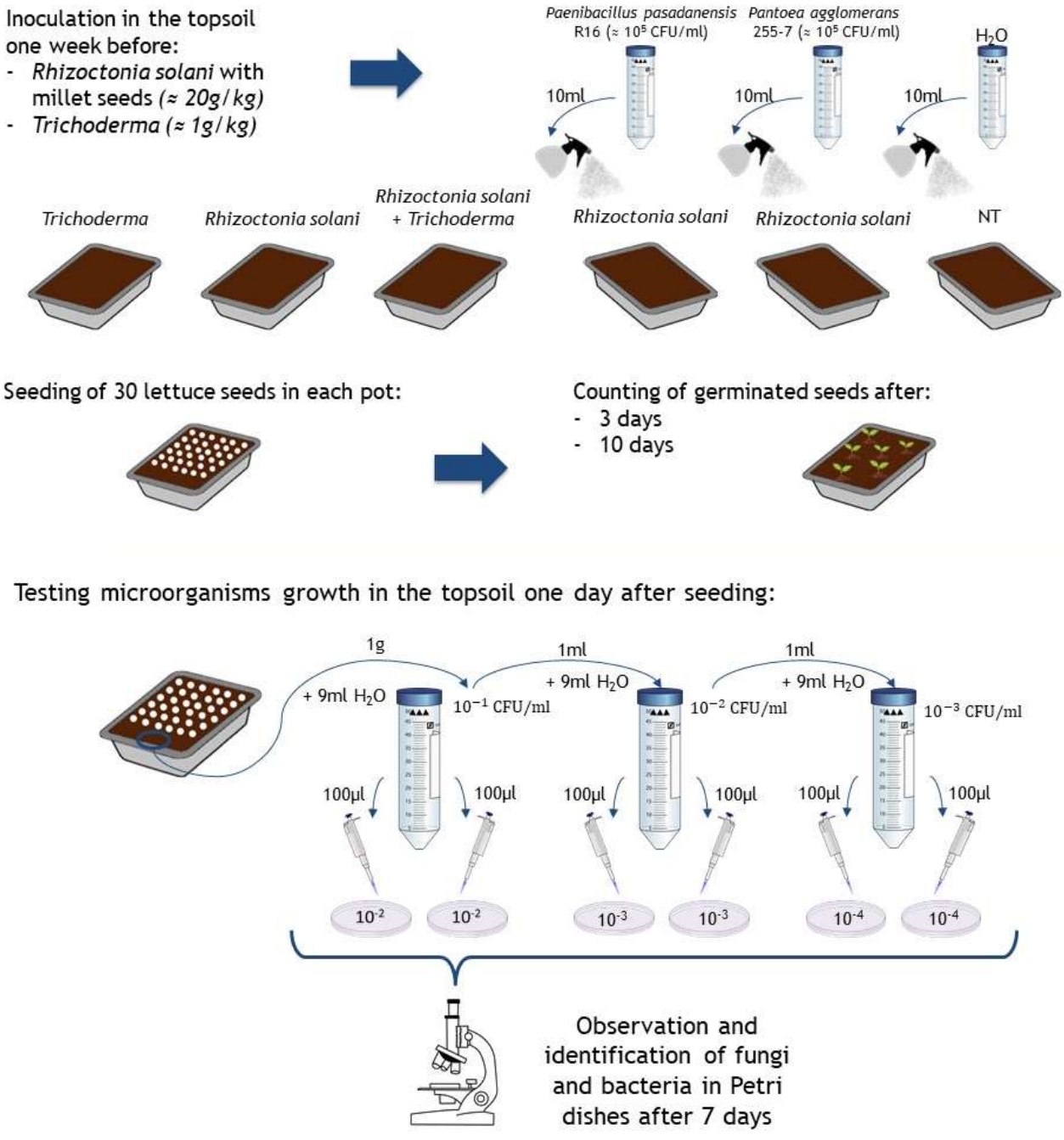

Fig. 1: Experimental set-up of the WP1 - Task a activities.

Task b: Phytotoxicity and capability of different concentrations of SI to prevent fungal infection and spreading (Protocol is described in Zendri 2006-2007 and Fig. 2).

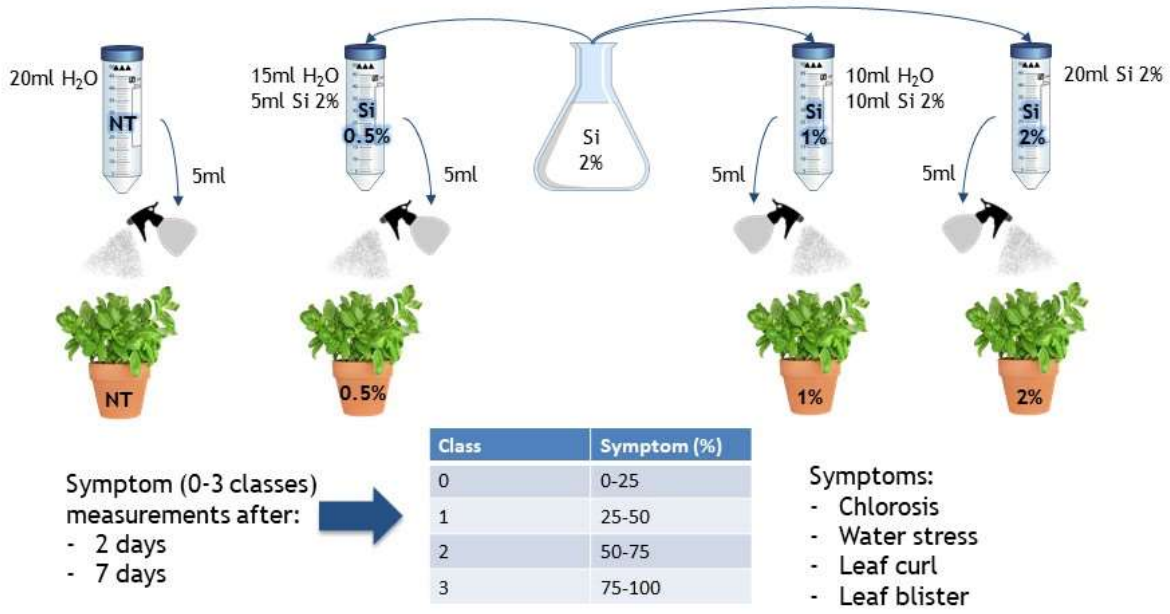

Symptom (0-3 classes) measurements after:
- 2 days
- 7 days

Class	Symptom (%)
0	0-25
1	25-50
2	50-75
3	75-100

Symptoms:
- Chlorosis
- Water stress
- Leaf curl
- Leaf blister

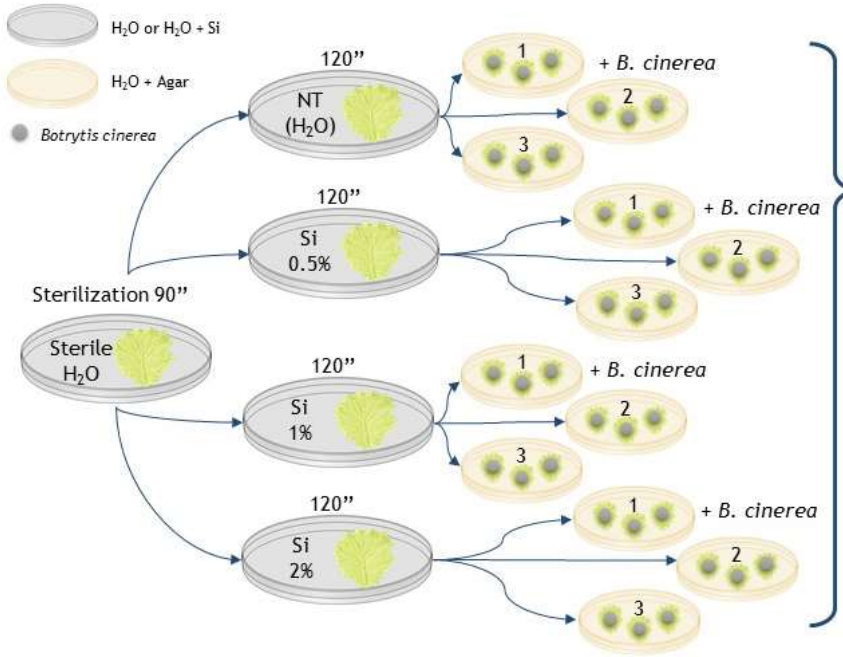

Symptom (0-7 classes) measurements after 7 days:

Class	Symptom (%)
0	0
1	1-5
2	5-10
3	10-25
4	25-50
5	50-75
6	75-100
7	100 and sporulation

Fig. 2: Experimental set-up of the WP1 - Task b activities.

WP2: Bioassay against TAV (Protocols are described in Voloudakis *et al.*, 2015 and Fig 3)

Task a: Induction of post transcriptional gene silencing by exogenous application of dsRNA

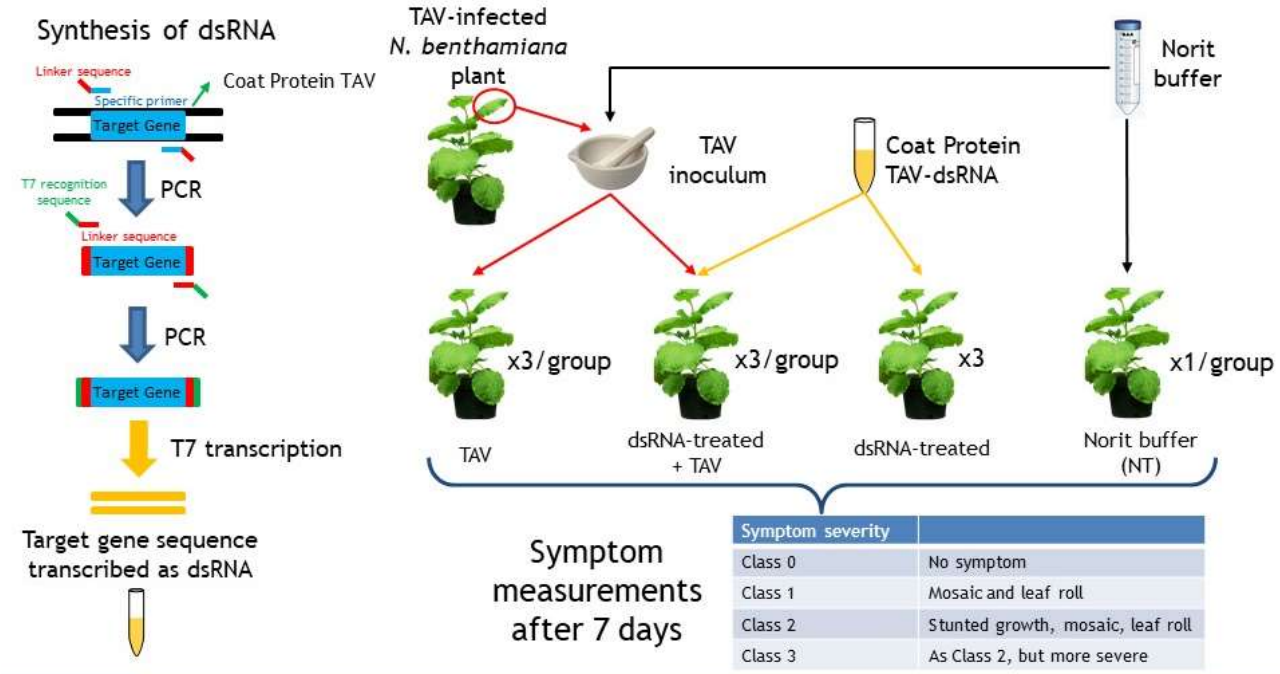

Fig. 3: Experimental set-up of the WP2 - Task a activities.

WP3: Bioassay against *Pseudomonas syringae* pv *tomato* (DC3000) (Protocols are described in Passera *et al.*, 2019 and Fig. 4).

Task a: BCA's interaction with *P. syringae* pv *tomato* (DC3000 strain).

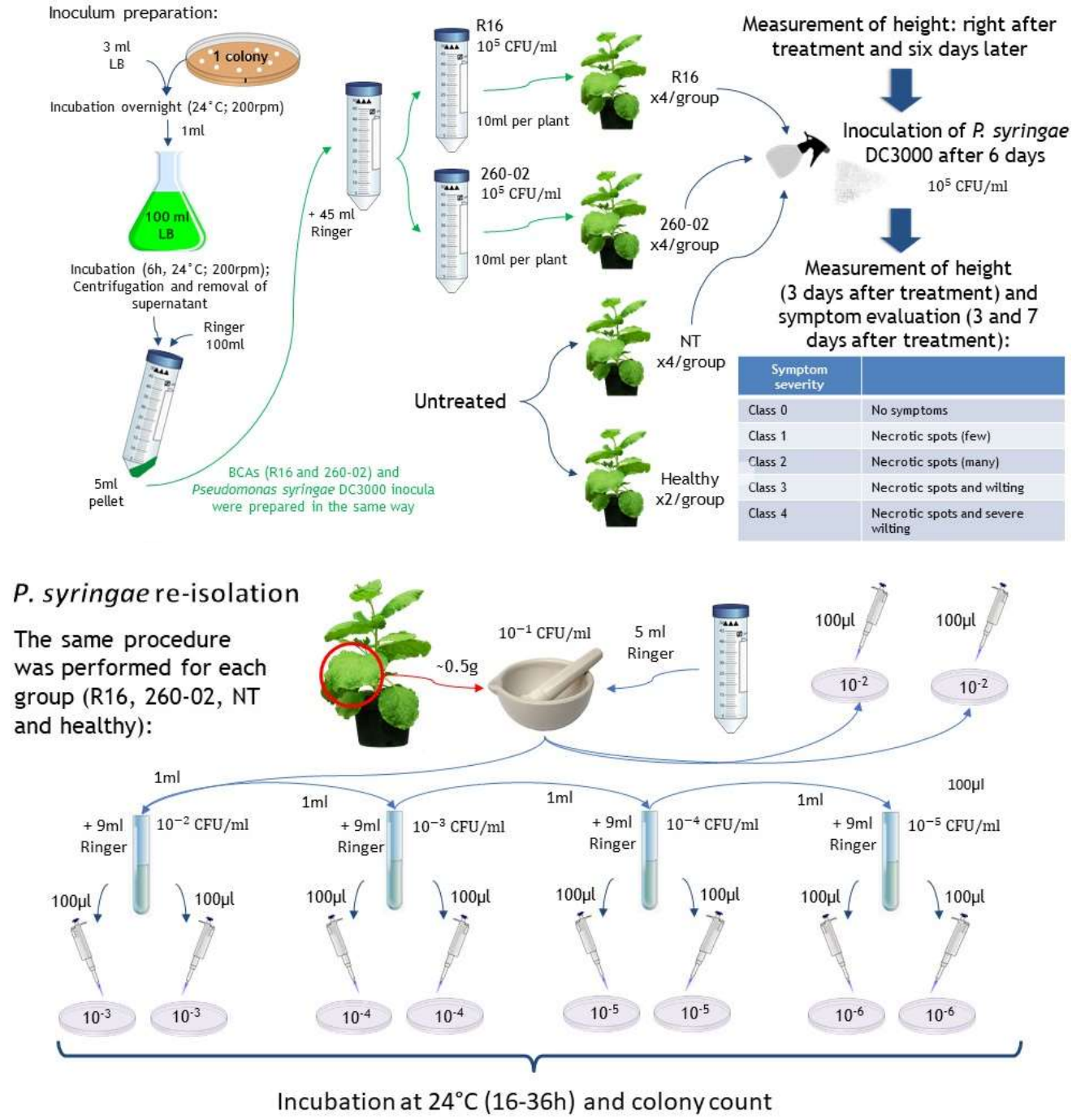

Fig. 4: Experimental set-up of the WP3 - Task a activities.

Results and Discussion

WP1_Task a: The results indicate that only treatment with Trichoderma shows significant results, with germination rate being similar to that of untreated, healthy controls (Fig.5).

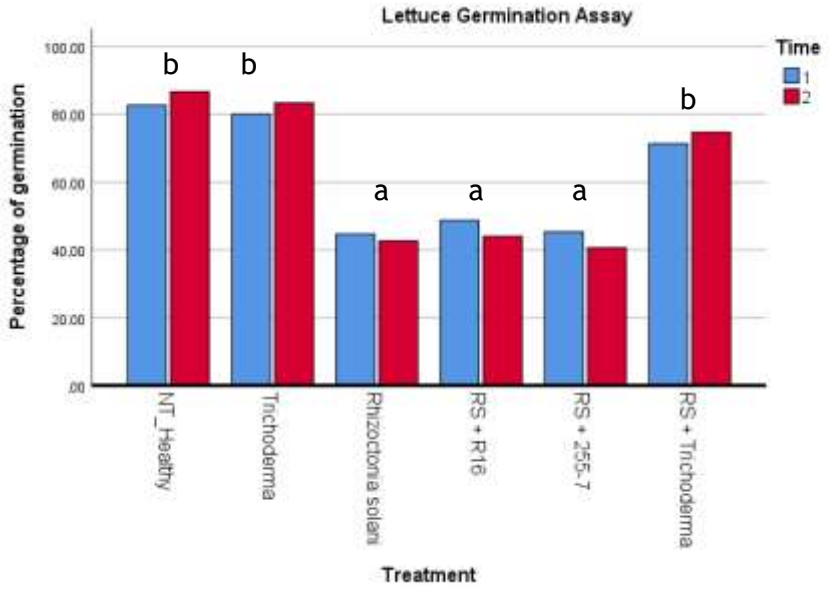

Fig. 5: Germination rate measurements. On the X-axis are reported the different treatments, while the Y-axis shows the percentage of germinated plants, out of a total of 30 per treatment. Blue indicates the germination at 3 dpi, while red shows germination at 7 dpi. Different letters (a, b) indicate significantly different results according to a general linear model, optimized for repeated measures, followed by Tukey's post-hoc test, p <0.05.

The aim of task_a is to evaluate ecological competition skills of the inoculated BCAs, which had better performance during *in vitro* assays. It is necessary to point out that *Trichoderma* spp. and *Rhizoctonia solani* were inoculated at the same time in the topsoil in order to allow the fungi to grow, as suggested in previous studies. Whereas bacteria strains were inoculated on the same day as sowing. The effectiveness of *Trichoderma* spp. could be related to its capability to colonize the rhizosphere of the seedling faster than RS.

WP1_Task b: Foliar distribution of SI seems to increase transpiration due to persistence of salt residues on basil leaves (Fig.2).

Fig.6: Photograph of basil leaves 6 days after spraying with silicates at 2% concentration. Salt residues on leaves can be seen, as well as some leaf curl symptoms.

Since no data about symptoms of toxicity of SI are available in literature, we classified recurrent damages related to their severity. Symptoms observed: chlorosis, water stress, leaf curl, leaf blisters. Higher SI concentration are associated to more severe damages over time (Fig.6 and 7).

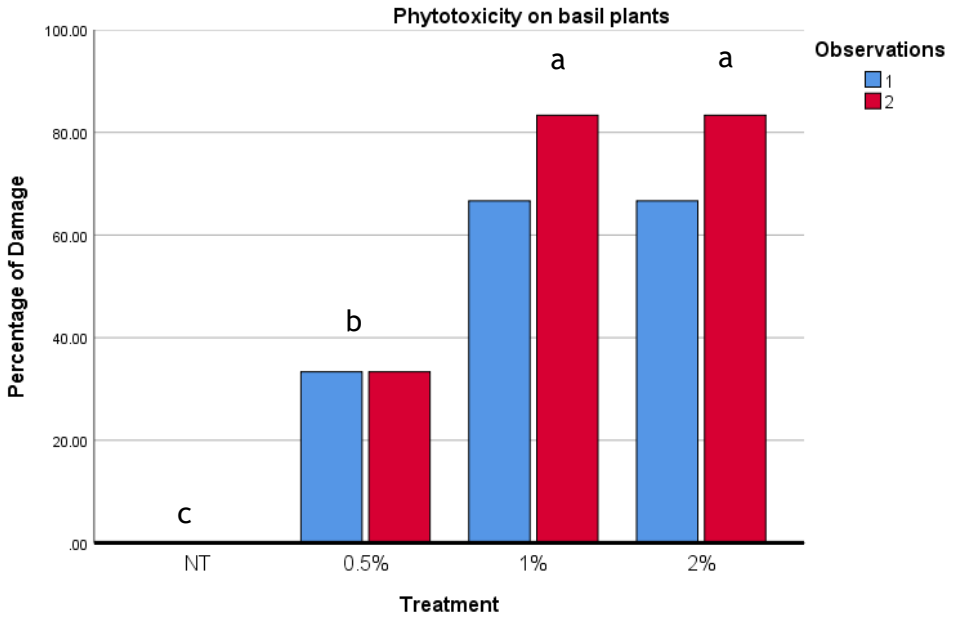

Fig.7: Graph showing the symptoms observed on basil plants treated with different concentrations of silicates. On the X-axis are the different treatments, while the Y-axis represents the percentage of damage, converted from symptom classes. Blue indicates the results of the first observation (6 dpi), while in red are the results of the second observation (10 dpi). Different letters (a, b) indicate significantly different results according to a general linear model, optimized for repeated measures, followed by Tukey's post-hoc test, $p < 0.05$.

The same treatments had contrasting effects on contrasting *Botrytis cinerea* spread (Fig. 8). Only 1% concentration managed to significantly reduce the infection index on lettuce leaves, while 0.5% (Fig 9) and 2% concentrations had no effect.

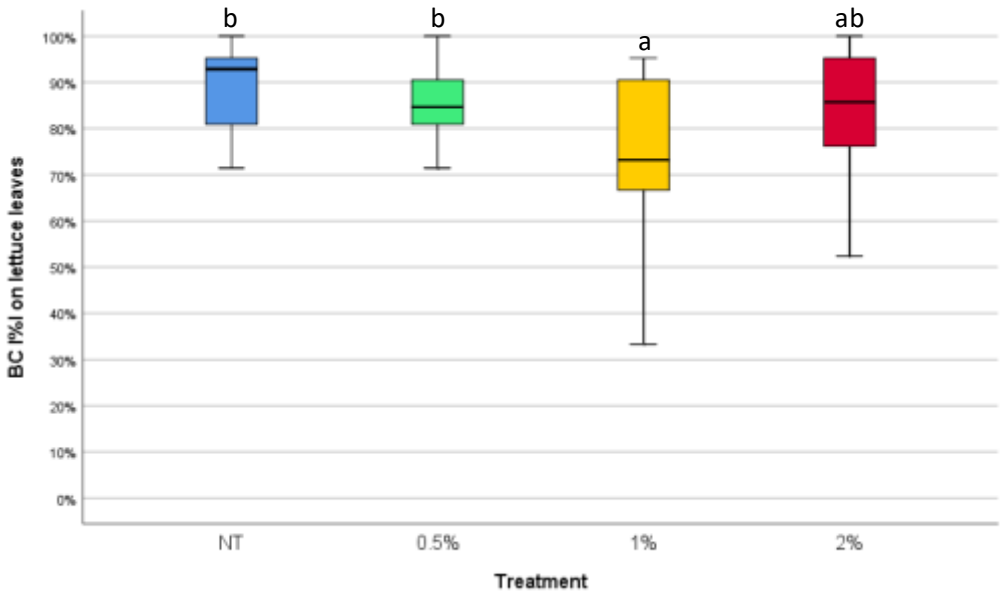

Fig.8: Box plot reports the effect of SI treatments on BC severity. On the X-axis are reported the different treatments, while the Y-axis reports the infection percentage index, calculated from the severity classes attributed to each leaf. Different letters (a, b) indicate significantly different results according to a general linear model, optimized for repeated measures, followed by Tukey's post-hoc test, $p < 0.05$.

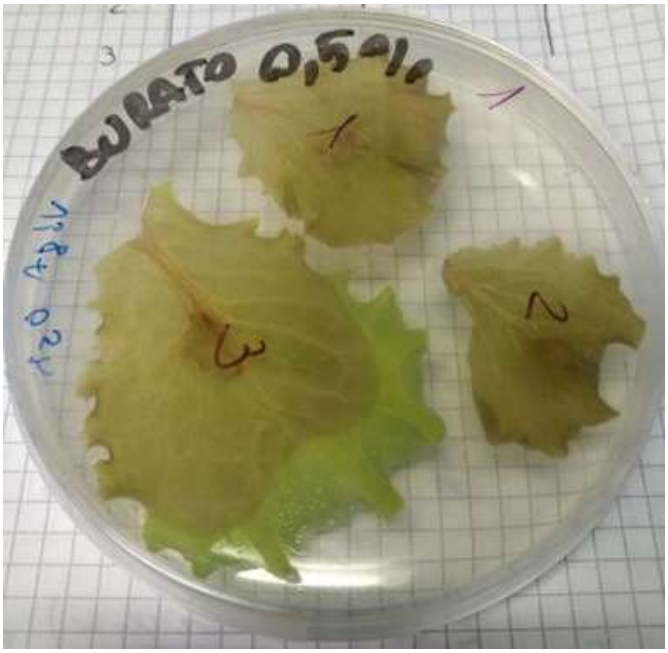

Fig.9: Example of a plate containing lettuce leaves inoculated with BC. The brown part of the leaf has been spoiled by the fungus, while the green part is still healthy.

- **WP2_Task a:** dsRNA neither induces negative effect on the plants when inoculated alone, and does not reduce TAV symptoms (Fig.10). Inoculation of dsRNA does not significantly reduce symptoms' severity of TAV infection (Fig. 11). Healthy plants inoculated just with dsRNA are asymptomatic (Fig. 12).
  Lack of efficacy could be related to the low concentration of dsRNA inoculum or to the use of a sequence which is not specific to the particular isolate of TAV that was used for the inoculation, therefore unable to silence CP protein expression.

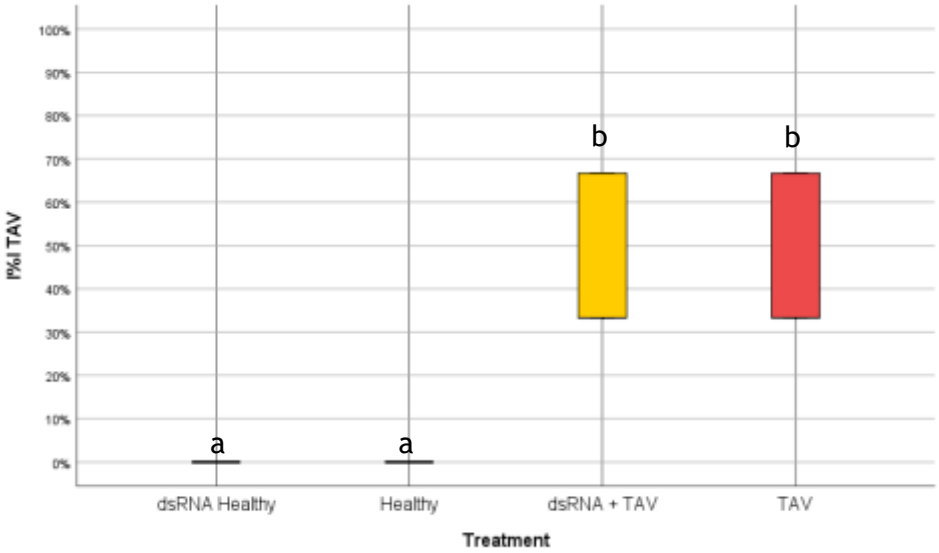

Fig.10: Box plot reports the effect of dsRNA treatments on TAV symptom severity. On the X-axis are reported the different treatments, while the Y-axis reports the infection percentage index, calculated from the severity classes attributed to each plant. Different letters (a, b) indicate significantly different results according to a One-Way ANOVA, followed by Tukey's post-hoc test, $p < 0.05$.

Fig.11: Example of a N. benthamiana plant showing severe TAV symptoms after inoculation.

Fig.12: Example of a healthy N. benthamiana plant, either non-inoculated or inoculated with dsRNA alone.

WP3_Task a: Soil inoculation with *P. pasadenensis* strainR16 and *P. syringae* strain 260-02 does not promote *N. benthamiana* growth in terms of height (Fig.13).

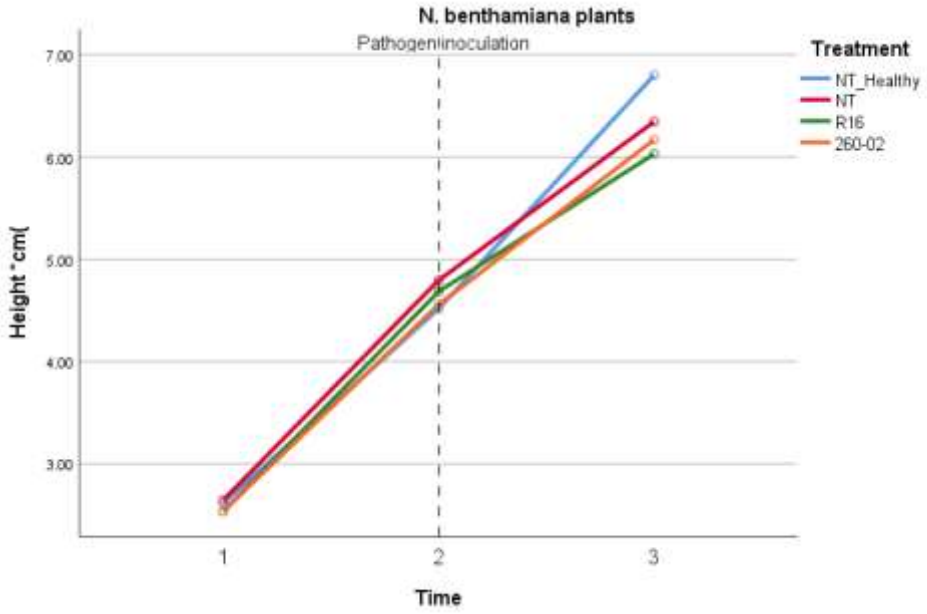

Fig.13: Graph reporting height measurements for N. benthamiana plants at 3 time points. Each line indicates a treatment, on X-axis are reported the 3 different measurement times, on the Y-axis are reported plant heights in centimeters. No significant difference was observed according to a general linear model, optimized for repeated measures, followed by Tukey's post-hoc test, $p < 0.05$.

These BCA's ability to interfere with strain DC3000 colonization of plants could not be assessed through UFC count (Tab.1). Only a few plates showed a countable number of bacterial, and therefore the counts cannot be properly compared. In particular, all plates with dilutions 10^{-4} and onwards were empty, while the initial ones were often too full of colonies to be counted.

Tab.1: UFC count obtained at different dilutions from plants treated in different ways

Dilution	10^{-2}	10^{-3}	10^{-4}	10^{-5}	10^{-6}
Treatments					
NT	183 UFC	17 UFC	2 UFC	0	0
NT	-	20 UFC	2 UFC	2 UFC	0
260-02	-	5 UFC	1 UFC	0	0
260-02	70 UFC	11 UFC	2 UFC	0	0
R16	42 UFC	311 UFC	90 UFC	0	0
R16	-	173 UFC	1 UFC	0	0
Healthy	0	0	0	0	0
Healthy	0	0	0	0	0
Healthy	0	0	0	0	0

There is no significant difference in symptom severity between treated and untreated plants (Fig.14 and 15)

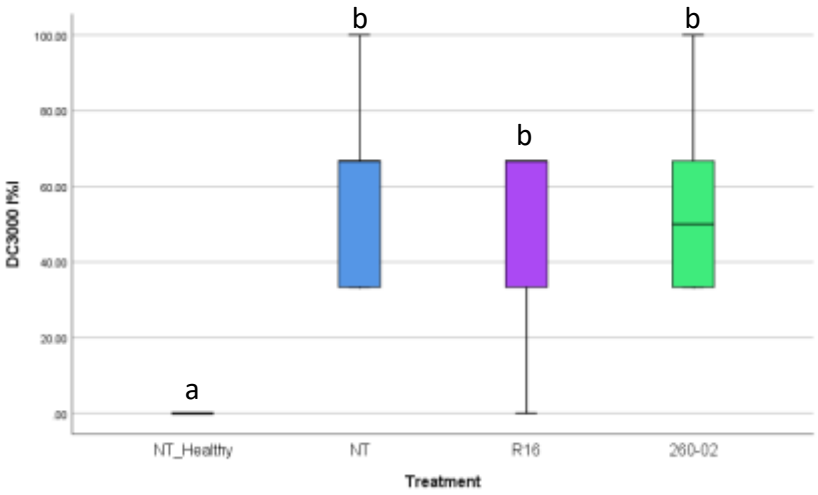

Fig.14: Box plot reports the effect of BCA treatments on DC3000 symptom severity. On the X-axis are reported the different treatments, while the Y-axis reports the infection percentage index, calculated from the severity classes attributed to each plant. Different letters (a, b) indicate significantly different results according to a One-Way ANOVA, followed by Tukey's post-hoc test, $p < 0.05$.

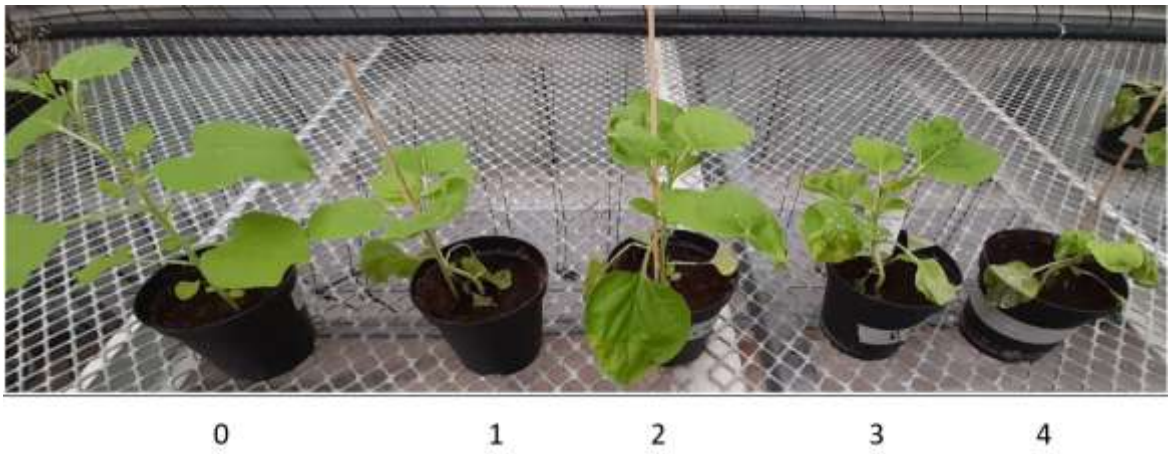

Fig.15: Picture showing example plants for each severity class identified for symptoms. Number and severity of chlorotic and necrotic spots increases from class 1 to 4, as the plant's architecture becomes more and more compromised.

Symptoms include chlorosis, necrotic spot and wilting as shown in Fig.16 and 17.

Fig.16: Example of symptom- spots.

Fig.17: Example of symptoms - wilting and necrosis.

References

Copping, L.G., and Menn, J.J. 2000. Biopesticides: a review of their action, application and efficacy. Pest management science 56:651-576.

Fatouros, G.,D. Gkizi, G. A. Fragkogeorgi, E. J. Paplomatas and S. E. Tjamos (2018). Biological control of Pythium, Rhizoctonia and Sclerotinia in lettuce: association of the plant protective activity of the bacterium Paenibacillus alvei K165 with the induction of systemic resistance. Plant Pathology (2018) 67, 418–425.

Junaid, J.M., Dar, N.A., Bhat, T.A., and Bhat, M.A. 2013. Commercial biocontrol agents and their mechanism of action in the management of plant pathogen. International journal of modern plant and animal sciences 1:39-57.

Passera A., Compant S., Casati P., Maturo M.G., Battelli G., Quaglino F., Antonielli L., Salerno D., Brasca M., Toffolatti S.L., Mantegazza F., Delledonne M., Mitter B. (2019). Not Just a Pathogen? Description of a Plant-Beneficial Pseudomonas syringae Strain. Front. Microbiol., https://doi.org/10.3389/fmicb.2019.01409.

Voloudakis A.E., Holeva M.C., Sarin L.P., Bamford D.H., Vargas M., Poranen M. M., Tenllado F. (2015). Efficient Double-Stranded RNA Production Methods for Utilization in Plant. Article Plant Virology Protocols, Methods in Molecular Biology, vol. 1236.

Zendri L. 2006-2007. Sviluppo di prodotti alternativi al rame per la viticoltura biologica nei confronti di plasmopara viticola. Tesi di Laurea.

Acknowledgments

The authors would like to thank for the support: Paola Casati, Piero Attilio Bianco, Fabio Quaglino, Alessandro Passera, Giuliana Maddalena, Stefania Prati, Andrea Giupponi, Anna Gilardoni.

Moreover, they would like to thank Riccardo Liguori, Alberto Pagliarini and Flavio Starace (Isagro).

CRISPRes

Genome editing of *Taraxacum kok-saghyz* to improve natural rubber production

Colombo A. & Tagliabue A.

Abstract

The Russian dandelium *Taraxacum kok-saghyz* (TKS) can easily become an interesting substitute of *Hevea brasiliensis* as natural rubber (NR) producer for our latitudes, given its adaptability to our climate and the quality of its rubber. As TKS is being known, many studies are released in the last years, allowing to understand its metabolism and genome structure. NR production for industrial application is influenced by the flux of metabolites and the presence of contaminant molecule which affect the physical properties. Our work explores the possibility to improve yield and quality of TKS's natural rubber. By the mean of genome-editing technique CRISPR/Cas9 we propose to knock-out OSC1 and OSC2 genes, which are involved in synthesis of pentacyclic triterpenes and GAS genes involved in synthesis of sesquiterpene lactones. We expect to observe a reduction in triterpenes and sesquiterpenes titre and also an improvement in NR yield.

Key words: *Taraxacum kok-saghyz* – Natural rubber - Oxidosqualene cyclase – Germacrene synthase - CRISPR/Cas9

Introduction

Nowadays rubber is one of most used material in the world, which find several applications above all in modern transports and consumable production. Globally the demand of natural rubber (NR) is increasing, determining the development of new sustainable rubber sources.

NR is a biopolymer mainly isolated from the sap of the Parà rubber tree (*Hevea brasiliens*), which is cultivated throughout Southeast Asia. Nonetheless, the production capacity is limited by the availability of suitable tropical land, the vulnerability to pathogens due to its narrow genetic background, long juvenile phase and labor requirements [1].

The Russian dandelion *Taraxacum kok-saghyz* (TKS) has drawn attention as an alternative rubber producing plant because of the high quality of its NR. TKS is a perennial plant, which produces NR in laticifers, a heterologous group of latex-producing cell structures that forms a continuous channel inside root. Like other dandelion, it grows quickly, can be cultivated across a wide range of environments and it is easier to manage [1,2].

TKS is a diploid, sexually reproductive organism with a genome size estimated about 1.04 Gb and can easily be genetically manipulated. Its self-incompatibility determines high heterozygosity, leading to sequence polymorphism and trait divergence among individuals [1,2]. Moreover, the genome sequence is poorly annotated and only the draft genome is currently available for research purposes.

NR or poly(*cis*-1,4-isoprenes) is a large molecule composed of more than 5,000 isophentyl diphosphate (IPP) units. IPP is produced by mevalonic acid (MVA) and methylerythritol (MEP) pathways and is consumed in several metabolic routes as the synthesis of triterpens, plant sterols, polyisoprenes and other secondary metabolites in TKS roots [3] (Fig. 1).

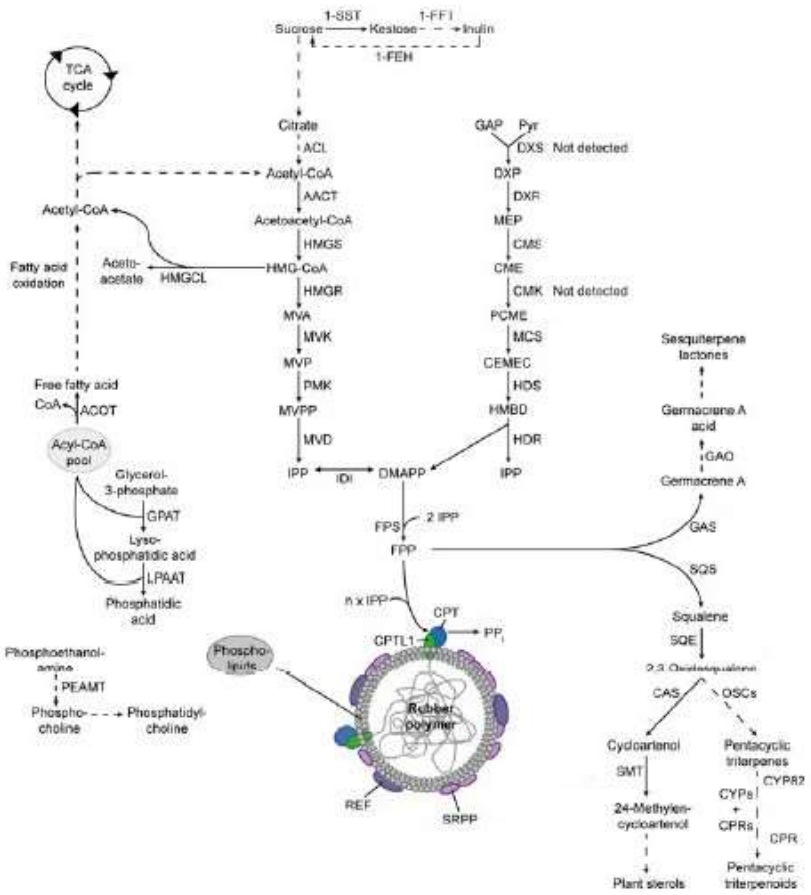

Fig.1: Illustration of the metabolic pathways of terpenes in TKS.[3]

For this reason, the latex composition is far from be pure and constant, affecting the quality of the rubber. An example, the polymer's properties are modified by the highly variable content of triterpenes [4].

Oxidosqualene cyclases (OSCs) catalyse the oxidation of 2,3-oxidosqualene which leads the production of pentacyclic triterpenes, a highly represented triterpene family inside TKS roots which play role in plant defence. The qRT-PCR revealed that OSC1 and OSC2 genes are the highest expressed in latex tissue, moreover seven different OSCs have been recently isolated and downregulated obtaining TKS population with a decreased triterpene titre, which could improve NR material properties [4,5].

Starting from farnesyl pyrophosphate (FPP), another metabolic, branch involves the synthesis of sesquiterpene lactones that exhibits anti-pest [6] activity. Germacrene synthases (GAS) are key enzymes for the cyclization of FPP to form germacrene, the precursor of these secondary metabolites, moreover differential expressed gene analysis showed that the majority of putative GAS genes are more expressed in TKS with lower rubber content[2] (Fig. 2), but no annotation study was performed yet.

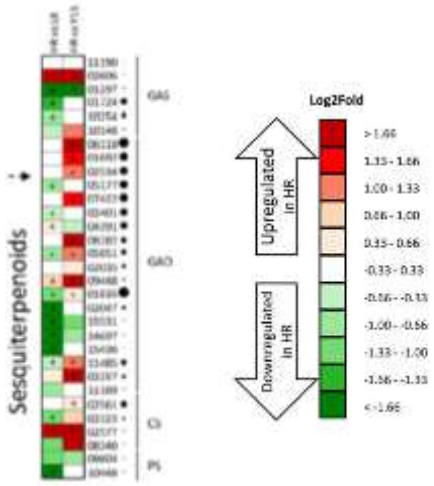

Fig. 2: Expression of contigs involved in sesquiterpenoid biosynthesis in higher (HR) and lower rubber (LR) content plant and a plant with no collectable latex (Y11). Asterisks indicate significant differences (P < 0.05). Black dots sizes are proportional to the number of reads [2].

GAS (Germacrene A synthase), GAO (Germacrene A oxydase), CS (Costunolide synthase), PS (Parthenolide synthase).

In this last decade, genome editing tools have been deeply revolutionized by CRISPR/Cas9 (clustered regularly interspaced short palindromic repeats/CRISPR associated protein 9) technology. It relies on the activity of the endonuclease Cas9 to perform a double strand break (DSB) on a site-specific genomic sequence. The specificity is determined by the complementarity of RNA sequence long 20 nucleotides called protospacer and 3 nucleotides called protospacer-adjacent motif (PAM) [7]. The genomic damage is recognized by the organism which would repair the damage via the non-homologous end joining DNA repair pathway (NHEJ), an error-prone repair method which may introduce insertion and deletions that can disrupt gene function if DSB was performed in it.

Aim

In this study, we want to exploit CRISR/Cas9 technology to knock-out OSC1, OSC2 and four putative GAS genes extracted from TKS draft-genome. We suppose that the modified plant will exhibit a reduce triterpenes or sesquiterpenes content and an increased NR yield.

Materials and Methods

Selection of target sequences within OSC1 and OSC2

The cDNA sequence of OSC1 (GWHTAAAA035384) and OSC2 (GWHTAAAA006225) were isolated from NCBI and they were also researched inside GWHAAAA00000000.genome, GWHAAAA00000000.RNA and GWHAAAA00000000.Protein files downloaded from Genome Warehouse (GWH; http://bigd.big.ac.cn/gwh/). A sequence alignment using NCBI Blast (https://blast.ncbi.nlm.nih.gov/Blast.cgi) was performed to determine the similarity level.

Potential CRISPR sites were identified using CRISPRdirect (https://crispr.dbcls.jp/), looking conserved sequences between several OSC proteins and functional domains[5], the gRNA protospacer recognition sites (Fig. 3) we selected are localized in the first two N-terminus functional domains involved in stabilization of carbocationic intermediates.

Selection of target sequences within predicted GAS genes

TKS GAS genes were not annotated in any database, therefore all the NCBI GAS genes belonged to phylogenetically close species and were compared in order to find conserved regions.

The RRPFHQGMPMVEAR aminoacid sequence is conserved in *Taraxacum officinale, Lactuca sativa, Cichorium intybus, Crepidiastrum sonchifoliu, Cichorium endivia, Helianthus annuus, Artemisia annua, Cynara cardunculus var. scolymus, Artemisia absinthium*. Using this oligopeptide as bait in GWHAAAA00000000.Protein file four putative GAS sequences (GWHTAAAA020498, GWHTAAAA020678, GWHTAAAA041876, GWHTAAAA041877) were detected.

There is no available information about GAS protein structure, thus the CRISPR site were designed by using CRISPRdirect on a conserved exon sequence common to the four genetic variants. The final gRNA can potentially target all the GAS identified variants (Fig. 3).

CCTCACACAAGAACACAAAAGGG

(**OSC1NCBI** / **OSC1GWH** / **OSC2GWH**)

GAACCGTGCGATTCAAGCTTGGG

(**OSC1NCBI** / **OSC1GWH** / **OSC2GWH**)

CCTTACACAAGACCACAAGAAGG

(**OSC2NCBI** / off-target in the contig of **OSC2GWH**)

TCTGCCCAATTGAGATTAAGAGG

(**GWHTAAAA020498** / **GWHTAAAA020678** / **GWHTAAAA041876** / **GWHTAAAA041877**)

Fig.3: The gRNA spacer sequences for OSC1 and OSC2 genes present in NCBI and GWH files (yellow, red, green), and gRNA spacer sequence for GAS genes present in GWH files (cyan).

In OSC2 conting in GWH a possible off-target is present for the green gRNA.

Cloning

Our experiment reckons on a maximum of four gRNAs: these were created by Golden Gate (GG) assemble, a method for assemble multiple DNA fragments which relies on the activity of type II endonuclease that cleaves outside its recognition site and T4 ligase. At first the gRNA spacer was split into two parts with 4 bp overlap in order to create the forward and reverse primer and each half of the spacer was synthesized within oligo primers with a BsaI site, a type II endonuclease. The 3'-end of the two parts contain also bases that anneal to gRNA scaffold and to the tRNA respectively. By GG assemble, the two oligomeric parts were assembled together to regenerate the gRNA spacer flanking the bases which anneal the scaffold and the tRNA. The regenerate gRNAs spacers were used as primer to synthesize the several parts of the polycistronic tRNA-gRNA (PTG). These were assembled together by polymerase chain reaction (PCR), creating the PTG [7, 8] (Fig. 4). Finally, after an amplification step of the PTG, it was inserted in a modified pRGEB32 plasmid for *Taraxacum kok-saghyz* after FokI digestion. The Cas9 promoter was replaced with 35PPDK.

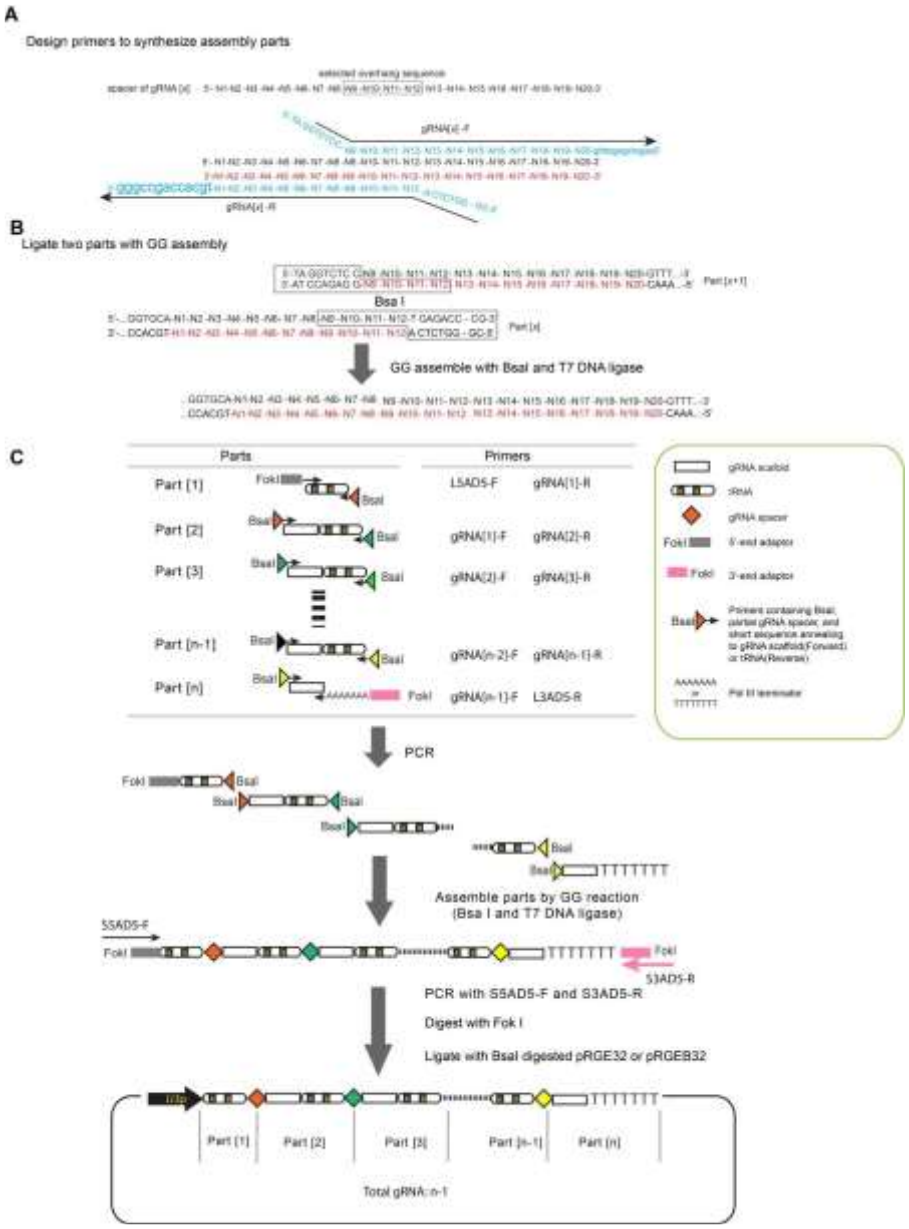

Fig.4: Strategy to synthesize PTGs with one step Golden Gate (GG) assembly [7].

***A**) Schematic guide to design gRNA spacer specific primers with 4 bp overlapping for GG assembly. The primers could be overlapped on any 4 consecutive nucleotides within the spacer. **B**) Mechanism to generate a* complete gRNA *spacer during GG assembly. After PCR amplification and BsaI digestion, the 4 bp overlapped sequence in the gRNA spacer was generated as overhangs to ligate two parts and the resulting ligation product would produce a complete gRNA without extra nucleotides. The DNA sequences in the box indicate BsaI cut site. (**C**) Schematic diagrams for one step GG assembly to synthesize PTGs from PCR parts and clone them into plasmid vectors pRGEB32. A PTG with n-1 gRNAs are divided into n. parts (Part[1]—Part[n], see the bottom). Each part was amplified with spacer-specific primers containing BsaI adaptor, except two terminal parts using gRNA spacer primer and terminal specific primers containing FokI site (L5AD5-F and L3AD5-R). These PCR parts were ligated together using GG assembly to produce the PTG with complete gRNA spacers. The assembled product was amplified with short terminal specific primers (S5AD5-F and S3AD5-R). After FokI digestion, the PTG fragment was inserted into the BsaI digested pRGEB32.*

Transformation

An *Agrobacterium tumefaciens*-mediated leaf disc transformation protocol was used: the plasmid was inserted in our vector *A. tumefaciens*, by electroporation. The bacteria was cultured at 28°C to the end of log phase and then centrifuged, and the pellet was suspended in coculture medium (4.4gL^{-1} Murashige and Skoog salt solution including vitamins, 10 mM MES, and 20 gL^{-1} Glucose, pH 5.6) supplemented with 200 µM acetosyringone. punched leaf discs of about 1 cm^2 from leaf of 6- to 10-week-old were punched and inoculated them with transformed *A. tumefaciens* for 30 minutes. The leaf discs were placed on regeneration medium (4.4 gL^{-1} Murashige and Skoog salt solution including vitamins, 18 gL^{-1} Glucose, and 8.5 gL^{-1} agar, pH 5.8) supplemented with 1 mgL^{-1} 6-benzyaldenine and 0.2 mgL^{-1} naphthaleneacetic acid for callus and shoot induction[9,12].

As needed, the elongation phase of the callus was maintained by adding zeatin, naphthaleneacetic acid and GA_3.

Rooting was induced by substituting the growth medium with a regeneration medium without hormones [9].

Transgenic plants were transferred to soil and will be cultivated at 16°C with a 16-h photoperiod.

Our transformed seedlings by PCR method were screened by amplifying the hypothesized mutated DNA regions by flanking primers to our site-specific genome editing target site in order to observe the polymorphisms occurring by High Resolution Melting technique (HRM). DNA extraction and PCR preparation performed following Fulton's protocol [10] on new leaves, about three weeks old. As outline of the process, we proceed with the cells lyse, achieved by mechanical means and the adding of buffer solution (0.35 M sorbitol, 0.1 M tris-base, 5 mM EDTA, pH 7.5). After precipitation of the proteins and separation of phases, isopropanol was used to make DNA precipitate and thus ethanol to wash the salt previously added. DNA pellet was retrieved by further centrifuge, dried it and resuspended it for further analysis.

Analysis

To get a better understanding how CRISPR/Cas9 acted on the genome and detect the presence of off-targets, the whole genome of wild type and mutants were sequenced by using PacBio RSII [1].

A Sanger sequencing of the targeted regions was used to compare and assess occurred mutations.

The quantification of secondary metabolites by gas chromatography-mass spectrometry (GC-MS) allowed us to evaluate the content in sesquiterpenes lactones and pentacyclic triterpenes before and after transformation. Previous studies were used as reference for the column set up and for the plant material preparation. For the sesquiterpenes lactones quantification Ruikar's protocol was adopted [11], instead for the pentacyclic triterpenes evaluation the protocol proposed by Post *et al.* [12].

Fresh root and leaf weight per plot were determined to estimate fresh root and total fresh biomass yield in grams per plant.

Rubber concentration in dry root mass was determined by a solvent-assisted extraction and gravimetric measurement to be expressed in grams of rubber over grams of root mass. Quantification was made as described by Panara[2]. Latex was harvested from excised roots, collected and weighted. After, the extraction buffer was added and centrifuge to fraction latex samples into three phases, rubber, aqueous and pellet phase. Coagulated rubber was removed and weighted [2].

Results and Discussion

Generation of knock-out TKS lines

In order to generate mutant TKS lines with an increase NR titer and a reduce sesquiterpenes and triterpenes level, we are going to use CRISPR/Cas9 technology to knock-out OSC1, OSC2 and GAS genes, creating three different mutant lines: KO OSC, KO GAS, KO OSC-GAS.

During the design of gRNA, we identified the presence of SNPs in our CRISPR target sites between OSC variants present in NCBI and GWH, therefore, to guarantee the knock-out we selected protospacer sequences in order to target both gene variants.

We were not able to search for possible off-targets in the genome due to the lack of enough computational power and full license software to deal with the draft genome of TKS. Moreover, an upstream sequencing of the specific *cultivar* of TKS we are going to use will optimize the gRNA design, assessing the possible presence of SNPs, and the off-target prediction.

How OSC1 and OSC2 knock-out affects triterpene titer and rubber yield

In previous studies, the knockdown of OSC1 by RNAi in TKS reduce the triterpene and pentacyclic triterpene level in TKS, the researchers analysed also the effect of a knockdown of all the OSC genes in TKS, showing a still higher triterpenes reduction [4]. In our experiment we suppose to obtain a higher reduction than the OSC1-RNAi knockdown in KO OSC and KO OSC-GAS. It is interesting compare the KO OSC line with the OSCs-RNAi line to understand which modification affect more.

Previous analysis showed that the OSCs knockdown didn't increase the NR yield [4], so we think to achieve a similar result in KO OSC and KO OSC-GAS.

During the gRNA design, we found an off-target inside the contig of OSC2 in GWH files for a specific gRNA, because it can be correlated to OSC2 genes, we decided to take the risk and knocked out it (Fig. 3).

How GAS knock-out affect phenotype, sesquiterpene titer and rubber yield

According to literature, this is the first project that aims to disrupt such a high number of putative GAS genes, therefore it is interesting characterize the phenotype of the KO GAS line. The silencing of *Taraxacum officinale* GAS1 showed a strong reduction of the sesquiterpene lactone taraxinic acid ß-D-glucopyranosyl ester which is correlated to a reduce root biomass due to an enhance insect susceptibility[6], similar studies on TKS KO GAS will show the sensitivity to pest compare to wild type (WT).

Focusing on the sesquiterpene level, we will expect a reduction compare to WT due to the gene silencing and a variation in rubber yield in KO GAS and KO OSC-GAS lines. Moreover, future analysis can characterize the effect of a low sesquiterpene content concerning the physical properties of the biopolymer extracted from KO GAS and KO OSC-GAS.

Risks and difficulties

TKS self-incompatibility and high heterozygosity remain a challenge for the development of a NR-producing crop and genome modification, therefore a bioinformatic effort must be done in order to distinguish the modification from natural polymorphisms, however the domestication of wild TKS is currently under development [1].

N. van Deenen. submitted a patent application related to their studies about the knockdown of OSC gene, it is called: "Method to obtain low triterpene/triterpenoid / containing natural rubber latex" [4], therefore the OSC knock-out by CRISPR/Cas9 could be covered by this patent.

Conclusions

Ambition of our work is to establish the Russian dandelium *Taraxacum kok-saghyz* as a valid alternative rubber source, therefore an improve production and a higher control about the standardization of the latex composition is important for the final application of natural rubber.

We believe that our work, in which we knocked-out OSC1, OSC2 and GAS genes by exploiting CRISPR/Cas9 technology, allow to the development of an industrial line of *Taraxacum kok-saghyz* and the study of this species metabolism to go one step further.

References

[1] Lin, T., Xu, X., Ruan, J., Liu, S., Wu, S., Shao, X., ... & Cheng, Z. (2017). Genome analysis of Taraxacum kok-saghyz Rodin provides new insights into rubber biosynthesis. National Science Review, 5(1), 78-87.

[2] Panara, F., Lopez, L., Daddiego, L., Fantini, E., Facella, P., & Perrotta, G. (2018). Comparative transcriptomics between high and low rubber producing Taraxacum kok-saghyz R. plants. *BMC genomics*, *19*(1), 875.

[3] Niephaus, E., Müller, B., van Deenen, N., Lassowskat, I., Bonin, M., Finkemeier, I., ... & Schulze Gronover, C. (2019). Uncovering mechanisms of rubber biosynthesis in Taraxacum koksaghyz–role of cis-prenyltransferase-like 1 protein. The Plant Journal

[4] van Deenen, N., Unland, K., Prüfer, D., & Schulze Gronover, C. (2019). Oxidosqualene Cyclase Knock-Down in Latex of Taraxacum koksaghyz Reduces Triterpenes in Roots and Separated Natural Rubber. Molecules, 24(15), 2703.

[5] Pütter, K. M., van Deenen, N., Müller, B., Fuchs, L., Vorwerk, K., Unland, K., ... & Prüfer, D. (2019). The enzymes OSC1 and CYP716A263 produce a high variety of triterpenoids in the latex of Taraxacum koksaghyz. Scientific reports, 9(1), 5942.

[6] Huber, M., Epping, J., Gronover, C. S., Fricke, J., Aziz, Z., Brillatz, T., ... & Triebwasser-Freese, D. (2016). A latex metabolite benefits plant fitness under root herbivore attack. PLoS biology, 14(1), e1002332.

[7] Xie, K., Minkenberg, B., & Yang, Y. (2015). Boosting CRISPR/Cas9 multiplex editing capability with the endogenous tRNA-processing system. Proceedings of the National Academy of Sciences, 112(11), 3570-3575.

[8] Khan, A. A., El-Sayed, A., Akbar, A., Mangravita-Novo, A., Bibi, S., Afzal, Z., … Ali, G. S. (2017). A highly efficient ligation-independent cloning system for CRISPR/Cas9 based genome editing in plants. Plant Methods, 13(1), 86. https://doi.org/10.1186/s13007-017-0236-9

[9] Collins-Silva, J., Nural, A. T., Skaggs, A., Scott, D., Hathwaik, U., Woolsey, R., … Shintani, D. (2012). Altered levels of the Taraxacum kok-saghyz (Russian dandelion) small rubber particle protein, TkSRPP3, result in qualitative and quantitative changes in rubber metabolism. *Phytochemistry*, *79*, 46–56.

[10] Fulton, T. M., Chunwongse, J., & Tanksley, S. D. (1995). Microprep protocol for extraction of DNA from tomato and other herbaceous plants. Plant Molecular Biology Reporter, 13(3), 207–209.

[11] Ruikar, A. D., Kulkarni, M. M., Phalgune, U. D., & Puranik, V. G. (2010). GC-MS Study and Isolation of A Sesquiterpene Lactone from Artemisia Pallens. Oriental Journal of Chemistry, 26(1), 143–146.

[12] Post, J., Deenen, N. van, Fricke, J., Kowalski, N., Wurbs, D., Schaller, H., … Gronover, C. S. (2012). Laticifer-Specific cis-Prenyltransferase Silencing Affects the Rubber, Triterpene, and Inulin Content of Taraxacum brevicorniculatum. Plant Physiology, 158(3), 1406–1417.

Aknowledgments

The authors would like to thank for the support: Carlo Pozzi, Vittoria Brambilla, Gabriella De Lorenzis, Silvia Toffolatti.

They would like to thank the other students who took part of the lab: L. Turino, A. Follador, A. Carrara, G. Fiscon, G. Patania, E. Marelli, S. Grisetti

FRU-BQE

Tree Fruit Breeding and Quality Evaluation

Vajani A., Centamore E., Lecchi B., Vuillermoz J., Basile A., Riva F., Floridi P., Bergna A., Linjouom H., Sironi A.

Abstract

Peach (*Prunus persica*) is a deciduous tree native to the region of Northwest China between the Tarim Basin and the north slopes of the Kunlun Mountains, where it was first domesticated and cultivated. Peaches were well known to the Romans since the 1st century AD, becoming one of the most important fruit crop in the 19th century in Emilia-Romagna region n(Italy).This REE (Research Enriched Education) called FRU-BQE is organized in the framework of the MASPes breeding program, a collaboration of CRPV (Centro di Ricerca per le Produzioni Vegetali)and the DISAA Department (University of Milan) and based in Imola (Bologna, Italy). Aims of this program is the varietal improvement of peach (and apricot). The program is aimed at the introduction of new cultivars adapted to the climatic conditions of the region, addressing disease resistance and outstanding fruit quality traits. The work presents a showcase of a typical evaluation trial and involves two varieties: Maura® and IFF1443. Maura® has white flash, instead IFF1443 has a yellow flesh. Both varieties start to ripe in the first week of July. Due to compare the post-harvest varieties, the following assessment were carried out: titratable acidity, fruits pigments, production of CO_2 and ethylene, organic acids content, firmness, weight, caliber and it was used an optical NIR instruments to allow a feedback. Field analysis lead to the conclusion that fruit thinning improved some quality parameters in both varieties. The post-harvest behavior was monitored by both standard destructive laboratory analysis and non-destructive approach (NIR instrument), suggesting a better shelf-life for IFF1443 selection.

Key words: peach, thinning, instrumental analysis, shelf-life, NIR

Introduction

The FRU-BQE experience is part of the Laboratorio REE (Research Enriched Education) project, taking place during the academic year 2019. FRU-BQE is organized in the framework of the MASPes breeding program, a collaboration of CRPV (Centro di Ricerca per le Produzioni Vegetali) and the DISAA Department (Universita' degli Studi di Milano), based in Imola (Bologna, Italy). Aim of this program is the varietal improvement of peach and apricot, along with the increase of the knowledge on fruit trees genomics and the characterization of germplasm resources. These objectives are pursued through agronomic and post-harvest management through on-field and laboratory analysis and instrumental monitoring planned along the entire supply chain. The program is focused on the development of resilient cultivars to biotic and abiotic stresses and characterized by superior organoleptic traits. After a preliminary evaluation by visual inspection and tasting, most promising selections were subjected to more extensive trials after grafting on commercial rootstocks, and compared with a range of materials (accessions, selection, commercial varieties).

This REE project is aimed at the active participation to the step of variety/selection evaluation trials. The activities consisted in a first part of on-field evaluation and a second part of laboratory analyses, focusing on main fruit quality traits. Two reference midseason peaches, harvested in the first decade of July, were considered: Maura®, a white-fleshed commercial peach and IFF1443, a yellow-fleshed nectarine selection. The aim is to evaluate fruits quality from harvesting to five days of storage under different conditions.

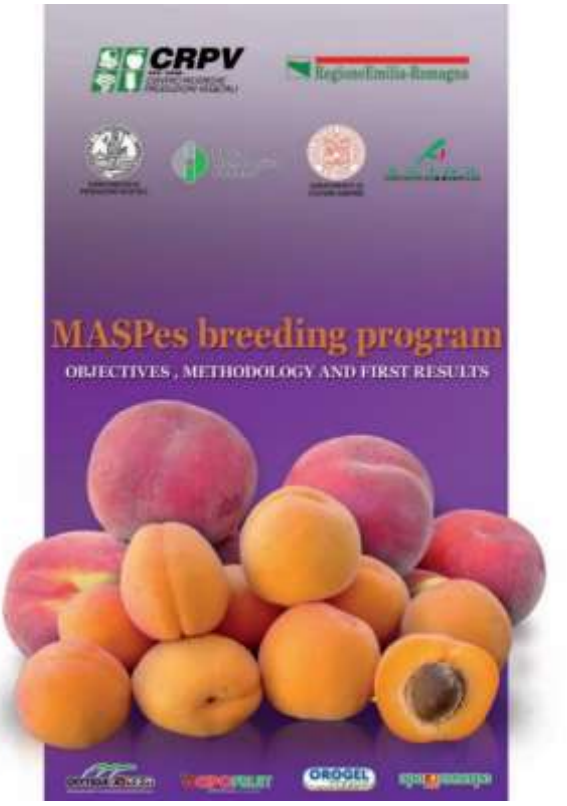

Materials and Methods

Plant material

The peaches that have been studied are Maura®(Figure 1) and IFF1443. Maura®is a commercial variety whit intermediate ripening date, high vigor, good constant productivity, strong bearing. The fruit is large, round, of AA caliber, epidermis of white background with red overtone extended on 100% of the surface. The flesh is white, firm, with a good balanced taste.

Fig. 1: Fruits of 'Maura' white peach.

IFF1443 is a non-commercial nectarine variety with yellow flesh that comes from a breeding program of CREA (Forlì).

Field activities

The study was carried out in the experimental fields of the University of Milan site at the ASTRA-Innovazione and CRPV Mario Neri's experimental farms in Imola (BO) and in Tebano (RA). The soil structure is clay-loam. The samples for this study were collected from three plants of Maura's® cultivars thinned respectively to 10 cm, 20 cm, and 30 cm apart and from two plants of IFF144 thinned respectively to 10 and 30 cm (Costa &Vizzotto, 2000, Costa & Vizzotto,2010).The activities were divided into two phases.

-The first phase consisted mainly in harvesting and counting of all fruits of each tree concerned and then, for each of them, choosing the 10 largest fruits that would be used for the subsequent analysis. The efficacy of the thinning process was assessed by manually counting the number of fruits.

- The second phase consisted in analyzing for each sample, the inner fruit quality (fruit weight and size, fruit flesh firmness, soluble solids content, DA index and titratable acidity):

- fruits were weighted individually by a precision scale and the size was measured by a digital caliper (Bassi*et al.,* 2016)
- The firmness was measured by a penetrometer with a Magness-Taylor probe. It is a destructive device to test the firmness of fruit flesh. The operation consists in cutting a small surface area (removing the epicarp) on each lateral side of the fruit in order to avoid his resistance that can false the analysis and then insert the tip of penetrometer. This instrument is ideal for determining the best time to harvest fruit or to test its progress to maturity (Bassi *et al.*,2016)
- The state of maturation of the fruit was assessed by measuring the IAD absorbance index with the DAmeter which is essentially an electronic instrument that provides an index representing the amount of chlorophyll present in a fruit (Costa *et al.,* 2009)
- Soluble solids content (SSC) in °Brix was obtained by a refractometer, which optically measures the refractive index of juice. SSC or Brix represents the percentage by mass of total soluble solids of a pure aqueous sucrose solution (Pereira et al., 2013).

Laboratory activities

The following measures (destructive and non-destructive) like fruit weight and size, DA index, hardness, dissolved solid content were repeated in 'Giuseppe Granelli' chemical-physical analysis laboratory at DiSAA. The tests were run in two different kinds of storage system to detect the effect of shelf life on fresh fruits. The fresh sample (t0) were submitted to these analyses:

- Spectrophotometer evaluation to determine the fruits pigments extension. A colorimeter is a light-sensitive instrument that measures the amount of color that is absorbed by an object or substance. The measured color difference, expressed in $\triangle E$ is a mathematical sum of the three values L, a, b (L = Light; white / black, a = green / red, b = blue / yellow) and should indicate the composite figure of the total color difference (Kamentsky*et al.*,1965, Braig*et al.*,1994)
- Automatic titrator used to evaluate the titratable acidity (g/L) expressed by the malic acid content (Wen-sheng *et al.,* 2009).
- Chromatograph gas used to estimate the production of CO_2 and ethylene (µL/kg h). The gases were sucked from glass jar containing peaches.
- HPLC (High Performance Liquid Chromatography) used to evaluate the major organic acids content in the peaches (Snyder *et al.,* 2012).
- Optical NIR instruments allow to measure qualitative parameters as weight, ethylene, CO_2, titratable acidity, color parameters -L *, a *, b *, hardness, SST, citric acid, galacturonic acid, malic acid, phenols, carotenoids *(*Magwaza*et al.,* 2012).

Non-destructive technology is based on optical sensors that use the interaction between light radiation and organic compounds (spectroscopy). Vis/NIR allowed the advantage of simultaneously analysis between the range 400 - 1000 nm (Rodriguez-Saona *et al.*, 2001).

The instrument management software can record the measure taken by the spectrophotometer thanks to the radiation produced by a lighting system formed by a central fiber that receive an input from the fruits reflections produced by the six around it (Nicolai *et al.*, 2007). The system is composed by the following elements: halogen lamp for lighting the samples; optic fiber cable; vis/NIR spectrophotometer; measurement management module with software for data acquisition, management and display (Rodriguez-Saona *et al.*, 2001). The same analysis, except for NIR, were done after 5 days (t5). Peaches were stored at 22°C in a hermetic glass jar, to show the shelf-life process.

Results and Discussion

Field analysis

Fruit fresh weight was affected by crop load in both 'Maura' and 'IFF1443' (**Figure 2**). In 'Maura', significant differences were found between thinning treatment at 10 cm (e.g. leaving an average distance of 10 cm among fruits in the fruiting shoots) and 30 cm, while fruits growth at 20 cm were not statistically different than those grown at 30 cm. A similar result was also obtained in 'IFF1443', in which fruit fresh weight was higher in the treatment at 30 cm. Thus, a lower fruit load (30 cm) resulted in higher fresh fruit weight, although 'Maura' yield fruits of higher size (about 210 g, on average) compared to IFF1443 (about 180 g).

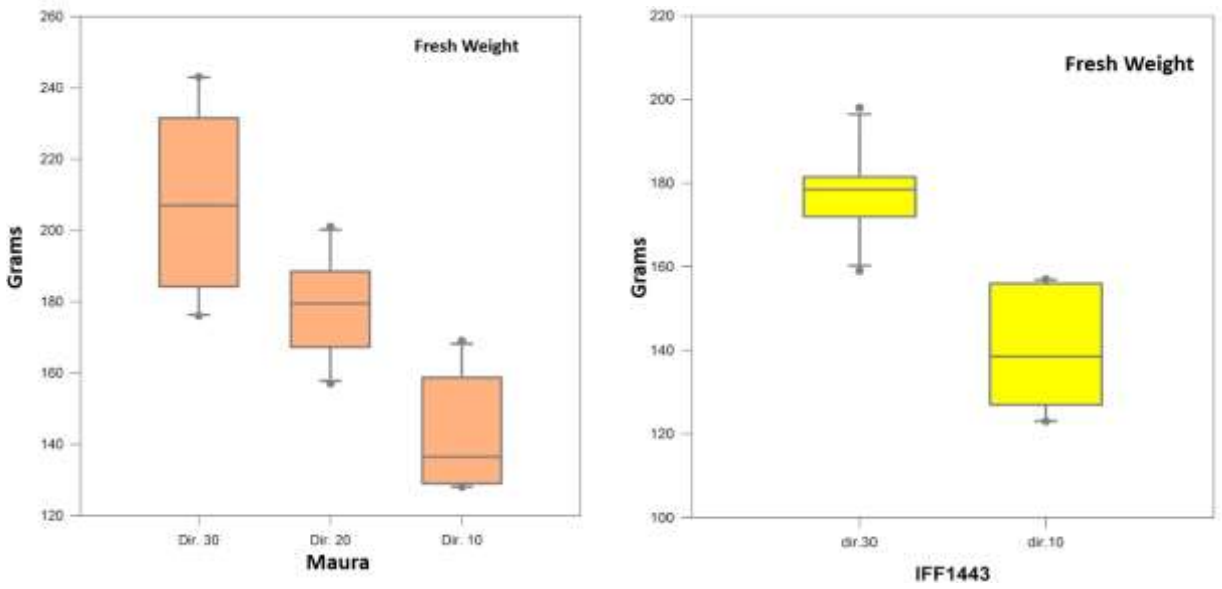

Fig.2: Fresh weight of fruits collected by 'Maura' and 'IFF1443', with different fruit thinning treatment. In Maura, Tuckey's test shows significative difference only between thinning 10 and 20 treatment. In IFF1443, significant differences were found by Wilcoxon's test.

The degree of fruit ripening, estimated using IAD index, also highlighted a significant effect of thinning treatment: IAD values tended to decrease along with the increase of thinning distance in both accessions (Figure 3). The two accessions showed a similar range of variation for this index. A similar trend was also observed for fruit firmness, although this parameter showed a higher variability between the two accessions (Figure 4).

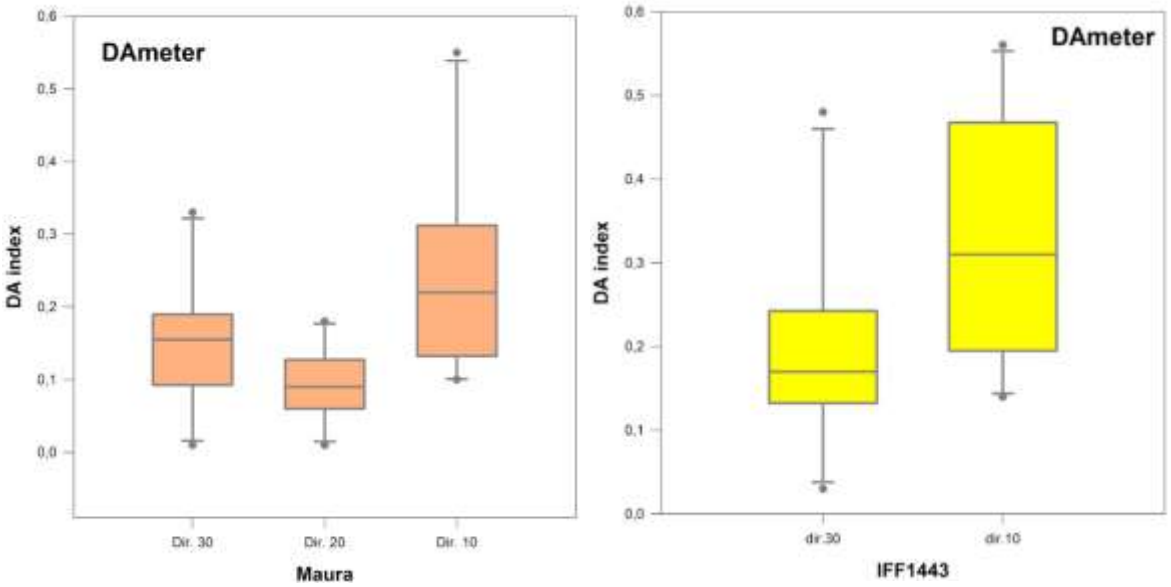

Fig.3: Graphical representation of IAD index values.

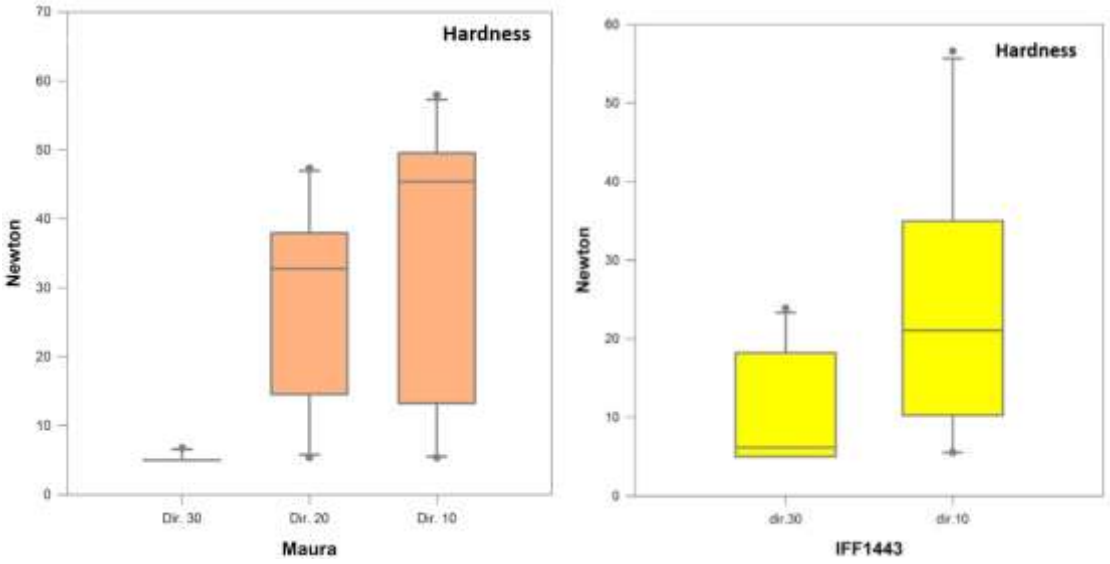

Fig.4: Graphical representation of firmness values (in Newton).

The effect of fruit thinning is also evident for SSC (expressed in °Brix), as SSC increase concomitantly to the increase of fruit density per shoot.

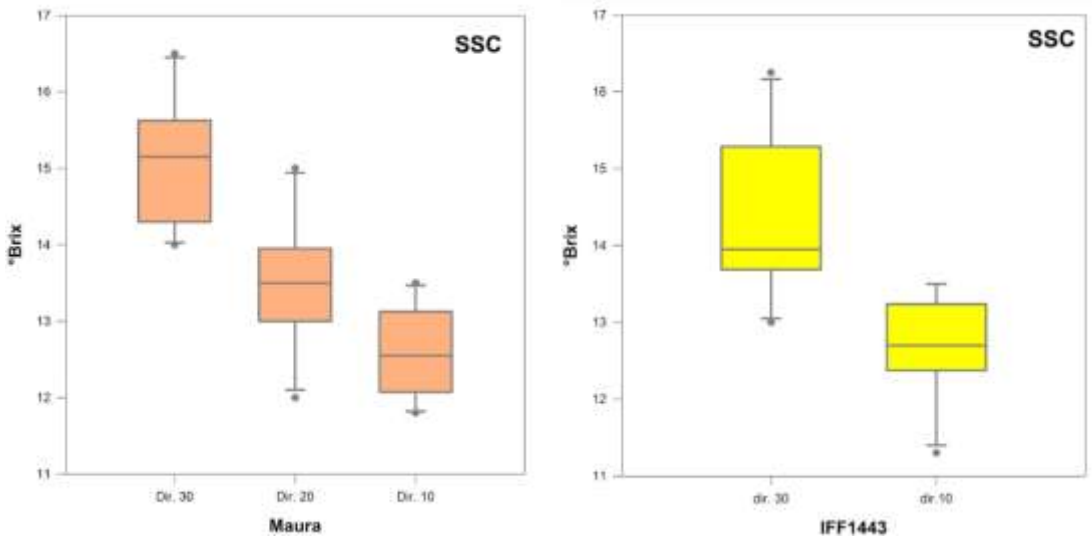

Fig.5: Soluble solid content. The treatment groups are greater than would be expected by chance; there is a statistically significant difference. Statistical analysis shows significative difference between all thinning treatment, either in Maura (Tuckey's test, P = 0,001) or IFF1443 (Student's test, P = 0,001).

In general, data obtained from the preliminary field analysis showed a remarkable effect of thinning treatment in both tested accessions. Thinning increase fruits fresh weight and solid soluble compounds (SSC) and decrease IAD index and fruit firmness. The advancing of fruit maturity at higher thinning treatment improves fruit size and solid soluble compounds (that are mostly composed by sugar).

Laboratory analysis

Laboratory analysis indicated differences between the two conservation steps (Table 1). The ethylene and CO_2 amount, and their increase with storage, were higher for IFF1443 than Maura. Firmness variation was greater in Maura than IFF1443, as well as SSC, at both the t0 and t5. The increase in titratable acidity during post-harvest storage maybe due to the sampling of fruits at different degree of maturity.

Tab.1: Analysis results.

Variety	FW (g)	Ethylene (µL/kg h^{-1})	CO_2 (mL/kg h^{-1})	TA (g/L)	L*	a*	b*	Firmness (N)	SSC (Brix°)
Maura T1	129,00	2,19	21,92	8,32	32,62	35,74	16,40	31,16	14,25
Maura T5	114,99	24,16	241,63	9,29	38,32	29,23	16,42	2,76	15,73
IFF1443 T1	131,88	5,71	57,10	7,48	33,61	29,78	25,14	5,46	13,45
IFF1443 T5	107,68	38,41	384,10	9,43	31,64	69,28	18,96	3,87	14,60

Fresh weight decreases due to a respiration and loss of water. Ethylene increase due to physiological ripening process (peach is a climacteric fruit; it means that increases respiration in the last stages of ripening). Increase in ethylene leads a major respiration ratio that leads to higher CO_2 production. In the spectrophotometer analysis we can notice an increase for IFF1443 in a* parameter, that means the peach T2 is redder then peach a T1, but this is not very significant because the fruit analyzed is not the same. As to be expected firmness decrease due to a ripening process: middle lamella of wall cells is degraded by enzymes. SSC increases due to a degradation

of acids and synthesis of sugars. The organic acid ratio from t0 to t5 has different behavior: the citric acid amount increases in both variety and is higher in IFF1443, galacturonic acid decreases in both. Malic acid decreases in Maura® and increases in IFF1443.

Tab.2: Analysis results.

Variety	Citric acid (ng/ µL)	Galacturonic acid (ng/ µL)	Malic acid (ng/ µL)	Phenols (mg/100g fw)	Carotenoids (µg/100g fw)
Maura T1	1891,13	86,03	5092,16	76,88	77,75
Maura T5	3483,40	45,79	3965,98	77,62	109,51
IFF1443 T1	3523,86	17,48	1954,87	118,44	760,97
IFF1443 T5	4865,01	0,00	2358,13	90,87	995,87

Phenols decline in IFF1443. Carotenoids rise in both varieties. Citric acid increases due to a sampling problem that was already described. Galacturonic acid, like the other acid, decreases during ripening: last value is 0 because we don't have the sample. The same thing happened at malic acid. Phenols, as to be expected, decrease in IFF1443 due to an effect of ripening. In Maura® they don't decrease significantly, maybe because of the same problem of sampling. A part of phenols, tannins are responsible for the sense of astringency, typical of not fully ripened fruit. Carotenoids, instead, increase, conferring color at fruit, they are synthetized from compounds derived from cellular respiration that increase during ripening, leading to an increase.

NIR

The use of NIR (Near InfraRed) instead of destructive analysis leads to results, reinterpreted through statistical analysis. Fruits products are chemically complicated, and so are the analysis system used for them. To extract the useful information from the spectra recorded with the instrument, it is necessary to use a specific statistical processing of the data (chemometrics). This program allows to transform the spectral data into an instrumental measure. Through the use of multivariate regression techniques, it's possible to create forecasting models able to estimate the parameters characterizing the peaches. Each calibration model (models built with all the samples available) corresponds to a validation model. The calibration model must be "tested" using a validation models, like cross-validation, leave one out. Following, the graphics reporting the R^2 notable values:
R^2> of 0.5 sufficient;
R^2> 0.7 good;
R^2> 0.8 excellent.

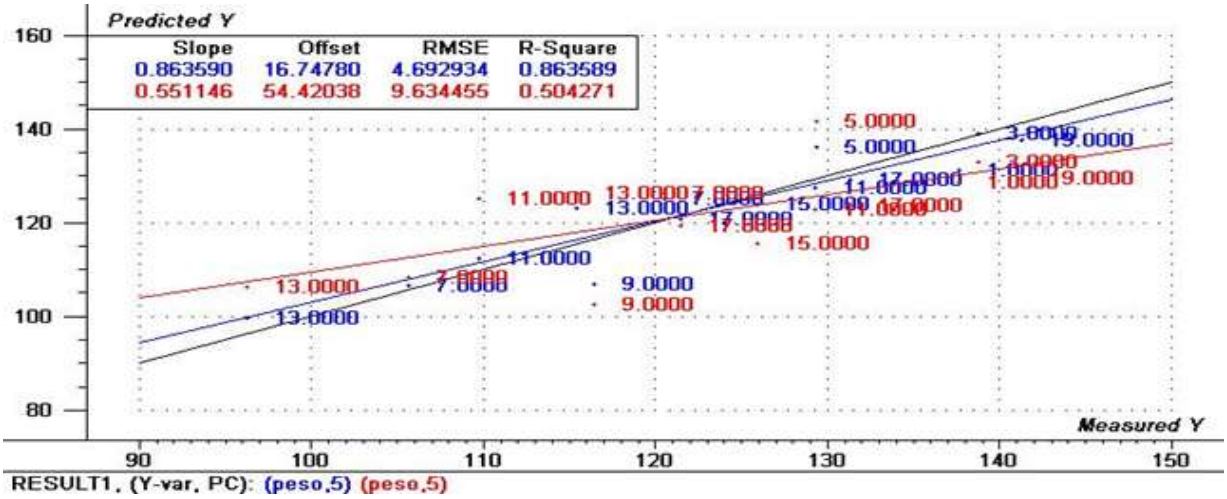

Fig.6: PLS Model to estimate fruit fresh weight.

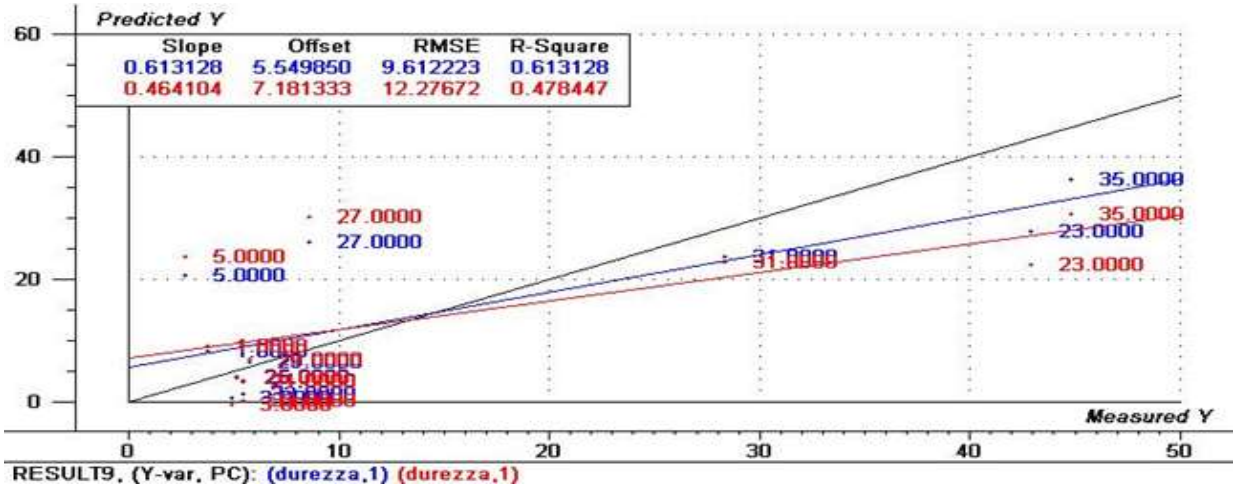

Fig.7: PLS Model to estimate the hardness.

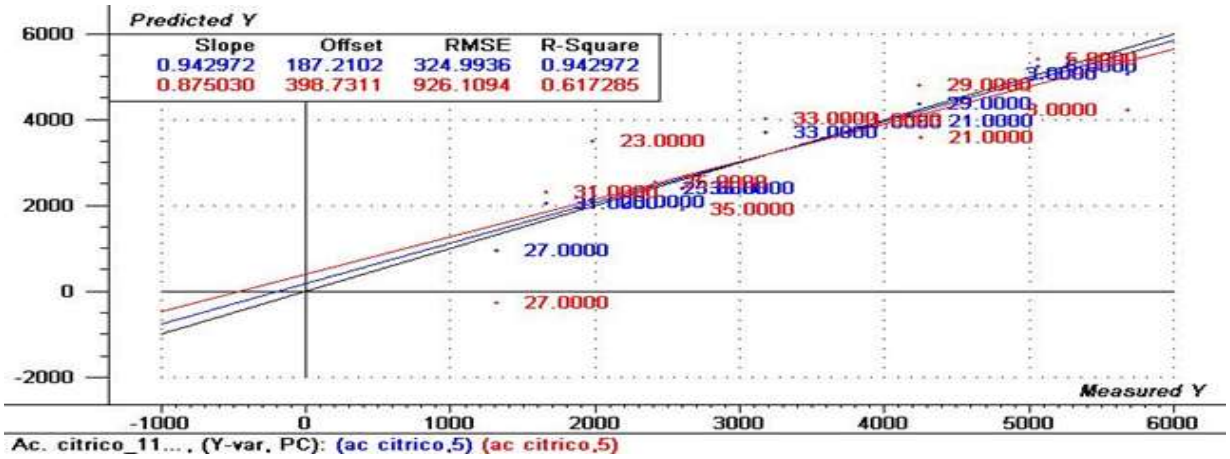

Fig.8: PLS Model to estimate the citric acid.

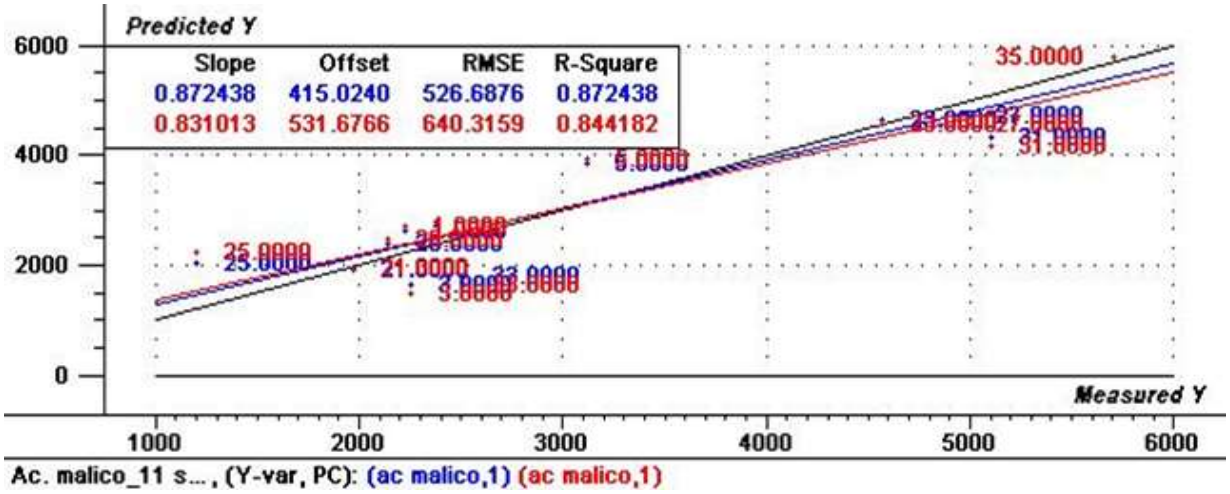

Fig.9: PLS Model to estimate malic acid content.

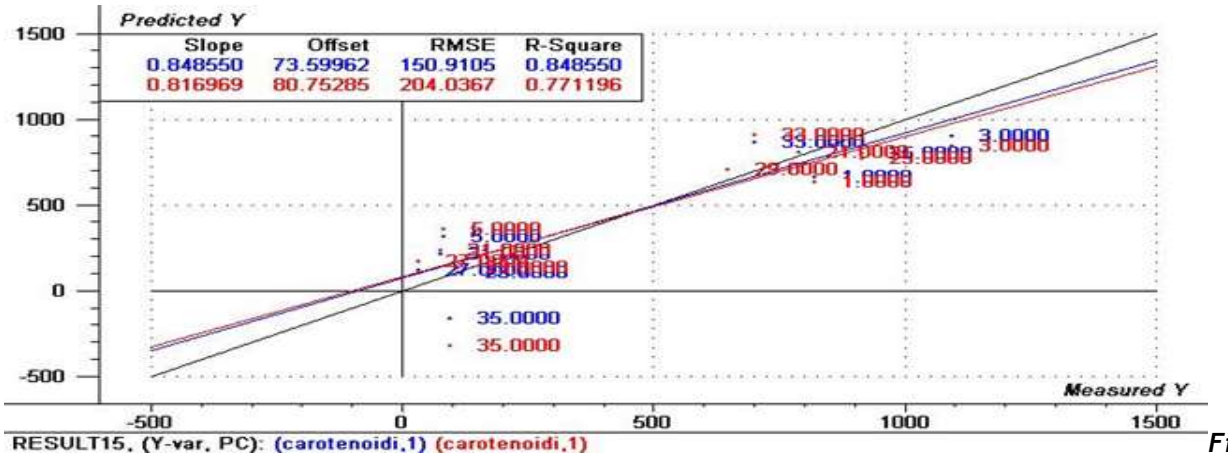

Figure

Fig 10: PLS Model to estimate total carotenoids content.

In this case the 14 peaches spectra were correlated with the weight (Fig. 5), ethylene, and CO_2 parameters. The spectra related to 11 other peaches were correlated with the parameters of titratable acidity, color L *, a *, b *, firmness (Fig. 6), SST, citric acid (Fig.7), galacturonic acid, ac. malic (Fig 8), phenols, carotenoids (Fig. 9). The following regression models were obtained by the Partial Least Squares regression (PLS) technique. Considering the contained quantities of the samples, good models were obtained for those parameters that show variability (table 3) of which: the weight, firmness, citric acid, galacturonic acid, malic acid and carotenoids. Parameters that vary little within sampling, acidity, SSC and color parameters, have obviously obtained estimation models with very low coefficients of determination. Due to the small number of samples, the validation models obtained lower R^2 values than the calibration models. These models can be easily improved by increasing the number of samples. Usually models are programmed with around 100 samples. When the NIR spectra are strongly correlated with destructive analysis, and model is developed it can be used to test a large amount of fruits without destroying them. This technology allows to test every single fruit during food supply chain to pursue the maximum of quality possible and serve to the final consumer a very high-quality product. To evaluate the quality of NIR model the data must to be compare to the destructive analysis data. The more the NIR value is near to the data from destructive analysis, the more the model is accurate. The NIR technology can be used instead of classic analysis and secure fruit quality. These tables show optimum results for some parameters like titratable acidity (malic acid) and solid soluble content because they are very similar in boot analysis, instead carotenoids and ethylene show very different results, so for these parameters the NIR analysis is not reliable (due also to a low number of samples).

Conclusions

The REE experience allows to improve the knowledge in the fruit sector, germplasm analysis to breed new varieties, like IFF1443, crop/agronomic management of the orchard, experiences of post-harvest management, instrumental monitoring planned along the entire supply chain. Field analysis lead to the conclusion that thinning improved some fruits parameters in both varieties, like fresh weight and DA index, especially in Maura®. Shelf life process is confirmed by standard laboratory analysis while the NIR analysis is useful to validate them. The results show IFF1443 variety has a longer shelf life than Maura®.
Further studies should be useful to repeat the experiment with a major number of samples for statistics soundness.

References

Bassi, D., Mignani, I., Spinardi, A., Tura, D., 2016. PEACH (*Prunus persica* (L.) Batsch). In: Simmonds, M.S.J., Preedy, V.R. (Eds.), Nutritional Composition of Fruit Cultivars. Academic Press, 535–571.

Braig, J. R., & Goldberger, D. S. (1994). *U.S. Patent No. 5,313,941*. Washington, DC: U.S. Patent and Trademark Office.

Costa, G., &Vizzotto, G. (2010). Flower and fruit thinning of peach and other Prunus. *Horticultural reviews*, *73*, 351.

Costa, G., Noferini, M., Fiori, G., & Torrigiani, P. (2009). Use of Vis/NIR spectroscopy to assess fruit ripening stage and improve management in post-harvest chain. *Fresh Prod*, *1*, 35-41.

Costa, G., &Vizzotto, G. (2000). Fruit thinning of peach trees. *Plant growth regulation*, *31*(1-2), 113-119.7

Kamentsky, L. A., Melamed, M. R., &Derman, H. (1965). Spectrophotometer: new instrument for ultrarapid cell analysis. *Science*, *150*(3696), 630-631.

Layne, D. R., &Bassi, D. (Eds.). (2008). *The peach: botany, production and uses*. CABI.

Magwaza, L. S., Opara, U. L., Nieuwoudt, H., Cronje, P. J., Saeys, W., &Nicolaï, B. (2012). NIR spectroscopy applications for internal and external quality analysis of citrus fruit—a review. *Food and Bioprocess Technology*, *5*(2), 425-444.

Nicolai, B. M., Beullens, K., Bobelyn, E., Peirs, A., Saeys, W., Theron, K. I., &Lammertyn, J. (2007). Nondestructive measurement of fruit and vegetable quality by means of NIR spectroscopy: A review. *Postharvest biology and technology*, *46*(2), 99-118.

Pereira, F. M. V., de Souza Carvalho, A., Cabeça, L. F., & Colnago, L. A. (2013). Classification of intact fresh plums according to sweetness using time-domain nuclear magnetic resonance and chemometrics. *Microchemical Journal*, *108*, 14-17.

Rodriguez-Saona, L. E., Fry, F. S., McLaughlin, M. A., &Calvey, E. M. (2001). Rapid analysis of sugars in fruit juices by FT-NIR spectroscopy. *Carbohydrate Research*, *336*(1), 63-74.

Sansavini, S., Bassi, D., &Gamberini, A. (2006). Peach breeding, genetic and new cultivar trends.

Snyder, L. R., Kirkland, J. J., &Glajch, J. L. (2012). *Practical HPLC method development*. John Wiley & Sons.

Wen-sheng, L. I., Xiao-yuan, F. E. N. H., Bao-gang, W. A. N. G., Zhen-zhong, G. U. O., Jun-jun, Y. A. N. G., & Chang-song, Z. H. A. N. G. (2009). Study on Determination of Titratable Acidity in Fruits Using Automatic Potentiometric Titrator [J]. *Food Science*, *4*.

www.maspes.org/index.html

Acknowledgments

The authors would like to thank for the support: Marco Cirilli, Anna Spinardi, Antonio Ferrante, Daniele Bassi, Riccardo Guidetti, Roberto Beghi, Ilaria Mignani, Remo Chiozzotto, Debora Tura.

IDRO-S-IP

Advanced Methodologies for the Hydrological Characterization of Soils and Creation of Prescription Maps for the Implementation of Precision Irrigation

Borelli F., Boscaini G., Maiocchi V., Morlacchi N., Riva R., Smiriglia E., Zanetti R.

Abstract

Modern agriculture must be more efficient in using agronomic inputs. Water in particular shall be used rationally, because most of the climate projections predict that changes will affect the hydrological cycle leading to a general reduction of the available water for agriculture. In this scenario, Precision Agriculture (PA) techniques can be seen as a solution to reach a better match between input demand and supply. The first step to be accounted for, is the identification of the spatial variability at the field level, to allow the creation of prescriptional maps, fundamental tools to apply PA techniques.
In this work, these procedures were applied in a maize field located in the experimental farm A. Menozzi in Landriano. An EMI sensor was used to investigate the soil Electrical Conductivity (EC) that, as well as shown in many studies, is strongly related to the Available Water Content (AWC) in the soil. Data acquired were used to parcel out the field into three homogeneous zones. Soil sampling was conducted to investigate soil physico-chemical (texture) and hydrological (soil water content availability and saturated hydraulic conductivity). All the acquired data were elaborated with statistical tool to obtain the prescription map, and finally data for each homogeneous zone were used to input an atmosphere-soil-crop model called CROPWAT (FAO, 2008), to compare the irrigation management carried out by the farmer with a hypothetical variable-rate irrigation management.

Key words: variable-rate management, variable rate irrigation, prescription map, geophysical sensors, CropWat.

Introduction

In agriculture an effective and efficient management of inputs is fundamental to make the crop production sustainable, for both environment and economics. Moreover, climate is changing and most of the projections predict that these changes will affect the hydrological cycle, leading to more frequent droughts and heat waves, to alteration of the spatial and temporal patterns of precipitation, to an increase in crop evapotranspiration, and to a general reduction of the available water for agriculture (Ortuani et al., 2019). In this scenario, precision agriculture (PA) techniques are rapidly spreading and improving. PA is an approach that tries to reach a better match between demand and supply of agronomic inputs like water, nutrients, pesticides. In order to achieve this goal, we need a detailed description of the variability at the field scale of soil and vegetation properties and status, to elaborate prescription maps which are fundamental to apply variable rate managing procedures. Following this approach, not only an improved water use efficiency can be reached, but also a higher quantity and quality of crop production. The goal is to maintain high levels of production, both quantitatively and qualitatively, but with a more sustainable use of field inputs. Within the field can be often recognized a spatial heterogeneity of soil characteristics, topography, microclimate, as well as of crop development, water status and yield; these factors result in a non-uniform inputs requirement (Ortuani et al., 2019). The

traditional method of investigating this factors is based on soil sampling at the vertices of a regular grid, then measuring soil properties affecting yields with analytic methods in the lab (texture, soil organic matter, pH, water retention), and finally interpolating data with geostatistical tools to produce detailed maps of the soil properties. This approach is extremely expensive and time-consuming (Ortuani et al., 2016). In PA, the intensive and relatively time-saving measurements of soil electrical conductivity (EC), acquired through non invasive geophysical proximal soil sensors are commonly used to create quick and high resolution soil maps, useful to delineate site specific management zones (SSMZ)(Ortuani et al., 2016; Corwin et al., 2003; Morari et al., 2009; Van Meirvenne et al., 2003). As a matter of fact, EC is strongly correlated to the soil properties affecting the crop yield, specifically soil physical parameters as soil texture (Doolittle et al.,2002; Moral et al.,2007), gravel contents (Morari et al., 2009), bulk density (André et al., 2012) as well as soil hydrological parameters (Hedley and Yule, 2009; Goodwin and Miller, 2003). A strong relation has been shown to exist between EC and the total soil available water-holding capacity (AWC) (Ortuani et al., 2019; Priori et al., 2013; Goodwin and Miller, 2003; Hedley and Yule, 2009; Fortes et al., 2015; Hedley et al., 2010). Cluster analysis of the soil maps elaborated from the EC data acquired at increasing soil depths is one of the most common methods to delineate SSMZ (Ortega and Santibanez, 2007; Priori et al., 2013; Ortuani et al., 2016; Ortuani et al., 2019). In this work, we illustrate the procedure to obtain a prescription map for the variable rate irrigation (VRI). We worked on a 4 ha field in the farm A.Menozzi, located in Landriano (PV). Firstly, EC measurements were acquired, through an electromagnetic-induction (EMI) sensor. The EC data were interpolated to obtain high-resolution soil maps, which were used to delineate the SSMZs within the field, by applying statistical procedures. Moreover, soil samples were collected at different depths (20 cm and 50 cm) in few points in each SSMZ, in order to measure in laboratory the soil texture and the soil water retention properties (specifically, the available water capacity, AWC). In the same points, also the soil saturated hydraulic conductivity (Ks) was measured through a field method. The AWC and Ks measurements were used to characterize each SSMZ. Finally, the FAO software 'CropWat' (FAO, 2008) was used to simulate the optimal irrigation management in each SSMZ, based on the different soil characteristics, crop and climate data, and the scheduling criteria for irrigation. The obtained variable-rate irrigation scheduling was compared with the irrigation management adopted by the farmer.

Materials and Methods

We worked on the "Bisella" field (4 ha) of the farm "A. Menozzi", located in Landriano (PV). The farm is located in the medium plain zone, rich in resurgences. This study is based on a first investigation on soil variability at farm scale (Bocchi et al.,2006), including also the experimental field of this study.

EMI surveys

A multi-frequency EMI sensor (Gem2, by *Geophex*) was used to investigate the spatial variability of soil properties at field scale. An EMI sensor acquires EC measurements, by transmitting an electromagnetic field that propagates throughout the soil depth. The EC measurements are average values relative to a specific depth of exploration (DoE), which depends on the operative frequency as well as on the soil properties. The EC measurements are recorded with their position, acquired by a GPS, to ensure that the data can be processed with a GIS.

The EC measurements were acquired along parallel lines with a distance of 7m; five different frequencies (15, 30, 40, 65 and 80 kHz) were used to describe the soil spatial variability at different depths.

SSMZ delineation

The EC measurements were pre-processed to recognize outliers, finally the valid data were interpolated using a GIS software (Qgis) to obtain the detailed EC maps at different depths. Only the maps relative to two of the five frequencies (30 and 40 kHz) were considered for further analysis. The maps relative to the frequencies 15, 65 and 80 kHz were not considered due to the prevalent background noise (80kHz) and the DoEs greater than the soil depth of agronomic interest (15 and 65 kHz).

The EC maps relative to the frequencies 30 and 40 kHz, characterized by decreasing DoEs, were integrated by applying the principal component analysis (PCA), carried out with the R software. Finally, in order to delineate the SSMZs within the field, the maps of the principal components explaining the most part of the EC variability at the different soil depths were processed through cluster analysis (CA), using the USDA software MZA. The optimal number of SSMZs was determined taking into account the FPI (Fuzziness Performance Index) and NCE (Normalized classification entropy) indices, representing the degree of zone separation and disorganization, respectively.

Soil sampling

For each SSMZ, three sampling points at most were selected, in order to characterize the soil properties of the zones. Different kinds of soil samples were collected: undisturbed samples at the depth of 20 cm, to measure AWC; disturbed samples at depths of 20 and 50 cm, to measure texture.

Soil characterization: soil texture, water retention curve, and hydraulic conductivity

In order to determine the soil physical and hydrological characteristics, laboratory analyses were conducted on the soil samples to measure the textural properties and the AWC properties of the soils. Moreover, in the same points, also the soil saturated hydraulic conductivity (Ks) was measured through a field method.

The disturbed samples were analysed following the II.5 method illustrated in "Metodi di analisi chimica del suolo" (MiPAAF, 2010), to measure soil texture. The AWC values were determined as the difference between the soil moisture at field capacity (FC) and the soil moisture at wilting point (WP). FC and WP values were measured with the pressure plate apparatus (Richards, 1948, 1965; Klute, 1986), considering pressures of 0.2 and 15 bar, respectively.

The Ks was measured in field, through the Simplified Falling Head technique (SFH) (Bagarello et al., 2004), based on the measurements of the height of infiltrated water at different time during a variable load infiltration process. For each point, three replicates were considered.

AWC mapping

Starting from the EC measurements acquired through the EMI sensor, a regression model was calibrated to estimate the AWC values at a detailed scale within the field, and finally mapping AWC with a high spatial resolution. This map was used to obtain the prescription map for the VRI (maize was considered). Since irrigation management refers to the water balance in the root zone (almost 1m depth for maize in the "Bisella" field), the AWC characteristics of this soil depth are required. The AWC values characterizing the root zone for maize were estimated considering the AWC measurements conducted on the soil samples collected at 20 cm depth) and the AWC dataset relative to a previous study (Ortuani et al., 2016) which investigated the soil hydrological properties of shallow and deep soils. The regression model to estimate the AWC values was calibrated considering the AWC values characterizing the root zones in each sampling point. These AWC values were calculated as average of the AWC measurements obtained in laboratory (relative to the soil samples collected at 20 cm depth) and the AWC values elaborated from the dataset of the previous study, to characterize the soil at depth greater than 50 cm.

FAO Model

After creating the hydrological prescription map for the Bisella field with the methods described above, it was carried out a comparison between the irrigation management conducted so far by the farmer, and a differentiated management for the three areas identified in the field. The goal was to evaluate the effectiveness and irrigation efficiency of the two irrigation schedulings. To simulate an optimized irrigation schedule for the different zones, the program 'Cropwat 8.0' was used. This FAO software is based on the method proposed in the FAO Irrigation and Drainage Paper 56 (FAO 1998).

The model, using *data input* (meteorological, soil, crop data) and *scheduling criteria* (Irrigation timing, irrigation quantity and irrigation efficiency) allows the simulation of the irrigation management of a crop, and proposes various indicators of management efficiency. Among the others, these include: the overall irrigation efficiency index, percolation losses, yield losses. To compare the different irrigation management, Cropwat was implemented for the year 2017 in two different ways:

1) simulation of the irrigation scheduling considering the irrigation events carried out by drip irrigation once a week from June 12 to the end of July, delivering 29 mm at each irrigation event (as stated by the farmer in his 'farm-diary');

2) optimization of the irrigation scheduling for each zone by considering the irrigation water to be delivered by drip irrigation when the 50% of the RAW is consumed, with an irrigation amount refilling the soil at the 80% of the TAW, and an irrigation method efficiency of 95%.

Results and Discussion

The detailed EC maps obtained interpolating the data acquired through the EMI sensor are shown in Fig. 1. These maps were elaborated through PCA and CA. Specifically, both the principal components explained 50% of the total variability, therefore the CA was applied on both the components. The optimal number of SSMZs was determined minimizing both the FPI and NCE indices produced with MZA software; four SSMZs were delineated. Fig. 2 shows the SSMZs and the selected sampling points.

The AWC map was elaborated from the EC map relative to 40 kHz, considering the regression model (Fig. 3) calibrated with the AWC values characterizing the root depth in the soil sampling points and reported in Table 1 (R^2=0,66; p-value=0). Fig. 4 shows the AWC map; due to the AWC spatial variability within the SSMZs, two of the four SSMZs are characterized with very similar mean AWC values (16 and 17,4%). Therefore, three SSMZs (A', B', C') were considered to obtain the prescription map for VRI (Fig. 2), merging C and D zones into one; Tab. 2 shows the mean AWC values for each of these SSMZs.

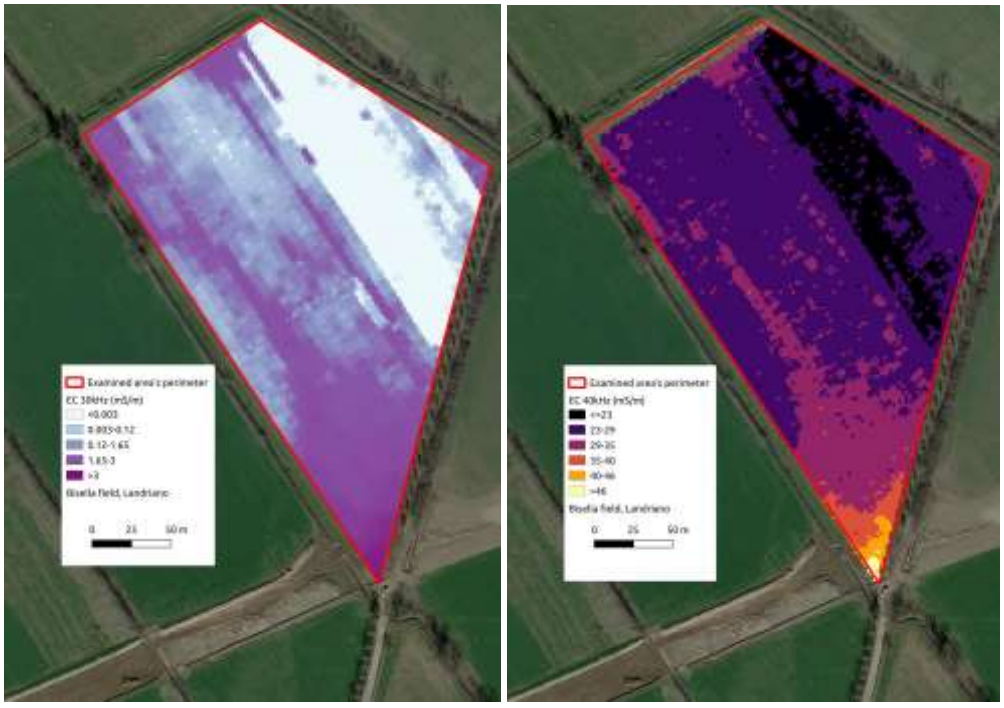

(a) *(b)*

Fig.1: (a) EC map from data acquired with operative frequency 30 kHz (deep soil); (a) EC map from data acquired with operative frequency 40 kHz (shallow soil).

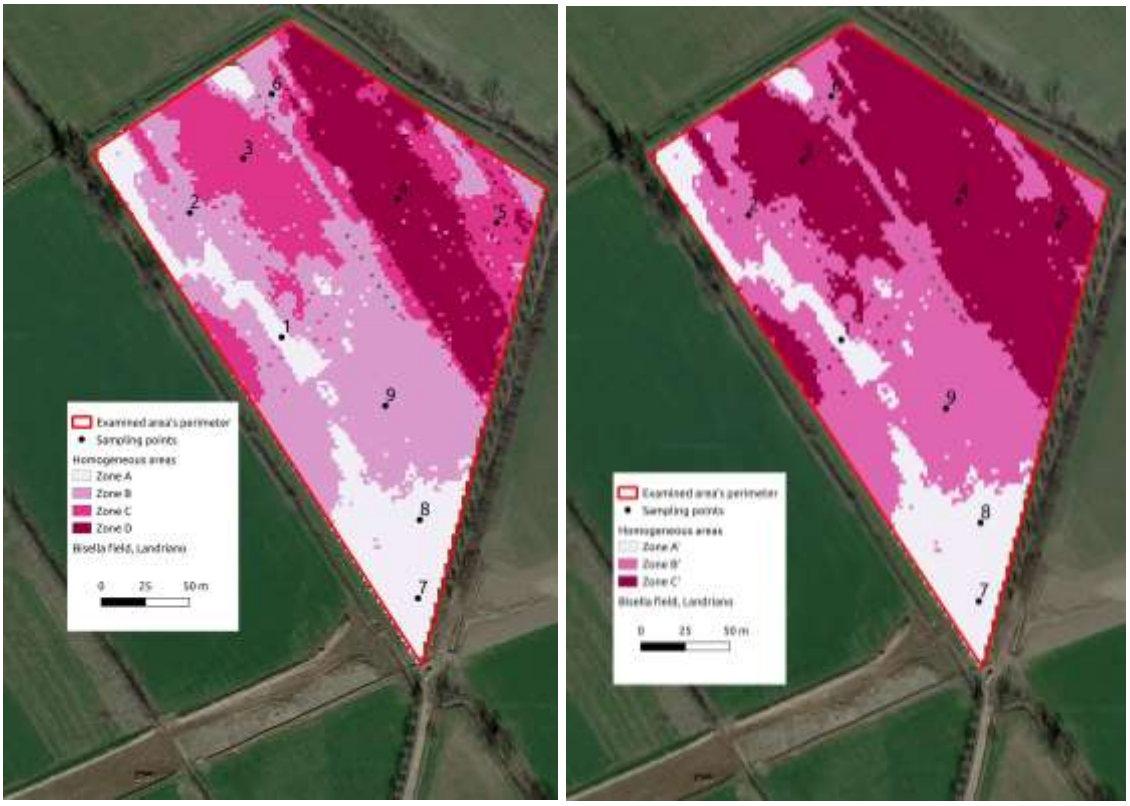

(a) *(b)*

Fig. 2: SSMZ maps: (a) four SSMZs, resulting from the EC maps; (b) three SSMZss, zones C and D were merged based on the spatial variability of the AWC values.

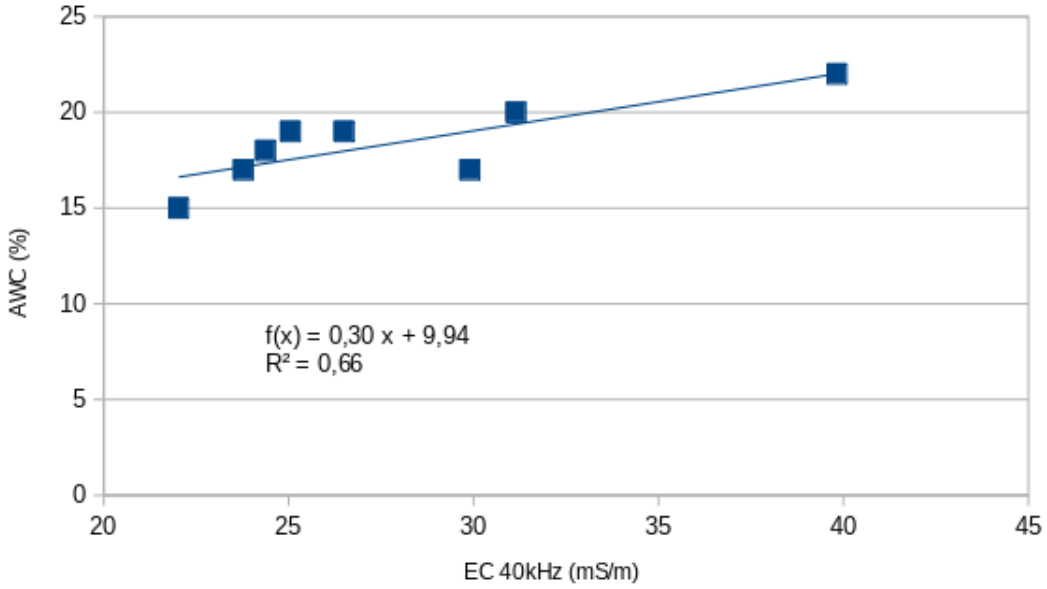

Fig. 3: Linear regression between EC and AWC.

The ks values were estimated from measurements obtained with an infiltration experiment at a depth of 20 cm. These values showed to be affected by uncertainty due to measurement errors. Once the datasets have been cleaned, the calculated conductivity values corresponded to those typical of a sandy loam soil (table 1). In order to obtain a Ks map, a regression model between Ks and EC was calibrated considering the Ks values in six points, because of three outliers (R^2=0,64 and p-value=0,05; Figure 4).

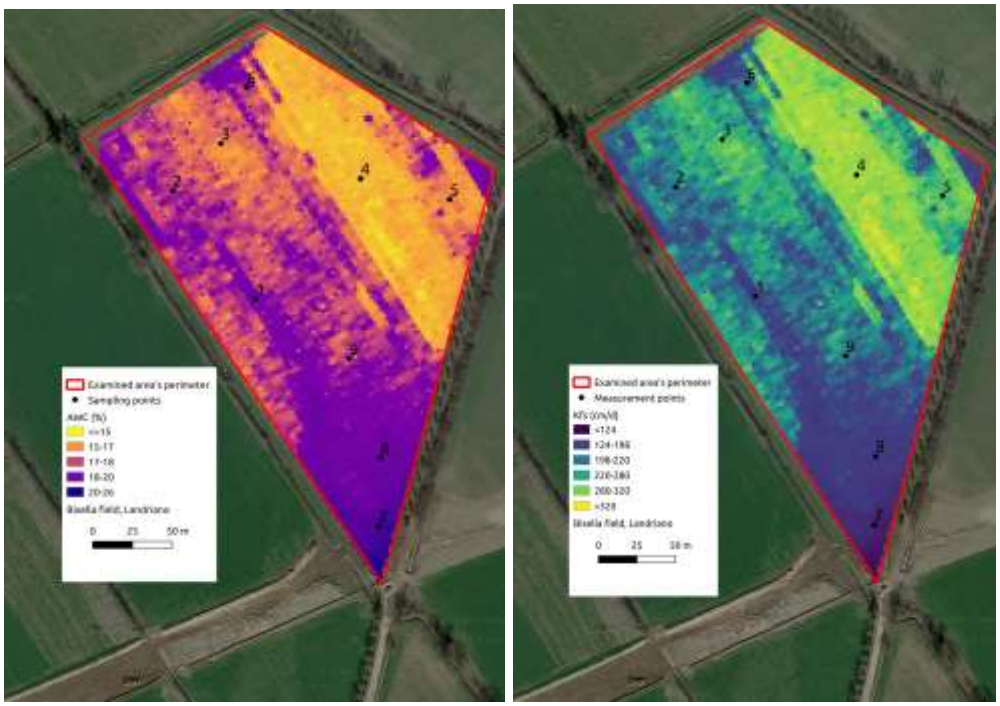

(a) *(b)*

Fig. 4: (a) AWC map; (b) Kfs map.

Tab. 1: Hydrological and physical characteristics of the soil for each sampling point.

Sample	Clay (%)	Silt (%)	Sand (%)	Texture (USDA)	EC 40 kHz (mS/m)	AWC (%)	Kfs (cm/d)
1	10	34	56	Sandy loam	29,9	17	198
2	3	34	63	Sandy loam	25,05	19	286
3	7	30	63	Sandy loam	23,775	17	320
4	1	34	65	Sandy loam	22,025	15	176
5	10	30	60	Sandy loam	24,075	21	243
6	12	28	60	Sandy loam	24,375	18	203
7	11	31	57	Sandy loam	39,825	22	218
8	12	31	57	Sandy loam	31,15	20	124
9	10	31	59	Sandy loam	26,5	19	384

Tab. 2: Average values for the three SSMZs.

Zones	Points	EC 40 kHz (mS/m)	Texture (USDA)	AWC (%)
A'	1 - 7 - 8	33,625	Sandy loam	19,6
B'	2 - 9 - 6	22,308	Sandy loam	16,7
C'	3 - 4 - 5	22,975	Sandy loam	11,1

Through the CropWat software, two different scenarios for the maize irrigation management in each zone were analyzed. Comparing the current irrigation management strategy and the optimized one, it is possible to observe a water saving in each zone (Fig. 5). Tab. 3 presents the overall results obtained with CropWat in this study.

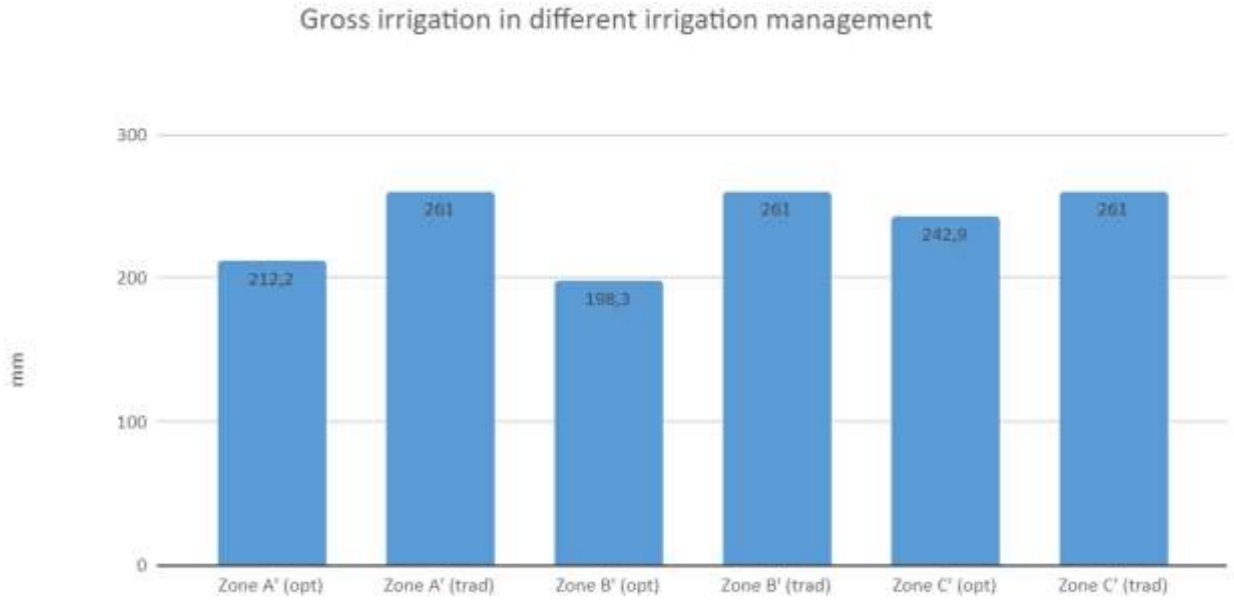

Fig. 5: Gross irrigation supplied to the maize crop in the case of the optimized and actually adopted irrigation strategies.

Furthermore, it is possible to see how the optimized method allows a reduction in irrigation water losses (Fig. 6).

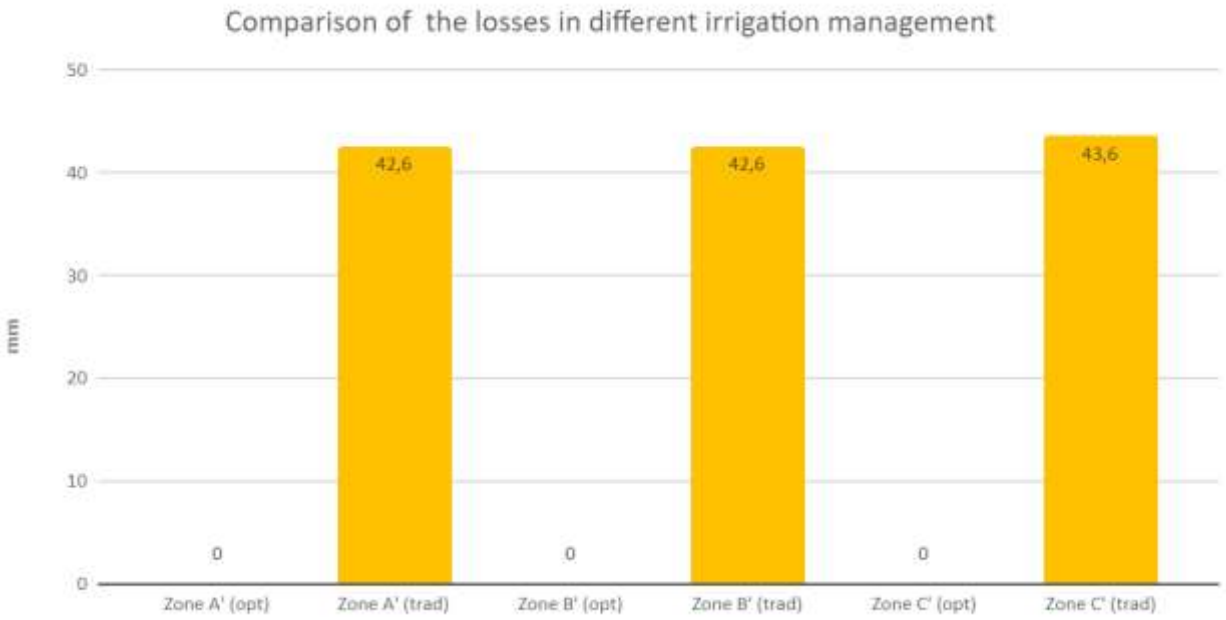

Fig. 6: Irrigation losses (percolation out from the root zone, mm) in the optimized and currently adopted irrigation strategies.

Tab. 3: Results obtained in the CropWat simulations.

	Zone A' (opt)	Zone A' (trad)	Zone B' (opt)	Zone B' (trad)	Zone C' (opt)	Zone C' (trad)
Irrigation efficiency (%)	100	83,7	100	83,7	100	83
Effective rain (mm)	95,8	81,5	95,8	81,5	85,3	81,5
Rain losses (mm)	88,6	102,9	88,6	102,9	99,1	102,9
Efficiency rain (%)	52	44,2	52	44,2	46,3	44,2
Yield reduction (%)	0	0	0	0	0	0,3
Gross irrigation (mm)	212,2	261	198,3	261	242,9	261
Percolation losses (mm)	0	42,6	0	42,6	0	43,6

Conclusions

A survey with an EMI sensor allowed the description of the spatial variability of soils in the Bisella field. EC data were used to subdivide the field in three homogeneous areas, which were then characterized through soil samplings. By implementing the CropWat model for each zone, it was possible to simulate a variable rate irrigation and compare it to the current irrigation management. The simulation showed that a differentiate scheduling would allow to lower the water volume applied by 16 %, and the percolation losses by 100%. The highest reductions were observed for zones A and B, which present higher EC values. These two areas are similar to each other in terms of soil properties, and predicted irrigation volumes and percolation losses, but they

show a significative difference when compared to the C area. For the C area the model predicted a yield loss of 3% in the case of the actual irrigation management. The loss of production was documented in another study (Ortuani et al., 2016) that, always on the Bisella field, verified the different mean production for the different parcels, which were statistically different (ANOVA test). For this reason, in view of a differentiated irrigation management we would advise separating the field into two parts, one comprising the zones A and B, and one comprising the zone C. Obviously, to operate a differentiated irrigation management in the same field, it must be shown that this solution would be economically sustainable, and this also depends on the type of crop cultivated in the field.

Geophysical tools such as EMI sensor have much potential in rapid soil characterization, but requires further experimentation to allow an easier interpretation of the results provided. This may increase the possibility of using this method to characterize soils with lower time and cost requirements, to further improve agriculture efficiency.

References

B.Ortuani, E.A.Chiaradia, S.Priori, G.L'Abate, D. Canone, A.Comunian, M.Giudici, M.Mele and A.Facchi, 2016. Mapping Soil Water Capacity Through EMI Survey to Delineate Site-Specific Management Units Within an Irrigated Field. Soil Science, volume 181, number 6.

B.Ortuani, G.Sona, G.Ronchetti, A.Mayer and A.Facchi. Integrating Geophysical and Multispectral Data to Delineate Homogeneous Management Zones within a Vineyard in Northern Italy. Sensors. 2019; 19(18):3974.

B.Ortuani, A.Facchi, A.Mayer, D.Bianchi, A.Bianchi and L.Brancadoro. Assessing the Effectiveness of Variable-Rate Drip Irrigation on Water Use Efficiency in a Vineyard in Northern Italy. Water. 2019; 11 (10):1964

Godwin R. J., Miller P. C. H.. 2003. A review of the technologies for mapping within-field variability. Biosyst. Eng. 84(4):393-407

Priori S., Martini E., Andrenelli M. C., Magini S., Agnelli A. E., Bucelli P., Biagi M., Pellegrini S., Costantini E. A. C.. 2013. Improving wine quality through harvest zoning and combined use of remote and soil proximal sensing. Soil Sci. Soc. Am. J. 77(4):1338-1348

Van Meirvenne M., Islam M. M., De Smedt P., Meerschman E., Van De Vijver E., Saey T.. 2013. Key variables for the identification of soil management classes in the aeolian landscapes of north-west Europe. Geoderma. 199:99-105

Ortega R. A., Santibanez O. A.. 2007. Determination of management zones in corn (*Zea mays* L.) based on soil fertility. Comput. Electron. Agr. 58:49-59

Corwin D. L., Lesch S. M., Shouse P. J., Soppe R., Ayars J. E.. 2003. Identifying soil properties that influence cotton yield using soil sampling directed by apparent soil electrical conductivity. Agron. J. 95:352-364

Doolittle J. A., Indorante S. J., Potter D. K., Hefner S. G., McCauley W. M.. 2002. Comparing three geophysical tools for locating sand blows in alluvial soils of Southeast Missouri. J. Soil Water Conserv. 57:175-182

Andre F., van Leeuwen C., Saussez S., Van Durmen R., Bogaert P., Moghadas D., de Resseguier L., Delvaux B., Vereecken H., Lambot S.. 2012. High-resolution imaging of a vineyard in south of France using ground penetrating radar, electromagnetic induction and electrical resistivity tomography. J. Appl. Geophys. 78:113-122

Fortes R., Millan S., Prieto M. H., Campillo C.. 2015. A methodology based on apparent electrical conductivity and guided soil samples to improve irrigation zoning. Precis Agric.

Hedley C. B., Yule I. J.. 2009. A method for spatial prediction of daily soil water status for precise irrigation scheduling. Agr. Water Manage. 96(12):1737-1745

Morari F., Castrignano A., Pagliarin C.. 2009. Application of multivariate geostatistics in delineating management zones within a gravelly vineyard using geo-electrical sensors. Comput. Electron. Agr. 68:97-107

Kumar P. 2016. Spatial analysis of soil properties using GIS based geostatistics models *Mod. Earth Syst*. Environ. 2:107

V. Bagarello, M. Iovino, D. Elrick, 2004. A Simplified Falling-Head Technique for Rapid Determination of Field-Saturated Hydraulic Conductivity. Soil Science Society of America Journal, 68: 66-73.

Elrick, D.E., R. Angulo-Jaramillo, D.J. Fallow, W.D. Reynolds, and G.W. Parkin. 2002. Analysis of infiltration under constant head and falling head conditions. p. 47–53. In P.A.C. Raats et al. (ed.) Environmental mechanics: Water, mass and energy transfer in the biosphere. Geophysical Monograph Series, Vol.129, AGU, Washington, DC.

Sitography: http://www.geophex.com/Pubs/gem2_-_how_it_works_detailed.htm

Aknowledgments

The authors would like to thank for the support: A. Facchi, B. Ortuani, A. Mayer, M. Rienzner, A. Moreno Carrera.

PHENOCROP

Field phenotyping for salt tolerance in japonica rice (*Oryza sativa* L.)

Miotti N., Tomasoni E., Korner F.

Abstract

A field phenotyping activity was carried out in order to confirm, by the evaluation of physiological parameters (flag leaf chlorophyll content, fluorescence emission characteristics and Na^+/K^+ ratio), the salt tolerance performance that some rice genotypes showed in previous greenhouse screenings. The trials were carried out in two paddy fields interested to natural soil salinization (Goro and Scardovari) and in a third non-salinized paddy field (Vercelli). Although, agronomic evaluations are currently in progresses, the results obtained confirmed the cultivar Galileo and the genotypes RIL267 as promising for future studies aimed at identifying of the molecular mechanisms conferring them salt tolerance that could be useful in breeding program.

Keywords: Oryza sativa L., salt tolerance, leaf chlorophyll and fluorescence, Na^+/K^+ ratio

Introduction

The Research Enriched Education (REE) laboratory named "Phenotyping: from the plant to the crop" was included in the framework of the H2020 NEURICE project (www.neurice.eu) whose main objective is to develop strategies for rice productivity, stability and quality by developing New commercial European RICE (*Oryza sativa*) harboring salt tolerance alleles to protect the rice production sector against climate change.

Trend of rising temperatures in the Mediterranean coastal regions is more evident than that observed in other regions at the same latitude. In areas close to the sea the water scarcity due to the in-progress climate modification determines alterations of the availability and quality of irrigation water (Appelo and Posta, 2004). The river delta areas are concerned by these events and it is particularly evident within the terminal stretches of the Po deltaic branches. Recent data evidence that in these areas the phenomenon of the salt wedge intrusion into the surface water courses is almost quintupled during the last decades especially due to the overexploitation of fluvial freshwater, and to the riverbed deepening (Simeoni and Corbau, 2009). These areas risk to became marginal for agriculture and less and less suitable for the rice systems here widespread. Indeed, among cereals rice is the most salt sensitive ones (Reddy et al., 2017). The possibility of having rice varieties tolerant soil salinity is a change of overcoming this problem (Ismail and Horie, 2017).

Previous studies carried out screening in greenhouse for salt tolerance about 500 rice genotypes among well-known accessions and F8-Recombinant Inbred Lines (RILs) obtained crossing the cultivar Vialone nano and Baldo, described as relatively salt sensitive and tolerant, respectively, parents, allowed the identification of two accessions (Galileo and Virgo) and three RILs (RIL87b, RIL267and RIL 39) as putatively salt tolerant.

Aim

The REE activities carried out were aimed at verifying in field trails the existence of physiological salt tolerance traits in the above cited rice genotypes at the beginning of the maturation periods. The physiological parameters considered were: a) flag leaf chlorophyll content; b) flag leaf fluorescence; c) flag leaf Na^+/K^+ ratio.

Materials and Methods

Preliminary activities

Preliminary activities were carried out in the green house of the UNIMI's Agricultural and Food Sciences Faculty in order to test the suitability of different instruments for measuring physiological parameter related to stress conditions during the plant growth. The Dualex optical sensor, the Handy Pea fluorimeter, the CIRAS-2 gas exchanger meter and the FLIR IR thermal camera were utilised to onset of abiotic stress condition (drought) in *Solanum lycopersicum* L. and *Nicotiana benthamiana* Domin and biotic stress condition in *Nicotiana benthamiana* Domin. inoculated with different virus and bacteria. All the instruments resulted useful in monitoring the different stresses in the plants, but only the Dualex and the fluorimeter devices were considered suitable for use in field. Indeed, they performances have been considered less susceptible to environmental conditions characterizing the field activities planned and, first of all, they resulted adapt for a fast collection of high number of data. In particular, the CIRAS-2 instrument resulted very reliable in measuring the stress effects on photosynthesis activity, but it needs too long time (more than 10 min); concerning IR camera, that measures leaf temperature in turn related to lea stomatal conductance, the images collected resulted to be marked influenced by environmental factors such as air temperature, light intensity and wind very variable in outdoor environments.

Experimental fields

Field trials were carried out at Vercelli (45°19'20,4" N; 8°22'25,35" E) and in the delta Po area, i.e. at Scardovari (44°51'58,0" N; 12°26'33,0" E) and Goro (44°50'01,9" N; 12°20'01,1" E; Fig. 1A). The field in Vercelli, whose soil electric conductance (EC_s) resulted was <1.0 dS m^{-1}, was considered as a control, whereas Scardovari and Goro paddy fields whose ECs during the 2019 growth season were in the range 2.5-4.0 dS m^{-1} were considered as salt treatments. All the fields were cultivated by the same agronomic techniques and flood watering regime. In each field a completely randomized block design was used, with plots of size 3 x 5 m; 7 rice genotypes (Vialone Nano, Virgo, Galileo, RIL 39, RIL 87, RIL 267, Baldo) were transplanted with three replicas, for a total of 21 plots. The edge of the field was delimited with fences to avoid damages from local fauna.

Physiological evaluations

About 12 days after flowering, when the sink activities of the developing grains is supposed to be the highest during maturation period, the flag leaf chlorophyll (CHL) content was evaluate by using the Dualex device (Cerovic et al., 2012). It is (Fig. 1B) an optical device that allows to obtain non-destructive measures based on the light absorbance and transmission properties of chlorophylls. Dualex performs repeated measures in short-time over a large number of samples and the quality of the measures are anyway influenced by environmental factors. Six measurements per plant were performed in the flag leaf: 3 on the upper, adaxial, and 3 on the bottom, abaxial, leaf lamina, in the proximal, median and apical part, respectively; thirty measures per leaf were obtained.

On the same leaf fluorescence measures were carried out by using the Handy-PEA portable fluorimeter (Fig. 1C). This device allows to obtain non-destructive measurements of the fluorescence signals, through the application of a continuous saturated light beam. In order to correctly detect the fluorescence values, the leaf photosystems were energy discharged by the application of clips obscuring for at least 20 min the measurement area. The ration between variable fluorescence (Fv) over maximum fluorescence (Fm), Fv/Fm, was considered as the main representative parameter, amongst those recorded by the instrument, of the efficiency of the leaf photosystems.

After Dualex and fluorometric measures, carried out on the flag leaf of 5 plant randomly chosen within each plot, the flag leaves were collected and then air dried. In them both Na^+ and K^+ concentrations on dry weight basis were evaluate by inductively coupled plasma mass spectrometry techniques (BRUKER Aurora-M90 ICP-MS, Fig. 1D) after mineralization in 65% HNO_3 in a microwave's oven.

Soil sampling and ECs measures

Four field prototype sensors have been installed around the experimental fields, which have detected the electrical conductivity of the soil along the entire duration of the season (Fig. 1E). To further verify the accrual ECs in the fields, four soil samples were taken around the perimeter of each experimental rice field, close to the position of the sensors, and with the Saturated Media Extract (SME) method the electric conductibility value was determined.

Statistical analysis

The SPSS software was used for data processing. For the comparison of the averages, the ANOVA variance analysis was used. The data were sorted according to the rice varieties and the place of data collection (Scardovari, Goro and Vercelli). The ANOVA analysis of data were carried out with post hoc tests (Tukey for unbalanced data and Ryan-Einot-Gabriel-Welsch for balanced data) on the base of: i) the assumption of Independence of Cases, that is the base of appliance of ANOVA analysis; ii) a normal distribution of residuals verified by Shapiro-Wilk test; iii) an Equality of Variances (homoscedasticity) verified by ANOVA on the absolute values of residuals. In the cases that the requirement of Equality of Variances was not verified a preliminary Brown-Fosythe test is carried out to verify the presence of significant differences between the averages, and if verified, the analysis with Games-Howell post hoc test has been done.

(A) (B) (C) (D) (E)

Fig.1: The experimental fields and the instrument used.

Results and Discussion

In Fig. 2 the content of chlorophyll, as Dualex CHL units, is showed for the different accessions tested in the three experimental fields. The outlier data were not considered for the statistical analysis. The statistical analysis has been done as described in material and method for Goro data, in the case of Vercelli and Scardovari, the assumption of Equality of Variances was not verified, so the second procedure of analysis was used (Brown-Fosythe test, followed by post-hoc Games-Howell).

In the control, non-saline, field of Vercelli the accessions showed different chlorophyll content with the presence of three groups of chlorophyll levels.

The same accessions grown in Scardovari and Goro fields with saline soils, ECs at 2.2 and 3.5 dS m^{-1}, respectively, showed a generalised increase of the level of chlorophyll content. Only RIL 39 and RIL 267 in Scardovari and RIL 267 and Galileo had a different chlorophyll content, while all

the other accessions had a same, and higher with respect to the control, level of the pigment. The RIL 267 showed the less increase in chlorophyll, while all the other accessions had an evident increase.

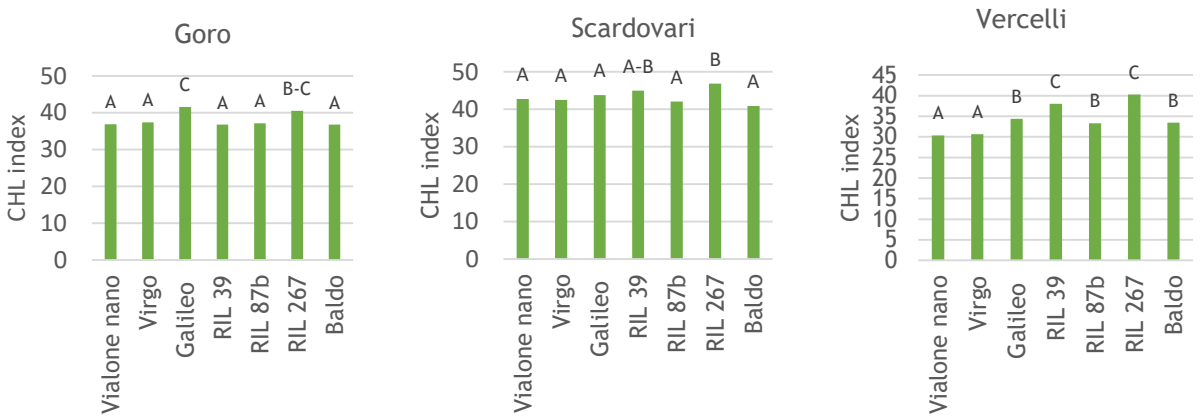

Fig.2: Chlorophyll content of flag leaf of rice accessions grown in Vercelli (control), Goro and Scardovari (saline soil).

In Fig. 2 the ratio between the Florescence variable (Fv) and the Fluorescence maximum (Fm) are reported. The statistical analysis was carried out for Scardovari and Goro data, in accord the method used for data on chlorophyll, utilising the Brown-Fosythe test, followed by post-hoc Games-Howell, since the Equality of Variances was not verified.

In terms of fluorescence the accessions Galileo and RIL 87b grown in control field, Vercelli, showed a significant higher level of Fv/Fm. This difference was lost both in Scardovari and Goro saline fields, were no significant statistically differences were recorded. This seems indicate that the growth in saline soil depress the genotype differences in the efficiency of photosystems in all the accessions tested.

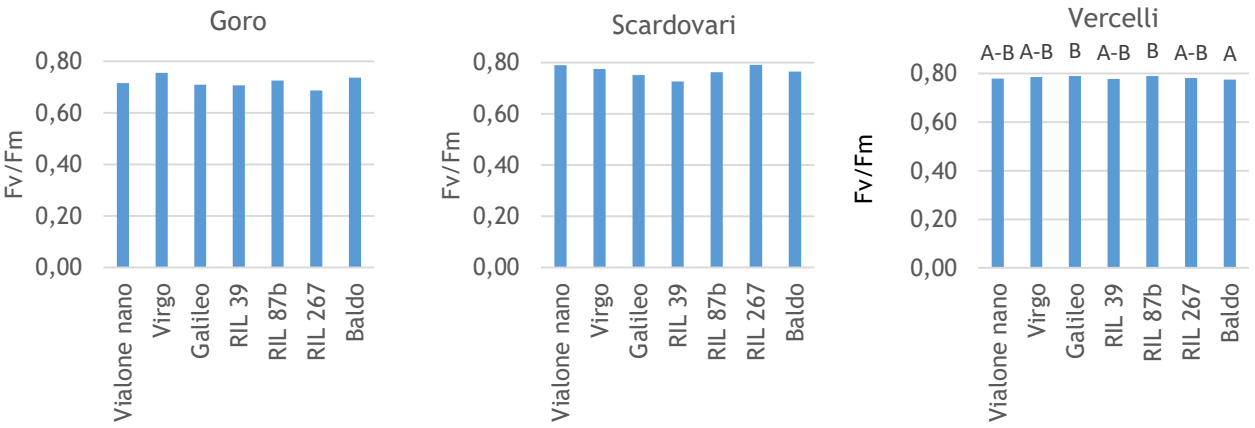

Fig.3: Fv/Fm measured in flag leaf of rice accessions grown in Vercelli (control), Goro and Scardovari (saline soil).

In order to investigate the effect of growth in saline soil on the leaf fluorescence, the above data are processed in a different approach, able to compare the different site of growth.

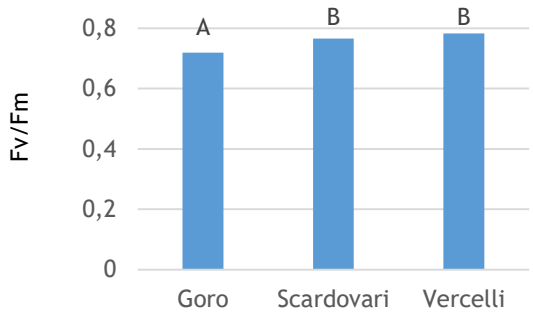

Fig. 4: Average of the Fv/Fm values in the three experimental fields.

The data of fluorescence were analysed considering the average of the total Fv/Fm ratio (Tsai et al., 2019) of all the rice accession in each field. The obtained results indicate that there is a significant reduction of the fluorescence in the field of Goro where, at the moment of the evaluation, there was the highest level of salinity (Ec 3.5 dS m^{-1}).

Taken together the results reported in Fig. 3 and 4 show that the salinity is able to affect the efficiency of the photosystems, mainly were the level salinity was higher, and that all the accessions are affected by this effect.

A well know traits conferring to plants salt tolerance consist in their ability in maintaining relatively low Na^+/K^+ in the leaves (Munns and Tester, 2008; Anschütz et al., 2014, Zhang et al., 2018). The data reported in Fig. 5 indicate that there is no difference in the Na^+/K^+ ratio in the flag leaf of plant grown in non-saline soil of Vercelli. The level of Na^+ (µmoli g^{-1}) in this condition is very low so the predominance of K^+ makes the ratio very low.

In saline soil of Scardovari and Goro the higher level of the ratio indicates the increase of Na^+ content in flag leaf of all accessions. In both saline soils there are differences among accessions in terms of Na+ content; in particular, the Galileo and RIL 267 had the highest Na^+/K^+ ratio. In the case of Goro also RIL 87b and Baldo showed an increase of Na+ content. The difference in the flag leaf Na^+/K^+ ratio at Goro and Scardovari could depend from the dynamics of the level of salinity in the two soils along the whole growth period. The measure of electrical conductivity that has been done by the soil media extract method, refers to the situation at the end of August, when all the measures have been performed. During the season the salinity of the soil water in the two sites close to the sea could be very different as a consequence of different effects, not last the inlet of the salt wedge.

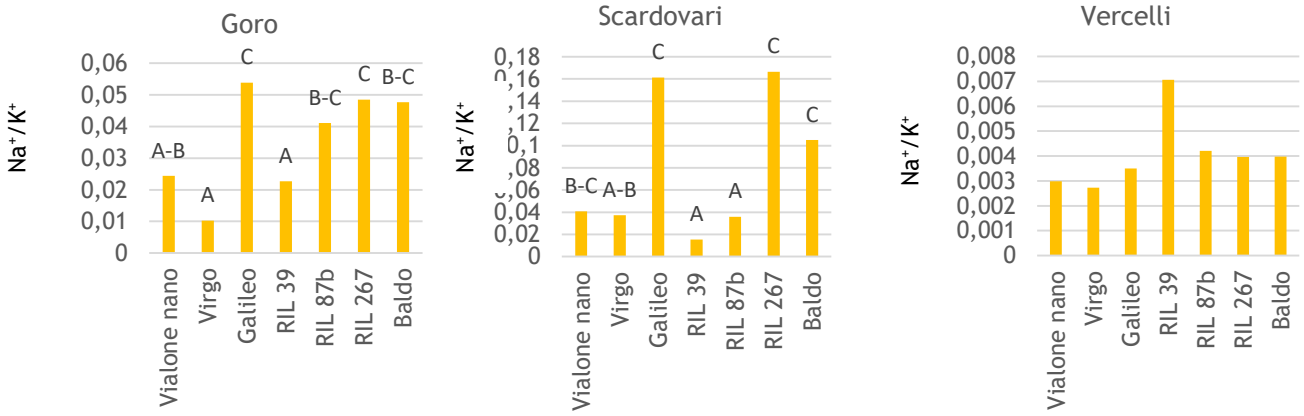

Fig. 5: Na^+/K^+ ratio measured in flag leaf of rice accessions grown in Vercelli (control), Goro and Scardovari (saline soil).

It is possible to conclude that the two accessions Galileo and RIL 267 appear to be the most interesting since they show the highest tolerance to the saline stress. In effect they accumulate more Na^+ in the leaf tissue without a reduction of chlorophyll content. This could counteract by antioxidant systems (Schmidt et al., 2013) the loss of the photosystems efficiency and allow the plant to support the growth and seed production.

Data about the grain yield of the different accessions that will be obtained at the end of the plants cycle, will indicate if the above indication are verified and the best accessions are indeed valuable in terms of seed production in presence of saline stress. In this case Galileo and RIL267 could have the most interesting genetic background to be utilise for the constitution of new cultivars tolerating the presence of salt in the soil.

Conclusions

The results obtained in the research activity of the REE course confirm, in field conditions, the data obtained by a previous activity, in a pot experiment and in glasshouse, about the saline tolerance of rice accessions. This mainly in the case of two genotypes (Galileo and RIL 267) that resulted the most promising to be utilised for the constitution of new cultivars tolerating the presence of salinity in the soil of cultivation.

References

Anschütz, U., Becker, D., and Shabala, S. (2014). Going beyond nutrition: regulation of potassium homoeostasis as a common denominator of plant adaptive responses to environment. *J. Plant Physiol*. 171: 670–687.

Appelo, C. A. J., Postma, D. (2004). Geochemistry, groundwater and pollution. CRC press.

Simeoni U., Corbau C. (2009). A review of the delta Po evolution (Italy) related to climatic changes and human impacts. *Geomorphology* 107: 64-71.

Cerovic Z.G., Masdoumierd G., Ben Ghozlena, N., Latouchea, G. (2012). A new optical leaf-clip meter for simultaneous non-destructive assessment of leaf chlorophyll and epidermal flavonoids. *Physiol. Plant*. 146: 251–260.

Ismail AM, Horie T. (2017). Genomics, physiology, and molecular breeding approaches for improving salt tolerance. Annu Rev Plant Biol. 2017;68:405–434.

Munns, R., Tester, M. (2008). Mechanisms of salinity tolerance. *Annu. Rev. Plant Biol.*, 59, 651-681.

Reddy, I.N.B.L., Kim, B-K., Yoon I-S, Kim K-H, Kwon, T-R. (2017) Salt tolerance in rice: focus on mechanisms and approaches. *Rice Sci.*, 24:123-144.

Schmidt R., Mieulet D., Hubberten H. M., Obata T., Hoefgen R., Fernie A. R., Fisahn J., Segundo B. S., Guiderdoni E., Schippers J. H.M., Mueller-Roeber B. (2013). Salt-responsive ERF1 regulates reactive oxygen species-dependent signaling during the initial response to salt stress in rice. *Plant Cell*, 25: 2115–2131.

Tsai Y-C., Chen K-C., Cheng T-S., Lee C., Lin S.H., Tung C-W. (2019). Chlorophyll fluorescence analysis in diverse rice varieties reveals the positive correlation between the seedlings salt tolerance and photosynthetic efficiency. BMC *Plant Biology* 19:403.

Zhang Y., Fang J., Wu X., Dong L., (2018). Na^+/K^+ balance and transport regulatory

mechanisms in weedy and cultivated rice (*Oryza sativa* L.) under salt stress. *BMC Plant Biol*. 18:375.

Acknowledgments

The authors would like to thank for the support: Alessandro Abruzzese, Piero Bianco, Paola Casati, Giorgio Lucchini, Roberto Oberti, Michele Pesenti, Stefania Prati, Gian Attilio Sacchi.

PRECIFEED

Evaluation of different diets for dairy cattle through on-field and laboratory analysis methods

Bonelli D., Frigerio S., Pampuri M., Stecconi A., Viganò F.

Abstract

In this laboratory different diets for dairy cattle were evaluated and, in particular, it has been considered fibre digestibility and peNDF. The diets were assessed through feed analysis, including both on-field methods (such as PSPS and NIR), most immediate and easily to execute, and laboratory techniques for measuring forage fibre fermentability, which allow more objective and precise analysis. The data collected with PSPS match with Zebeli's references, with the exception of the values concerning the diet containing soy silage that deviate slightly from the recommended values. The values of dry matter and other parameters obtained by NIR analysis were put in CNCPS software to rectify and estimate diet and consider some improvements for a better assessment of the current diet of the lactating cows. A further study concerning diet allowed the evaluation of the actual digestibility of the samples of corn silage and soy silage through two instruments: Gas Endeavour and Daisy. The data obtained through those instruments showed a different trend: the gas production curves, achieved through the Gas Endeavour, had a biphasic trend, while the curves obtained by processing data from Daisy had a monophasic trend. The analysis carried out showed a lower quality of the fibre of soy silage compared to corn silage in terms of potential fibre digestibility. However, the rate of fibre digestion resulted higher for soy silage.

Key words: *kd, peNDF, CNCPS, precision feeding, gas production*.

Introduction

Precision feeding of livestock is becoming an increasingly more important part in farm management. This gives the possibility to acquire and manage numerical data of raw materials and diets, which must be valorised and used to help farmers and nutritionists on making better decisions. By a punctual management of this information it is possible to identify in real time alert situations, like important variations of dry matter on silages. This, subsequently, allows solving problems with targeted, corrective actions, but mostly, it is possible to analyse farm productive systems defining their efficiency and their improvement possibility. In fact, "feed purchased" voice represents about 30% of dairy farm production costs (Pirondini, 2014). The improvement of cows' efficient use of nutritional factors and finding solutions less expensive but equally effective to feed them, now, is a primary goal to lead profitable dairy farms. Livestock feeds analysis includes both on-field methods, most immediate and easily to execute, and laboratory techniques, which allow obtaining an analysis more objective and precise.

Aim

The aim of this laboratory was to evaluate different diets for dairy cattle using the Cornell Net Carbohydrate and Protein System (CNCPS) software (v. 6.5) through on-field and laboratory analysis methods and tools. In particular, it has been considered chemical analysis and fibre digestibility of the main forages used in the ration and physically effective fibre (peNDF) of the total mixed ration (TMR) for a more appropriate utilization of the software evaluation.

Materials and Methods

In this laboratory, the *Azienda didattico-sperimentale A. Menozzi* (Università degli Studi di Milano) in Landriano (PV), a typical farm of Lombardy, based on crop cultivation of raw materials for livestock diet, was chosen for this evaluation. On the actual diet was used NIR analyzer and Penn State Particle Separator (PSPS). The NIR analysis, provides quickly analytical components of raw materials and diet with a good precision. Particle size, calculated with PSPS, is an important parameter to evaluate mixer wagon's work and to verify if there is the right amount of physically effective fibre (peNDF), which affects rumen functions and productive capacity of dairy cows. Another interesting analysis made during laboratory was the fibre digestibility measure, made through two different *in vitro* methods: DAISY II, a discontinous method to calculate NDF digestibility in batch, and GAS ENDEAVOUR, a new generation method to evaluate gas production (which is comparable with the NDFD because only NDF residues were analysed). This last parameter has a very practical importance influencing energetic feed values, conditioning dry matter intake and milk production. In a perspective of efficiency improvement and costs reduction, being able to measure easily fibre quality to ensure a costancy of this value is a valid choice to increase profitability. It was not possible to make this analysis for the diet currently used in Landriano due to lack of time for sample preparation, but, in order to experience these methods, samples of feeds from an experiment performed in March and April 2019 were evaluated. The two evaluated diets were characterized by the use of soybean silage as partial replacement of corn silage.
On these diets granulometry analysis was also made.

Farm

The samples analyzed were collected in *Azienda didattico-sperimentale A. Menozzi* in Landriano, a typical lombard farm based on crop cultivation of raw materials for livestock diet. It's a dairy farm which milk is sold for cheesemaking.
During laboratory, the diets for dairy cattle were evaluated through both on-field and laboratory analysis methods and tools.
The first thing to do is asking the farmer information about farm structure, in particular the forage system and some data about breed animals and their production. Farm's data are reported in the following tables:

Tab.1: Crop systems

First crop	Second crop	ha
Barley	Soy	16
Barley	Corn	5
Corn	/	22

Tab. 2: Herd composition

Cattle	N°
Lactation	91
Dry	20
Replacement heifers	105
Total	216

Tab. 3: Farm's breed

Breeds	% of total
Holstein	75
Jersey	15
Pezzata Rossa	10

Sampling

In the farm, samples of lactation diet total mix ration (TMR) and of raw materials like corn silage, barley silage, alfalfa hay and wheat hay were taken. TMR sampling was performed following the method suggested by Hall (2014), while for raw materials it has been used a toothed core drill.

On-field methods

For on-field analysis, two instruments were mainly used: PSPS: (Fig.1), composed of four sieves and a solid pan. It was used to separate the ration in five fractions based on the particle size and to define the value of peNDF (Penn State Extension). The values obtained were evaluated with Penn State (2002) and Zebeli's (2012) references.
Near Infra-Red (NIR), is a quick, precise, multifunctional and non-destructive instrument used to determine chemical composition and digestibility of rations, feeds and faeces. It's based on measuring electromagnetic radiation absorption of the sample analyzed. It gives information about dry matter, crude protein, NDF, ADF, ash, starch and others in a very short time, without any chemical analysis.

Fig. 1: PSPS and obtained fractions.

Laboratory methods

Regarding laboratory analysis, two instruments were used to evaluate *in vitro* fibre digestibility: DAISY II Incubator (Ankom Technology, Macedon, NY) and Gas Endeavour (Bioprocess control AB, Lund, Sweden). For each method it is required ruminal fluid taken from donor fistulated cows.

Fig. 2: DAISY II incubator and filter bags.

The Daisy II incubator (Fig.2) was used for the *in vitro* estimation of neutral detergent fibre digestibility (NDFD), following the procedure of ANKOM Technology, on soybean silage and corn silage. It was decided to calculate fibre digestibility at three times of incubation: 6, 48, 288 hours. This method allows to simulate the rumen digestion process at several hours of incubation and to estimate the potential degradability of NDF at 288 hours. Moreover, applying the curve fitting method by eye (Orskow and McDonald, 1979), it was possible to calculate the degradation rate (kd) of the potentially degradable fibre.

Fig. 3: Gas Endeavour.

Otherwise, Gas Endeavour (Fig.3) measures in-continuo the digestibility in relation with gas production by fermentation of the samples, operated by ruminal microorganisms. This instrument measures steadily gas production of every reactor in which have been put milled sample, rumen fluid and buffer solution, following the procedures of Menke and Steingass (1988). Data of cumulative gas production, obtained from Gas Endeavour, and all kinetic parameters were estimated by the nonlinear regression procedure of SAS with Orskow and McDonald's (1979) model. Because the samples used in this evaluation were treated before with neutral detergent solution, the kinetic parameters of gas production were assumed to be equal to that of fibre degradation. Moreover, digestion rates were also estimated by CNCPS model based on values obtained by Daisy. To calculate dry matter, samples were dried at 60° C for three days up to constant weight. For last, data taken from NIR were entered in CNCPS software to evaluate the current diet.

Results and Discussion

PSPS results

The use of separator made it possible to measure the different fractions of the diet and, consequently, to evaluate peNDF and compare it with Zebeli et al. (2012) reference. The separator was used to assess the following TMRs:

- TMR control with corn silage
- TMR with soy silage
- TMR actually used on farm (Landriano)

The first two samples were collected in April (twice in two different periods) while the last sample represents the current TMR used on farm.

Tab. 4: PSPS data compared to Penn State references

	TMR (Penn State)	TMR Soy silage	TMR Control	TMR Current
Size (mm)	%			
>19	2-8	15.2	6.2	8.9
8-19	30-50	31.4	36.3	35.8
4-8	10-20	17.1	15.6	15.8
<4	30-40	34.6	40.7	37.2

Data collected (Tab. 4) appear to be in accordance with the data of the Penn State University, except for the coarser fraction of the soy silage (>19 mm). This value could be caused by not an adequate mixing time (too short) during TMR preparation.

Tab. 5: peNDF of analysed rations

Sample	%DM>8mm	%DM<8mm	%NDF>8mm	%NDF<8mm	peNDF>8mm-NDF (%DM)
TMR contr. 10/4	39.7	60.3	53.3	46.7	17.8
TMR contr. 12/3	39.0	61.0	52.4	47.6	17.7
TMR soysil. 10/4	43.4	56.6	53.0	47.0	16.9
TMR soysil. 13/3	52.2	47.8	60.4	39.6	20.3

Similary peNDF was consistent with the indications reported by Zebeli et al. (2012) with the exception of the values concerning soy silage TMR that deviate slightly from the recommended values.
According to Zebeli et al. (2012), an optimal value of peNDF>8 mm is 17-18% (DM): this value does not excessively limit the ingestion of dry matter and at the same time maintains an optimal level of rumen pH, limiting the risk of SARA (Sub-Acute Ruminal Acidosis).

NIR analysis and Dry Matter results

NIR analyser allowed to obtain more reliable data about the analytical composition of sampled feeds used in the September 2019 diet. For each forage, it has been estimated dry matter and chemical composition (Tab. 6). The following values were subsequently inserted in CNCPS software to estimate diet and consider some improvements for a better assessment of current diet adequacy.

Tab. 6: Raw materials composition by NIR

	% DM[1]	CP[2] (% DM)	ASH (% DM)	NDF[3] (% DM)	ADF[4] (% DM)	STARCH (% DM)
Alfalfa Hay	90.09	9.75	10.23	62.89	45.56	
Wheat Hay	89.70	9.75	9.01	64.21	51.28	
Corn silage	32.07	6.80	2.94	41.23	23.90	31.05
Barley silage	28.35	10.80	7.32	53.86	32.76	18.85

[1]: dry matter
[2]: crude protein
[3]: neutral detergent fibre
[4]: acid detergent fibre

Tab.7: Obtained dry matter after oven drying

CROP	% DM
Corn silage coring	30.84
Barley silage	31.40
TMR	53.09
Corn silage	32.42
TMR heifers	37.70
Alfalfa hay	91.86
Wheat Hay	90.80

In Tab. 7 the values of dry matter determined by oven are reported. The data from NIR and dry matter analysis are very similar to the values of CNCPS database. This means that NIR analyser is a good and rapid instrument for collecting information about feeds.

NDF digestibility

Two different methods to calculate NDF digestion rate (kd, %/h) were compared: Daisy and Gas Endeavour. Data obtained from Daisy were fitted to the exponential equation as described by Orskov and McDonald (1979), subsequently the following results were obtained:

Tab. 8: Digestion hour rate of different forage

	kd Daisy	kd GP nlin
Soy silage	3.75	5.00
Corn silage	3.03	3.08

The kinetics of gas production registered continuously by the automatic system had a biphasic trend. Hence, to be able to compare the results (Daisy vs GP) the same model (Orskov and McDonald monophasic model) was applied to GP data.

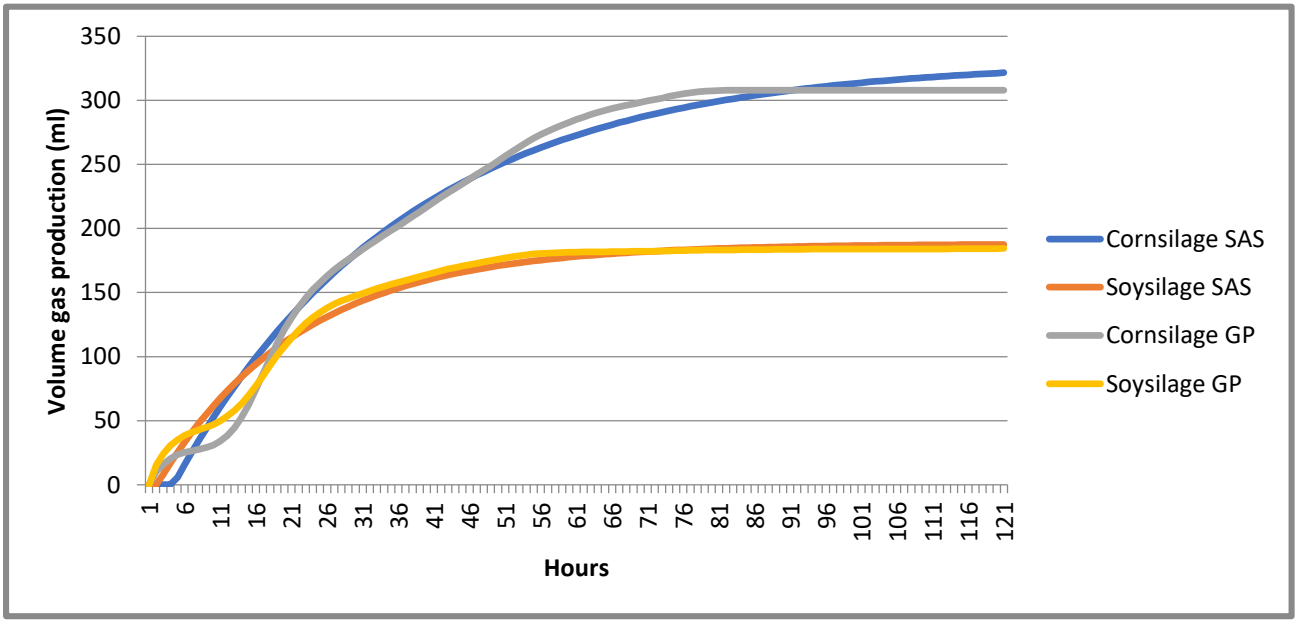

Fig. 4: Kinetics of gas production.

In Fig.4 it is possible to observe the curves relating to the gas production of corn silage and soy silage samples over 120 hours which are obtained through the use of Gas endeavour and those processed with SAS. For each silage, it is possible to observe the different trend of the two curves in the first 19 hours where the biphasic trend of the Gas Endeavour's data is evident. Despite this, the curves reach the asymptote at the same time: the digestibility calculated through the two valuations is very similar.

CNCPS results for the diet uses actually in Landriano

To evaluate the current diet CNCPS evaluation guidelines were used. In Tab. 9 and Tab. 10 the recipe output and the current diet are reported.

Tab. 9: CNCPS recipe output

Inputted DMI (kg/day)	23.278
Min-Max Expected DMI (kg/day)	21.125 - 22.589
Inputted/Min Expected DMI	110.2
DM (%)	54.7
Cost/head	EU 4.82
Cost/100 kg Milk	EU 17.54
Cost/100 kg ECM	EU 16.17
IOFC	EU 8.78
IOpurFC	EU 9.54
Milk:Feed	1.54
ECM:Feed	1.67

	ME	MP
Supply	61.9	2516
Maintenance	17.6	726
Pregnancy	0.0	0.0
Lactation	32.3	1375.0
Growth	0.0	0.0
Reserves	0.0	0
Balance	12.0	414.7
% Required	124	120
Allowable Milk kg/day	37.73	35.79
Inputted Milk kg/day	27.50	
Inputted ECM kg/day	29.83	

CP (%DM)	14.8
SP (%CP)	33
RDP (%DM)	9.63
Ether Extract (%DM)	3.1
LCFA (%DM)	2.5
Total Unsaturate (g/day)	423.9
NFC (%DM)	45.6
Starch (%DM)	29.4
Sugar (%DM)	7.7
Total Ferm. CHO (%CHO)	65.3
Forage (%DM)	46.6
aNDFom (%DM)	28.64
Forage NDF (%DM)	23.26
Forage NDF (%NDF)	81.24
Forage NDF (%BW)	0.77
Lignin (%NDF)	9.95
Lignin (%DM)	2.85
uNDF (%NDF)	0.00
uNDF (%DM)	0.00
ME (Mcal/kg)	2.66
NEm (Mcal/kg)	1.74
NEg (Mcal/kg)	1.13

Days To Gain 1 BCS	50
RumenNH3 (%Rqd)	123
peNDF (%DM)	21.1
Rumen_pH	6.32
MP From Bact (%)	58.8
MP From Bact (g)	1480.3
MUN (mg/dl)	10.0
Urea Cost	0.48 Mcal

	%Rqd	%MP
Met	108.6	2.21%
Lys	116.0	6.74%
His	134.3	2.61%

Lys:Met	3.04

Tab. 10: Landriano's current diet

Feed-ID	kg/day (DM)	kg/day (AF)
Mix Hay 13 CP 56 NDF 14 LNDF-CNCPS-4063	2.1587	2.3500
fieno frumento landriano-CNCPS-3084	0.9080	1.0000
uni essential-CNCPS-C101438	3.4721	3.8996
Soybean Meal 47.5 Solvent-CNCPS-2027	2.7000	3.0000
Corn Grain Flaked 24 lb-CNCPS-1044	1.2900	1.5000
Corn Grain Ground Fine-CNCPS-1039	3.1680	3.6000
orzo silo landriano-CNCPS-3002	3.1700	10.0000
silomais landriano-CNCPS-3015	4.6200	15.0000
Molasses Cane-CNCPS-1079	1.1680	1.6000
dairy speed 40 pellet landriano-CNCPS-C101510	0.3885	0.4000
Sodium Bicarbonate-CNCPS-5070	0.2348	0.2360
Total	23.2781	42.5856

DM intake (23.3 kg/d) is a bit over the predicted maximum value estimated (22.6 kg/d) which correspond approximately to 4%. This means that dairy cows, with this diet, are eating too much in comparison with how much milk they produce. Maybe this diet has a problem of digestibility which can compromise the optimal use of ingested nutrients. This can be also seen in the Metabolizable Energy and Protein balances: each of these two values are equal or over 120%. The peNDF (21.1 %DM) coincides with the minimum reference value from the guidelines and the rumen pH (6.32) is acceptable. NFC (45.6 %DM) and starch (29.4 %DM) are a bit high compared to CNCPS' guide and this can mean that the farmer used too much grain in the dairy cows' diet. The fact that aNDFom (28.64 %DM) is under the standard value of 33% combined with the excess of starch and sugars could mean that dairy cattle may be at risk of rumen acidosis. On the protein evaluation there is a good value of CP (14.8 %DM). Even if the Lys/Met (3.04) is an acceptable value the required % of MP of each amino acid are below the recommended values in the guidelines (2,6% for Met and 7,1% for Lys). There is a very good MP from bacteria (the minimum recommended is 45%). The rumen NH_3 (123 %Rqd) and the urea cost (0,48 Mcal) are in line with the values in CNCPS guideline, too.

Conclusions

The values of diets particle size evaluated with the Penn State method are in line with the references of Zebeli et al. (2012), with the exception of the TMR with soybean silage that presents the fraction >19 mm a little bit high: the greatest coarseness of the soy silage could be the cause of this effect.
Increasing the stay time of the TMR inside the mixer wagon could solve the problem related to the length of the soy silage: it depends mainly on the cutting efficiency of the knives and on the "stay time" of the TMR inside the mixer wagon.
The results obtained by calculating the peNDF comply with the guidelines of Zebeli et al. (2012) in the case of corn silage, while in soy silage they are slightly outside the recommended range. In particular, in the first period, this may mean a small reduction of the dry matter intake.
Through the evaluation of the difference in digestibility of the fibre between soy silage and corn silage, it was observed that the second one, which contains more NDF and less lignin than soy silage, is more digestible. The difference between the two curves is given by the fact that, while the soy silage reaches the asymptote (120 hours), the digestible fibre of the corn silage has not been completely degraded in the same time interval. In a dairy cattle ration, introducing self produced soy silage could be a good alternative to the purchase of other soy by-products (for example soybean meal) allowing a reduction of environmental impact and feeding costs. Soy's limit is that, compared to corn silage, has a less digestible fibre content. As a result of these considerations it is possible to affirm that it is not possible to entirely replace corn silage with soy

silage. In addition, it could be interesting to calculate kd from biphasic gas production curve to achieve a better precision of CNCPS parameters and to process calibration curves for NDFD in NIR analyzer. Diet actually used in Landriano's farm has an energetic surplus and a lack of fibre which could cause rumen acidosis problems. To solve this problem a possible solution can be replacing partly or totally corn meal or flacked corn with soybean hulls or other raw materials characterised by high quality fibre content. This can also lead to a reduction of feeding costs.
In conclusion, precision feeding is nowadays crucial for the improvement of animal diets and for a greater farm sustainability.

References

Mullenix K., Johnson J., 2014, Collecting Forage Samples for Laboratory Analysis, Alabama A&M University and Auburn University)

Zhang H., Redfearn D., Caddel J., 2017, Collecting forage samples for Analysis, Oklahoma Cooperative Extension service - Division of Agricultural Sciences and Natural Resources

Glunk E., Van Emon M., Malisani R., 2016, Collecting a Forage or Feed Sample for Analysi, Montana State University Extension

Hall H., Ishler A., 2001, Forage Quality Testing: Why, How, and Where; Penn State Extension,

Hall M. B., 2014, Feed analyses and their interpretation, Veterinary Clinics of North America: Food Animal Practice,Volume 30, Issue 3, Pages 487-505

Penn State Particle Separator, 2016, Penn State Extension, https://extension.psu.edu/penn-state-particle-separator, Visitato 2018

Heinrichs J. and Kononoff P, 2002, Evaluating particle size of forages and TMRs using the New Penn State Forage Particle Separator, Penn state: College of Agricultural Sciences, Cooperative Extension, http://www.dairyweb.ca/Resources/USWebDocs/PSPS.pdf

Brouillette J. (2011), Forage particle size: What's ideal?, Progressive Dairyman, https://www.progressivedairy.com/topics/feed-nutrition/forage-particle-size-whats-ideal

Kononoff P.J., Heinrichs A.J. (2011), New Developments in TMR Particle Size Measurement, Extension.org, https://articles.extension.org/pages/26270/new-developments-in-tmr-particle-size-measurement

Haan M. M. (2015), Can On-Farm NIR Analysis Improve Feed Management?, Penn State Extension, https://extension.psu.edu/can-on-farm-nir-analysis-improve-feed-management

Percy-Smith C. (2016), On farm silage testing with NIR, NIR Performance, http://nirperformance.com/2016/08/15/farm-silage-testing-nir/

Guidelines for Interpreting CNCPS 6.5 Outputs for Lactating Dairy Cows L. E. Chase, T.R. Overton, and M. E. Van Amburgh (Dept. of Animal Science - Cornell University)

Pirondini M. (2014), La digeribilità della fibra neutro detersa dei foraggi, Ruminantia,

https://www.ruminantia.it/la-digeribilita-dellafibra-neutro-detersa-dei-foraggi/

Chase L. E. (2016), Guidelines for Interpreting CNCPS 6.5 Outputs for Lactating Dairy Cows

Orskov, E.R. and McDonald, I. (1979) The estimation of protein degradability in the rumen from incubation measurements weighted according to rate of passage. J. of Agricultural Science Cambridge, 92,499-503.

Qendrim Zebeli, Dominik Mansmann, Burim N. Ametaj, Herbert Steingaß & Winfried Drochner (2010) A model to optimise the requirements of lactating dairy cows for physically effective neutral detergent fibre, Archives of Animal Nutrition, 64:4, 265-278.

Q. Zebeli,*1 J. R. Aschenbach,† M. Tafaj,‡ J. Boguhn, ‡ B. N. Ametaj,§ and W. Drochner ‡, © American Dairy Science Association®, 2012. Invited review: Role of physically effective fibre and estimation of dietary fibre adequacy in high-producing dairy cattle, J. Dairy Sci. 95 :1041–1056.

Acknowledgments

The authors would like to thank for the support: L. Rapetti, G.M. Crovetto, G. Galassi, S. Colombini, I. Toschi, P. Roveda, M. Chiaravalli, D. Reginelli, M. Battelli

PROAGRA

Influence of nutritional solutions with different ammonium-nitrate ratio on yield and nutritional quality of *Eruca sativa* (Mill)

Bosio P., Galli G., Gamba P., Pasini L., Perucco E., Rinaldi L., Spreafico N., Zen G.

Abstract

Eruca sativa (Mill), commonly known as rocket salad, is a plant of growing interest for consumers and producers because of its numerous beneficial effects on human health and cultivation characteristics. In this study, different N-ratios (NH_4^+/NO_3^-) in nutrient solutions were tested during a hydroponically cultivation cycle in order to verify changes in the yield, chemical composition and contents of secondary metabolites in rocket salad. Significant differences were founded analyzing the content of chlorophyll, NBI index (both increasing with major ammonium concentration); several ions and secondary metabolites also exhibited a decreasing trend with increasing ammonium concentration. The other analysis did not reveal significant differences between treatments.

Keywords: nitrogen, eruca sativa, pal, ammonium, secondary metabolites, food quality

Introduction

In the last years, consumers developed an "health consciousness" that leads them to choose those foods that, in addition to a good appearance, have beneficial effects on health. A food that combines this request with several advantages for the production is rocket salad (*Eruca sativa* Mill.). *Eruca sativa* is an edible annual plant, commonly known as rocket salad or arugula. It's a green leafy vegetable, member of the *Brassicaeae* family that originates from Mediterranean countries. Hydroponic cultivation is a good cultivation technique that reduces the production cycle and also improves the shelf life (*i.e.* control of nitrate content) (Esiyok et al., 2010).

Like the entire fresh-cut vegetables, rocket salad is the protagonist of considerable growth on the market; it's appreciated for its pungent aroma and flavour, and for its proven beneficial properties on human health (Bell et al., 2015). Most of the benefits of rocket is due to the content of antioxidants and glucosinolate compounds (GLS). In particular, GLS are secondary metabolites rich in nitrogen and sulfur that give to the leaves of the plant the pungent taste and the smell typical of the product (Cavaiuolo and Ferrante, 2014).

One of the ways by which we could fight the underconsumption of nutraceutical foods without increasing the quantities consumed is to increase the content of active molecules in the plant; this feature depends mainly on the genetic characteristics of the plant, the conditions of cultivation, and nitrogen and phosphate nutrition (Chun et al. 2015; Bell et al 2015). It's also known that the amount of antioxidant compounds and glucosinolates is increased by stress conditions (*i.e.* water and nutritional shortage, high density, etc.) (Bell et al, 2015; Kim et al 2006). A less known factor of influence concerns nitrogen nutrition and, in particular, the ammonium-nitrate ratio (Chun et al, 2015; Kim et al, 2006). Ammonium (NH^+_4) and nitrate (NO^-_3) are the two major sources of inorganic nitrogen taken up by roots of higher plants. The effect of these two forms on plant growth is dependent not only on plant species, but also on their ratios and concentrations (Marschner, 1997). An important aspect of *Eruca sativa* is that it accumulates large amounts of nitrogen, and this fact constitutes a risk for the consumer health. Studies of rocket salad obtained in Italian markets have shown it to be the vegetable with the highest NO^-_3 content (Santamaria et al., 1999). The maximum daily diet intake of nitrates (0.06 mg / kg body

weight) and nitrites (3.65 mg / kg body weight), while the maximum leaf nitrate contents for the commercialization of rocket is reported in the European regulation n. 1258/2011. The NO^-_3 content in plants can be reduced by decreasing it in the nutrient solution or replacing it with NH^+_4 a few days before harvest.

Aim

The aim of this work was to find qualitative and quantitative differences in *Eruca sativa* related to different nitrogen fertilization. In particular, the effect of different ratio of ammonium and nitrate in the nutrient solution was assessed. The work aims to understanding the influence of the two mineral nutrients and their biochemical interactions in the metabolism. The timing of the activities is summarized in the following table:

Tab.1: Program

Greenhouse cultivation	
13-June	*Preparation of nutritional solutions*
14-June	*Sowing*
18-June	*Addition of the solution in the tank*
02-July	*Non-destructive analysis*
03-July	*Non-destructive analysis + harvesting*
Laboratory analysis	
11-July	*Extraction of phenols, chlorophyll and carotenoids*
12-July	*Spectrophotometer readings on extractions*
15-July	*Protein fraction extraction and sample preparation*
16-July	*Determination of protein contents*
17-July	*Western blotting*
18-July	*Protein dosage and PAL activity*

Materials and Methods

Experimental design

The work started with the preparation of a hydroponic cultivation system consisting of 12 tanks of 33 liters. In each tank there was a polystyrene alveolar container floating on the nutrient solution. Every tank was filled with agri-perlite where were placed rocket seeds. Three treatments were set, each one with four replies, for a total of 12 tanks (Fig.1).

The nutrient solution was added after germination under black film, to avoid undesirable algal proliferation. The three nutrient solutions are shown in the table 2 and represent the three treatments: 0% NH_4^+ - 100% NO_3^-; 25% NH_4^+ - 75% NO_3^-; 50% NH_4^+- 50% NO_3^-. The total nitrogen was maintained constant, corresponding to 168.84 mg L^{-1} (12 mM). Previous work reported that *E. sativa* growth is strongly inhibited by percentage of ammonium above 50%, as suggested by the comparison of phytotoxicity phenomena, such as chlorosis and necrosis (Sun-Ju et al., 2010).

At the time of sampling, leaves were separately collected, frozen in liquid N_2 and stored at −80°C.

Tab. 2: Salts uses for the nutrient solutions preparations

0% - 0 mM NH_4			25% - 3mM NH_4			50% - 6mM NH_4		
	mg/L	g for 40 L/tank		mg/L	g for 40L/tank		mg/L	g for 40L/tank
$CaNO_3$	842	33,68	$CaNO_3$	421	16,84	$CaCl_2$+2HO	588	23,52
KNO_3	385	15,4	NH_4NO_3	247	9,88	NH_4NO_3	494	19,76
$KHPO_4$	269	10,76	$CaCl_2 + 2H_20$	294	11,76	$KHPO_4$	269	10,76
KSO_4	335	13,4	KNO_3	192	7,68	KSO_4	371	14,84
$MgSO_4$	200	8	K_2HPO_4	269	10,76	$MgSO_4$	200	8
			K_2SO_4	193	7,72			
			$MgSO_4$	200	8			
microelement (added in every treatments): Fe-EDTA al 6% Fe 0,02 g/L (0,8 g/tank) and Oligon Green 0,02 g/L (0,8 g/tank)								

Fig.1: Setting up of the floating system.

Fig.2: Non-destructive analyses.

Non-destructive analyses

The first *in-vivo* measurement took place 14 days after sowing. The following parameter were detected: NBI (nitrogen balance index), chlorophyll and flavonoid contents with DUALEX (chlorophyllometer); chlorophyll content with SPAD-hansatech-CL01 (chlorophyllometer); performance index (PI) measurement and Fv/Fm (maximum quantum efficiency of photosystem 2) with Handy PEA (fluorimeter) (Fig.2).

After 16 days from sowing, the measurements with SPAD and handy PEA were repeated. In both analysis sessions, 5 measurements were made with SPAD, 5 with DUALEX and 3 with Handy PEA for each tank. At the end of the cultivation phase, sample disks were cut out from leaves and were used for the biochemical analyses (see below).

Content of carotenoids, chlorophylls, polyphenols and nitrate

The analysis of the content of chlorophylls, carotenoids, and polyphenols involved the preparation of the disk samples with pure methanol (for polyphenols was also added hydrochloric acid, see below). Then, after 12 hours in a dark cold room, the samples were analyzed with a spectrophotometer measuring the specific absorbances for the measurements of carotenoid (470 nm), chlorophyll-b (652.4 nm) and chlorophyll-a (665.2 nm). The data were interpreted with the Lichtenthaler formula (1987) to know the value in mg/g. For the extraction of phenolic compounds and anthocyanins, around 1 g of leaves were homogenized in 3 mL of acidified methanol (1% HCl V/V) and extracted overnight in the dark. The phenolic index was calculated as the absorbance at 320 nm of the extracts, normalized to fresh weight (Ke and Saltveit, 1989). Anthocyanin content was determined, measuring in the same extract used to evaluate phenol index, the absorbance at 535 nm.

Nitrate content was measured by a procedure in which were used 5% p/v salicyl-sulfuric acid and 1.5 M NaOH that was added to stop the reaction. Nitrate content were measured reading the absorbance of the samples at 410 nm.

Analysis of macro- and micro-elements: ICP-MS

The acidic digestion of rocket leaves was performed by a heat-controlled microwave system after the addition of HNO_3 to samples previously dried (48h at 80°C). The samples were then analyzed by ICP-MS, Inductively Coupled Plasma-Mass Spectrometry (Bruker, Aurora M90): a very sensitive technique that allows the determination of mineral elements based on their mass/charge ratio (m/z) up to the order of ppb (10-15 g Kg^{-1}). The instrument uses a plasma torch (ICP: with Argon flow) to induce ionization, and a mass spectrometer to detect the positive ions produced. The analyses permitted to quantify the following elements: K; Ca; P; Mg; Na; Mn; Fe; Zn; Cu; Ni; Mo; Co; Se; As; Cd; Pb; Cr.

HPLC-MS/MS

For the measurement of the content of glucosinolate compounds and polyphenols, the samples were analyzed with a mass spectrometer (HPLC, High Pressure Liquid Chromatography; ESI, Electro-Spray Ionization; Tandem mass) (Fig. 3). The extraction involved the following steps: grinding of the leaves in liquid nitrogen, collection of 100g of material and addition of the extraction solvent (methanol 70% and 0,1% formic acid) in a ratio of 1:10 g/v), incubation at 4 °C and shaking for 30 min in the dark, centrifugation (10,000 *g* for 10 min), collection of the supernatant and filtration (nylon filter 0.45 µm), dilution sample 1:10 in formic acid 0.1% and analysis with the mass spectrometer. After dilution, the samples were analyzed by an Agilent Technologies 1200 series capillary pump coupled with a dual ESI source on a 6520 Q-TOF mass spectrometer. LC runs were done on an XDB-C18 column (2.1 × 50 mm, 1.8 µm, Agilent Technologies) in acidic condition [FA 0.1% (v/v)] applying a gradient from 5 to 70% of acetonitrile

with a flow rate of 200 µL min−1. The ESI source was set at 350 °C at -3000 V. Data acquisition was performed in negative mode. Molecule identification was verified according its fragmentation profile in MS/MS mode.

Fig.3: HPCL-MS/MS.

Fig.4: Electrophoretic separation.

Gel electrophoresis and western blotting

Gel electrophoresis followed by Western blot analysis were performed to detect and quantify Phenylalanine ammonia lyase (PAL) enzyme. The determination of protein content in the samples, previously obtained by SDS buffer extraction procedure, was performed using the 2-D Quant Kit (GE Heathcare) kit. The samples were then prepared for the one-dimensional electrophoresis (1D-SDS-PAGE). Electrophoresis was performed on 12% polyacrylamide gel according to Laemmli (1970) method. After the preparation of gel and samples, the equipment for electrophoretic run was prepared (Fig. 4).

At the end of the run, the gel was divided into two portions: one containing the coloured standards, the other for blotting. Proteins were then electrophoretically transferred to a polyvinylidene difluoride (PVDF, Sigma-P0682) filter using a semidry blotting system (NovaBlot, Pharmacia, Sweden). At the end of WB,a part of the PVDF membrane corresponding to control sample was was coloured with Comassie Blue to verify the efficiency of blot procedure.

Filter was incubated for 1 h with TBS-T buffer [50 mM Tris–HCl (pH 7.6), 200 mM NaCl, and 0.1 % (v/v) Tween 20] supplemented with 3% (w/v) of albumine. The TBS-T buffer was used as incubation medium throughout the procedure. The PVDF membrane was then placed in a solution with antibodies against the enzyme PAL 1:3000 (anti PAL parsley - Anti Rabbit). The membrane was then transferred in a solution containing anti-Rabbit antibodies conjugated with alkaline phosphatase. After incubation, Sigma Fast BCIP/NBT dye solution was added. At the end the protein bands corresponding to the enzyme PAL were visualized.

The profiles of both gels and PVDF membrane were graphically examined using the *ImageJ* software. The intensity of band of PAL was normalized against the intensity of RuBisCO band.

Determination of PAL enzyme activity

PAL enzyme was extracted, and its activity was determined by spectrophotometric assay. Samples were ground at 4 °C in 5 volumes of 100 mM Tris-HCl buffer (pH 8.8), containing 2 mM Na-EDTA,

5 mM Ascorbic acid, 1 mM PMSF and 5 mM MSH. Supernatant was then clarified by centrifugation at 12.000 g for 20 min. Protein content was measured by Bradford method, according to manufacturer's instructions (Biorad protein assay kit), using BSA as the standard (Fig. 5 and 6).

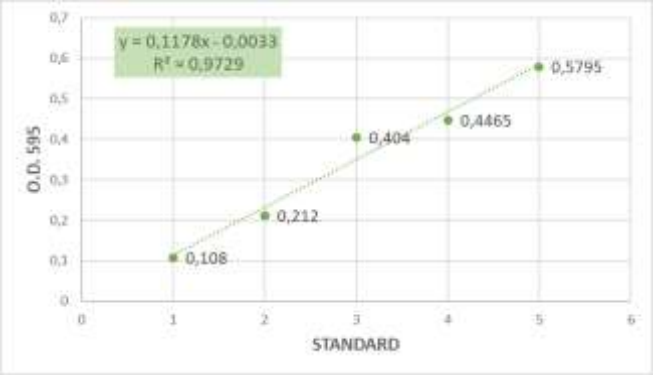

Fig.5: Protein dosage calibration.

Fig.6: Spectrophotometer.

Activity was evaluated at pH 8.8 measuring the formation of cinnamic acid after the addition of phenylalanine to reach a final concentration of 2.8 mM. The assay was performed at 38°C. Reaction was stopped after 0 or 60 min of incubation adding 6N HCl and then it was measured the absorbance at 290 nm. The specific activity was calculated trough the following equation:

Specific activity (nmol cinnamic acid h^{-1} mg $prot._{-1}$) = [(ΔAss_0-60') x ε x l]/ mg protein

Results and Discussion

Biomass production

At the end of the cultivation the total biomass produced by each biological replicate was evaluated (Tab. 3). The results did not show any significant differences among the three experimental conditions.

Tab.3: Total biomass measure at the sampling time. Values are the mean ± SE of four independent biological samples (n = 4). Samples indicated with the same letters do not differ significantly according to Tukey test (p < 0.05).

Treatment	Biomass (kg/tank)	±SE
0%	0.51125a	0.01007782
25%	0.47250a	0.03682730
50%	0.47875a	0.05956002

Non-destructive analyses

The results of non-destructive analyses are presented in Figure 7. The data revealed significant differences in the values of chlorophyll and NBI. In particular, for the NBI values there was a significant difference among 0% NH_4^+ condition with 25% and 50% NH_4^+ ones. Differently, chlorophyll values showed only significant differences between control condition (0% NH_4^+) and higher concentration (50% NH_4^+). There are no significant differences between treatments for flavonoid values (Fig.7).

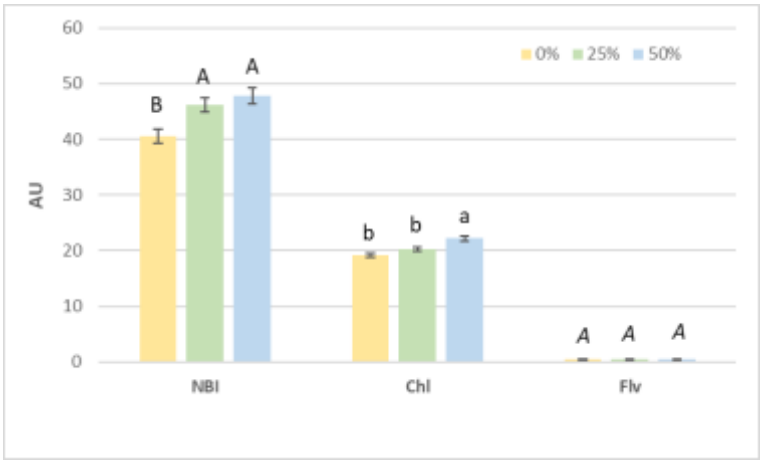

Fig.7: Evaluation of nitrogen balance index (NBI), chlorophyll (Chl) and flavonoid (Flv) contents evaluated by Dualex. Values are the mean ± SE of four independent biological samples analyzed in quintuple (n = 20). Samples indicated with the same letters do not differ significantly according to Tukey test (p < 0.05).

The results of non-destructive analyses conducted by chlorophyllmeter (SPAD) at two different time are reported in figure 8. The comparison of the results obtained at the two sampling times did not reveal any differences. In both times considered, the presence of ammonium induced a significant increase in chlorophyll content.

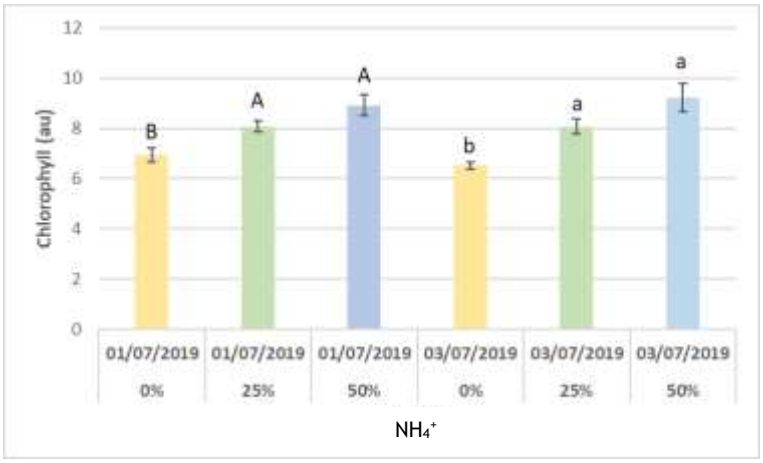

Fig.8: Evaluation of chlorophyll (Chl) contents evaluated by Chlorophyllmeter. Values are the mean ± SE of four independent biological samples analyzed in quintuple (n = 20). Samples indicated with the same letters do not differ significantly according to Tukey test (p < 0.05).

In all experimental conditions, the maximum quantum efficiency of photosystem 2 (PV/Fm), evaluated by Handy PEA instrument, resulted to be higher than 0.8, indicating a good efficiency of this photosystem (Schreiber et al., 1995) (Fig. 9). No differences were observed between the two dates.

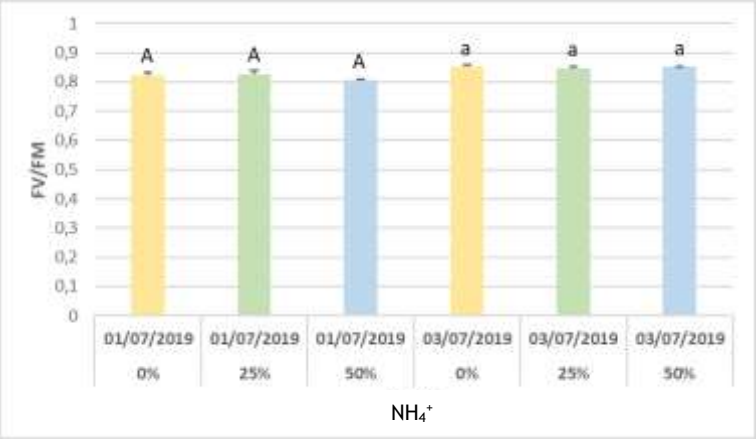

Fig.9: Evaluation of maximum quantum efficiency of photosystem 2 (FV/Fm). Values are the mean ± SE of four independent biological samples analyzed in triplicate (n = 12). Samples indicated with the same letters do not differ significantly according to Tukey test (p < 0.05).

Destructive analyses

The destructive analyses did not reveal significant differences when comparing treatment values for chlorophyll, carotenoid, anthocyanin and nitrate levels as well as there were not differences in phenol index (Tab. 4).

Tab.4: Evaluation of chlorophyll, carotenoid, anthocyanin and nitrate levels and phenol index. Values are the mean ± SE of four independent biological samples (n = 4). Samples indicated with the same letters do not differ significantly according to Tukey test (p < 0.05).

Treatment	NO3 (mg/kg)	±ES	Total Carotenoids (µg/mg)	±ES	Total Chlorophyll (mg/g)	±ES	phenolic index (ABS320 nm/g f.w.)	±ES
0%	1409.946a	150.671	0.203a	0.004	1.255a	0.028	25.560a	1.405
25%	1171.825a	89.288	0.234a	0.009	1.454a	0.043	25.434a	1.102
50%	1569.926a	174.507	0.235a	0.023	1.524a	0.159	24.747a	1.497

The ionomic analyses highlighted several significant differences (Tab. 5). At the higher NH_4^+ a decrease in the levels of K, Ca, Mg, Mn took place. On the contrary, Se content resulted to increase in same experimental condition.

The evaluation of PAL activities did not show significant differences, even if, in plants exposed to the higher NH_4^+ was observed an increasing activity (Fig. 10).

To obtain further information, a Western blot analysis to study PAL enzymes was conducted (Fig. 11). An evident difference between two replicates was founded. For this reason, area of the band referred to PAL was normalized against the large subunit of RuBisCO. This analysis revealed an opposite trend, so any consideration on quantitative changes could not be done. Further experiments must be performed to clarify this aspect.

Tab.5: Evaluation of ion contents. Values are the mean ± SE of three independent biological samples (n = 3). Samples indicated with the same letters do not differ significantly according to Tukey test (p < 0.05).

mg DW^{-1}	% NH4					
	0%	**±ES**	**25%**	**±ES**	**50%**	**±ES**
K	135.3151 a	20.1205	108.2642 a	7.0425	88.5391 b	12.6371
Ca	28.2667 a	3.7615	19.4674 ab	0.8361	12.0666 b	2.2121
P	11.2910 a	1.1092	11.0615 a	0.8425	9.0222 a	1.3446
Mg	6.1142 a	0.9408	3.8496 ab	0.2681	2.5537 b	0.4515
Na	1.2346 a	0.2984	0.8396 a	0.0899	0.6165 a	0.1321
Mn	0.2134 a	0.0331	0.1376 ab	0.0114	0.0931 b	0.0165
Fe	0.1294 a	0.1290	0.1552 a	0.8980	0.1220 a	0.2301
Zn	0.0747 a	0.0043	0.0642 a	0.0055	0.0577 a	0.0111
Cu	0.0144 a	0.0014	0.0108 a	0.0021	0.0129 a	0.0015
Ni	0.0062 a	0.0018	0.0038 a	0.0007	0.0029 a	0.0009
Mo	0.0057 a	0.0004	0.0061 a	0.0001	0.0063 a	0.0010
Co	0.0005 a	0.0003	0.0002 a	0.0001	0.0001 a	0.0001
Se	0.0003 b	0.0001	0.0010 ab	0.0003	0.0012 a	0.0002
As	0.0007 a	0.0003	0.0005 a	0.0000	0.0004 a	0.0001
Cd	0.0001 a	0.0000	0.0001 a	0.0000	0.0000 a	0.0000
Pb	0.0003 a	0.0001	0.0002 a	0.0001	0.0001 a	0.0000
Cr	0.0012 a	0.0002	0.0008 a	0.0001	0.0010 a	0.0003

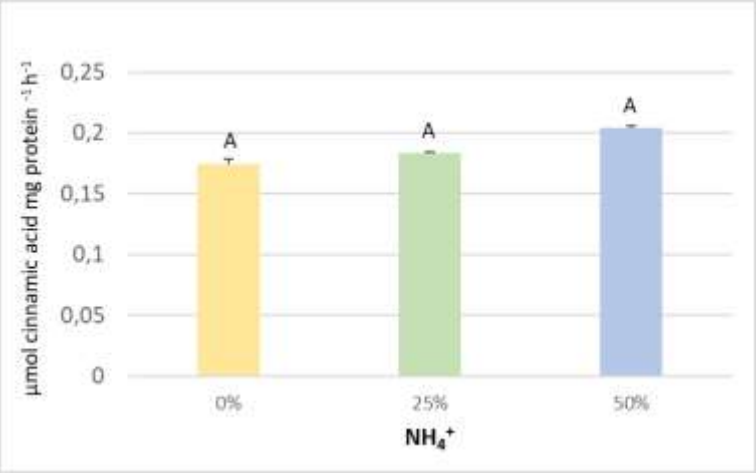

Fig.10: Evaluation of PAL activity. Values are the mean ± SE of two independent biological replicates (n = 2). Samples indicated with the same letters do not differ significantly according to Tukey test (p < 0.05).

The results of the analysis conducted with HPLC-ESI-MS are show in table 6. The analysis permitted to detect the most common secondary metabolites that are known to be accumulated in this species. In details, two glucosinolate compounds [*4-mercaptobutylGLS (Glucosativin) and 4-methylthiobutyl GLS (Glucoerucin)*] and three different flavonoids [Quercetin-3,3,4-Triglcucoside,

Kaempferol-3,4'-diglucoside and Quercetin-3,4-diglucoside-3-(6-sinapoyl-glucoside)] were identified and quantified. The presence of ammonium did not affect glucosinolate compounds. Differently, the Quercetin-3,3,4-Triglcucoside and Quercetin-3,4-diglucoside-3-(6-sinapoyl-glucoside) were not detectable in leaves of plants grown in the presence of NH_4^+; this last compound resulted significantly different from statistical point of view.

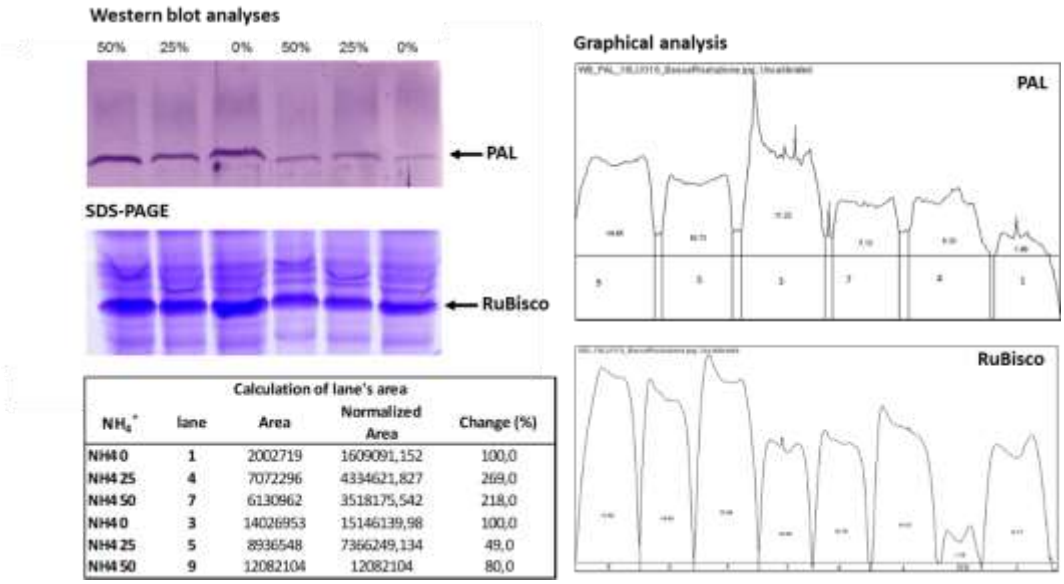

Calculation of lane's area

NH_4^+	lane	Area	Normalized Area	Change (%)
NH4 0	1	2002719	1609091,152	100,0
NH4 25	4	7072296	4334621,827	269,0
NH4 50	7	6130962	3518175,542	218,0
NH4 0	3	14026953	15146139,98	100,0
NH4 25	5	8936548	7366249,134	49,0
NH4 50	9	12082104	12082104	80,0

Fig.11: Localization of the PAL in the 1D profile of rocket salad leaves by Western Blotting. Proteins were separated by 10% SDS-PAGE and analyzed by WB against PAL antibody. The analyses were conducted on two independent biological samples. The Area of the band referred to PAL was normalized against the RuBisCO band.

Tab.6: Evaluation of amounts of glucosinolate compounds and polyphenols by HPLC-ESI-MS/MS. The values are expressed as % abundance of each compound among the different conditions. Values are the mean ± SE of three independent biological samples (n = 3). Samples indicated with the same letters do not differ significantly according to Tukey test ($p < 0.05$). [M-H]$^-$: molecular weight / charge (m/z) of the molecule, RT: retention time in HPLC (min).

	Reference ion	Rentention time	Treatment (% NH_4^+)					
			0%		25%		50%	
	[M-H]^-	RT	$\bar{X}$	±ES	$\bar{X}$	±ES	$\bar{X}$	±ES
4-mercaptobutylGLS (Glucosativin)	406	1.94 ± 0.04	109.49a	6.74	94.46a	5.31	96.05a	19.84
4-methylthiobutyl GLS (Glucoerucin)	420	3.37 ± 0.08	142.27a	46.4	91.97a	6.59	65.75a	
Quercetin-3,3,4-Triglcucoside	787	1.37 ± 0.02	100.00a	63.37	N.R. b		N.R. b	2.11
Kaempferol-3,4'-diglucoside	609	8.09 ± 0.03	103.93a	17.34	99.12a	8.01	96.94a	21.23
Quercetin-3,4-diglucoside-3-(6-sinapoyl-glucoside)	993	2.79 ± 0.01	100.00a	18.81	N.R. b		N.R. b	

The analysis of the rocket plants grown in the presence of only nitrate or of increasing ammonium levels (25 and 50%, respectively) showed several differences, suggesting that the nitrogen form affected some metabolic activities. However, the addition of ammonium until 50 % of total nitrogen did not affect the biomass production, suggesting that a general toxic effect did not occur at this concentration (Tab. 3).

Non-destructive analysis, highlighted differences in the NBI index and chlorophyll content. In plant grown in ammonium-free medium, NBI was significantly lower, even if this effect was not

confirmed by laboratory analyses (Tab.4). In addition, the analyses established that the nitrate content was in compliance with legal requirements.

Significant differences in chlorophyll content were found in plant grown in 50% ammonium. Similar results were observed after 17 and 19 days from sowing, even if the fluorescence index (Fv/Fm) did not show differences (Fig. 9). In this view, also the destructive analyses did not show significant differences in chlorophyll and carotenoids values (Tab.4). Taken together, the results highlighted that the presence of ammonium until 50% of total nitrogen (12 mM) not reduce the growth of rocket salad even if it affected some metabolic activities.

Ionomic analysis highlighted that ammonium negatively affected the level of some ions, such as K, Ca and Mg (Tab. 5). This effect was in accordance with previous works (Barlas et al., 2011; Villatoro-Pulido et al., 2012; Tripodi et al., 2017). This effect was attributed to the fact that NH_4^+ share the same channel with K^+, so reducing the capacity to uptake this last cation (Haynes and Goh, 1978; Marschner, 1997; Shun-Ju et al., 2010). The significant increase in Se content induced by the presence of ammonium could open an interesting possibility to improve organoleptic properties of this edible plant.

PAL is a key enzyme in the production of phenolics, producing trans-cinnamic acid that is the precursor of a large part of these secondary compounds. At the same time, there is a direct relation with nitrogen metabolism, because the reaction generates ammonium. The evaluation of the PAL activity did not show changes among the different experimental conditions (Fig. 10) and the Western blot analysis produced contradictory results (Fig. 11). Further work will be needed to verify this point.

The HPLC-ESI-MS/MS analysis confirmed the presence of secondary metabolites typical of *Eruca sativa* (Pasini et al. 2012). The analyses showed that Quercetin-3,3,4-triglucoside and Quercetin-3,4-diglucoside-3-(6-sinapoyl-glucoside) disappeared under NH_4^+ exposure, whilst other metabolites were not influenced by the presence of this cation. Overall the results suggest that in this experimental condition NH_4^+ could affect only specific point of the phenolic pathway and do not have a generalized effect on the synthesis of this class of compounds.

Conclusions

On the basis of the data collected by the different analyses, no significant differences from compositive point of view were found in shoot of plants exposed to increasing concentration of ammonium, as regards the composition in pigments, ions and in the activity of the PAL enzyme.

While, with regard to secondary metabolites, the expected toxic effect due to high ammonium ratio (and generally responsible for a decrease in the content of glucosinolate compounds) was not observable by our analysis; except for the content of a polyphenol that was not detected in the ammonium's treatment. According to this scenario, was not founded negative effects on the plant grow. These results, that are different to those reported by other studies (Kim et al. 2006), could be due to grown condition adopted, but also to be linked to peculiar genetic characteristics.

In this view, this work open to the possibility of the use of ammonium as an alternative to nitrate in nitrogen fertilization, considering also the prices offered on the market.

References

Barlas, N. T., Irget, M. E., Tepecik, M. 2011. Mineral content of the rocket plant (Eruca sativa). African Journal of Biotechnology, 10(64), 14080-14082. http://dx.doi.org/10.5897/AJB11.2171

Esiyok, D., Bozokalfa, M. K., Yagmur, B., Kaygisiz Asciogul, T. 2010. Nutrional value and economic plant properties of E. sativa accessions. Cruciferae Newsletter, 29, 42-45.

Haynes, RJ and Go, KM. 1978. Ammonium and nitrate nutrition of plants. BiolRev, 53: 465–510.

Jin-Hyuk Chun, Silbia Kim, Mariadhas Valan Arasu, Naif Abdullah Al-Dhabi, Doug Young Chung, Sun-Ju Kim. Combined effect of Nitrogen, Phosphorus and Potassium fertilizers on the contents of glucosinolates in rocket salad (Eruca sativa Mill.). Saudi Journal of Biological Sciences (2017) 24, 436–443

Ke, D.; Saltveit, M.E. Wound-induced ethylene production phenolic metabolism and susceptibility to russet spotting in Iceberg lettuce. Physiol. Plant. 1989, 76, 412–418.

Luke Bell, Maria Jose Oruna-Concha, Carol Wagstaff. Identification and quantification of glucosinolate and flavonol compounds in rocket salad (Eruca sativa, Eruca vesicaria and Diplotaxis tenuifolia) by LC–MS: Highlighting the potential for improving nutritional value of rocket crops. Food Chemistry 172 (2015) 852–861

Marina Cavaiuolo and Antonio Ferrante. Nitrates and Glucosinolates as Strong Determinants of the Nutritional Quality in Rocket Leafy Salads. Nutrients 2014, 6, 1519-1538; doi: 10.3390/nu6041519

Marschner, H. 1997. Functions of Mineral Nutrients, Macronutrients. In Mineral Nutrition of Higher Plants, 231–255. San Diego: Academic Press.

Santamaria, P, Elia, A, Serio, F and Todaro, E. 1999. A survey of nitrate and oxalate content in fresh vegetables. Journal Science Food Agricolture, 79: 1882–1888.

Schreiber, U., Bilger, W., Neubauer, C 1995. Cholorophyll Fluorescence as a nonintrusive indicator for rapid assessment of in vivo photosynthesis. In: Ecophysiology of Photosyntesis. Schulze, E.D., Caldwell, M.M. (eds). Berlin, Heidelberg, New York: Springer-Verlag

Sun-Ju Kim, Kawaharada Chiami & Gensho Ishii (2006) Effect of ammonium: nitrate nutrient ratio on nitrate and glucosinolate contents of hydroponically-grown rocket salad (Erucasativa Mill.), Soil Science and Plant Nutrition, 52:3, 387-393, DOI: 10.1111/j.1747-0765.2006.00048.

Sun-Ju, K. ,Kawaharada, C. ,Gensho I., 2010. Effect of ammonium: nitrate nutrient ratio on nitrate and glucosinolate contents of hydroponically-grown rocket salad (Eruca sativa Mill.). Soil Science and Plant Nutrition 52(3), 2006, 387-393.

Tommaso R. I. Cataldi, Alessandra Rubino, Filomena Lelario and Sabino A. Bufo. Naturally occurring glucosinolates in plant extracts of rocket salad (Eruca sativa L.) identified by liquid chromatography coupled with negative ion electrospray ionization and quadrupole ion-tra mass spectrometry. Rapid Commun. Mass Spectrom. 2007; 21: 2374–2388

Tripodi, P., Francese, G., Mennella, G. 2017. Rocket salad: crop description, bioactive compounds and breeding perspectives. Advances in Horticultural Science, 31(2), 107-113. http://dx.doi.org/10.13128/ahs-21087.

Villatoro-Pulido, M., Rojas, R. M., Munoz-Serrano, A., Cardenosa, V., Lopez, M. A. A., Font, R., Del Rio-Celestinod, M. 2012. Characterization and prediction by near-infrared reflectance of mineral composition of rocket (Eruca vesicaria subsp. sativa and Eruca vesicaria subsp. vesicaria). Journal of the Science of Food and Agriculture, 92(7), 1331–1340. http://dx.doi.org/10.1002/jsfa.4694

Acknowledgments

The authors would like to thank for the support: B. Prinsi, G. Cocetta, G. Lucchini, A. Ferrante, L. Espen, R. Bulgari

RITMO

Reducing rockfall and shallow landslide hazards by forest: the study case of Andrista (Cevo – Valle Camonica, Northern Italy)

Acrami P., Arrigoni F., Castelli L., Cavenaghi S., Crippa A., Gaspari T., Macchi F., Orifici C., Porseo C.

Abstract

Mountain areas are typically threatened by gravitational natural hazards. It is well known from ages that forests have a protection function against natural hazards as they can mitigate and/or control several soil degradation processes, as soil erosion, shallow landsliding, rockfall, water runoff, etc. Such protection is always exerted in general terms, but a specific forest can also mitigate or avoid the effects of a natural disaster event on a specific human asset, and in such case, it is defined as a direct protection forest.

Forests can mitigate natural hazards in different ways. In the case of rockfall and shallow landsliding, the protection effect of the forest is due to the barrier made by standing and lying trees, slowing down, deviating and stopping falling rocks, and to the soil stabilizing effects and water content reduction by root systems.

In such a framework, the aims of this work are, firstly, to evaluate the direct protection capacity of a chestnut forest located in Cevo, loc. Andrista (Northern Italy, BS) against rockfall and shallow landslide hazards that threaten a nearby passing road; secondly, to propose a silvicultural management that should maintain and improve the protection function of the forest.

Hazard landslide maps have been produced using the PRIMULA model to achieve the first objective, and the results have been compared with Regione Lombardia's hazard landslide maps.

RockForNet, a software that estimates the level of protection against rockfall, was used to achieve the second objective. The model produces an ideal and a minimum requirement in terms of diameters class distribution, given specific forest conditions, and the level of protection is given as the percentage of stones stopped by trees.

This approach could be used to improve the silvicultural management of the Italian forests that have a protection function, which conditions can be very poor due to many different factors, such as abandonment of the rural areas.

Keywords: Direct protection forests, Rockfall, Shallow landslides, Forest management

Introduction

Forests have a general protection function against natural hazards as they can mitigate several soil-degradation processes and reduce the effects of potentially dangerous phenomena. When a specific forest can mitigate or avoid the effects of a given natural disaster event on a specific human asset, such as a settlement, infrastructures or any human activities, it is defined as a direct protection forest (*Berger and Rey, 2004; Dorren et al., 2004*). Direct protection can be achieved only by forests with defined characteristics (composition, density, texture, etc.) suited for a specific natural hazard (*Regione autonoma Valle d'Aosta, Regione Piemonte, 2006*). If the protection function of the forest prevails over any other role (e.g. recreational, ecological,

production), its silvicultural management shall be aimed at keeping and/or improving this function (*Wilford el al., 2006*).

Mountain areas are typically threatened by gravitational natural hazards, amongst which rockfalls and landslides (Fig. 1). A rockfall is triggered when a fragment of rock detaches from a cliff face to propagate downslope by falling, bouncing and rolling (*Moos et al., 2018*). Forests can mitigate this natural hazard acting as a barrier made by standing and lying trees, and slowing down, deviating and stopping the falling rocks (*Meloni et al., 2006; Moos et al., 2018*). Shallow landslides (typically with a sliding surface less than 2 m deep) are caused by the excess of shearing forces respect to soil strength and the latter can be increased by the mechanical reinforcement and soil water reduction exerted by trees' roots.

The aim of this paper is, first, to evaluate the protection capacity of a chestnut forest located in Cevo (BS, Italy), loc. Andrista, against rockfall and shallow landslide hazards that threaten a nearby passing road. The adopted materials and methods are presented, along with the results and their discussion. Second, to propose silvicultural management that should maintain and improve the protection function of the forest for the next decades.

Fig. 1: a) A huge rockfall in Dolomiti mountain, Italy. (Ph: Braxmeier H.); b) A landslide in Merano, northern Italy. (Ph: Calanni A.)

Materials and Methods

Description of the study area

The fieldwork was carried out in Andrista, a small settlement included in the municipality of Cevo (BS). The study area is located in the middle of Valle Camonica in the Adamello Park, with geographical coordinates: 46 ° 04′54 ″ N 10 ° 21′11 ″ E (Fig. 2). The area is part of the central-eastern esalpic region, with an average annual temperature of around 8 ° C and an average annual rainfall of 800mm. It is characterized by a silicate substrate and a particularly friable acid rock (Gneiss).

The forest survey for the rockfall hazard protection study was carried on in a transect plot divided into 3 subplots, each 30 m wide and 25 m high, for a total surface area of 90x25 m, with a slope of 33° at an altitude of 750 m a.s.l. located in the rockfall transit and deposit area; it is characterized by the presence of a slow-growing Chestnut grove with the presence of *Fraxinus ornus, Ostrya carpinifolia* and *Corylus avellana*. Position, species, number of rock impacts, presence of animal browsing, and diameter at breast height (DBH) of all trees (DBH>7.5 cm) were recorded. The height and core samples were collected for the most common species on 6 representative trees for a total of 35 trees of chestnut, manna ash and hop-hornbeam. The rock damage was considered when bending of the trunk, debarking or stones at the base were found.

The root survey was carried out within a circular plot with a radius of 40 m and slope of 24° at an altitude of 650 m a.s.l., characterized by a fruit chestnut grove with the presence of *Fraxinus ornus* and *Ostrya carpinifolia*. Position, species, height and DBH of all trees (DBH> 7.5 cm) were recorded.

The vertex was used to measure distances and heights, whereas an increment borer was used to extract tree cores.

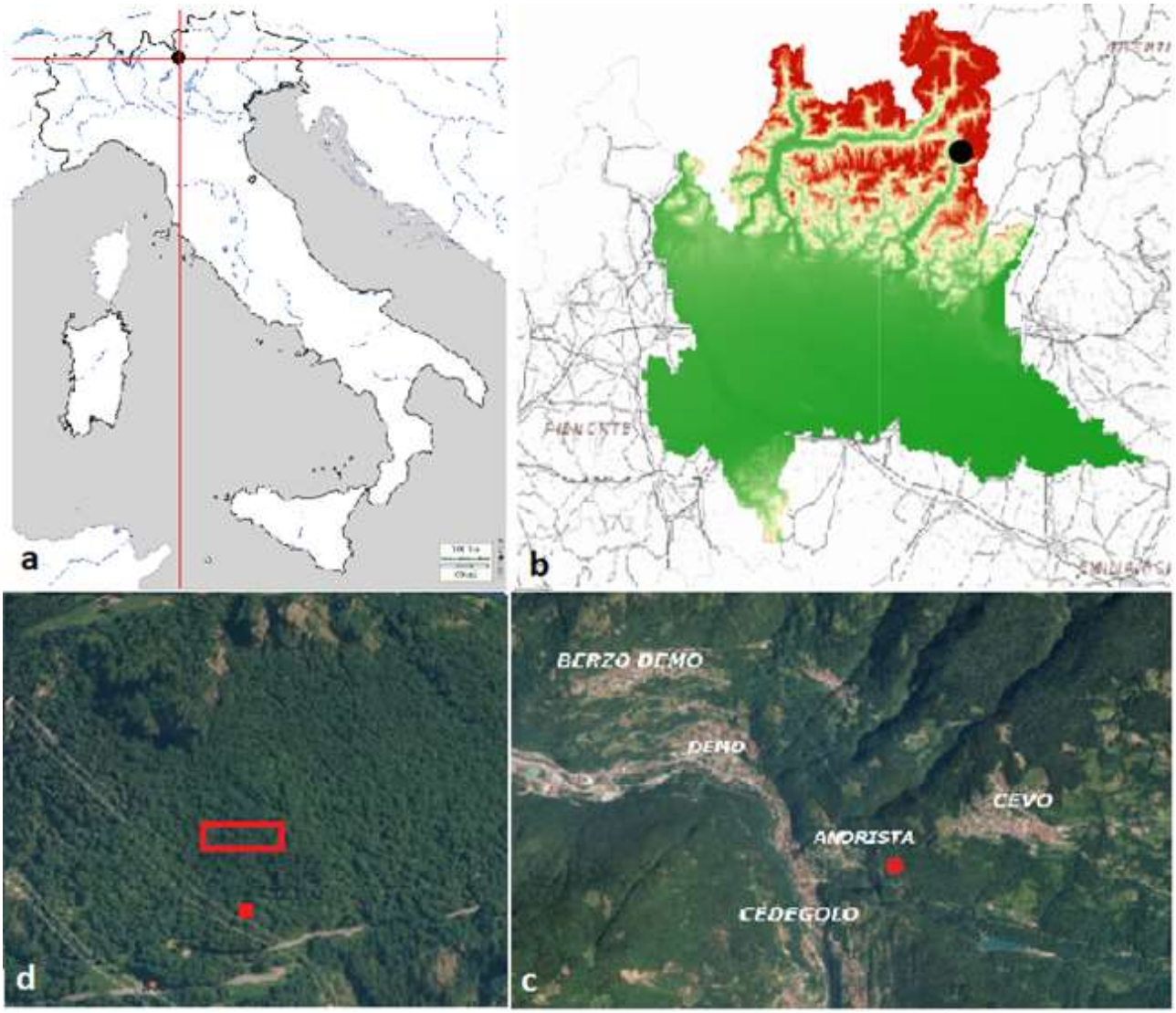

Fig. 2: The study site is located in northern Italy (a), in the middle of Valle Camonica situated in the Lombardy region (b).The study site is included in the municipality of Cevo (BS),(b), and the field surveys is carried out in transect plot - delimited by a red polygon and red point (d.).

The trench method was adopted to quantify the root reinforcement (*Bohm 1979, Zobel and Wisei, 2010; Xu et al., 1997; Schmid and Kadza, 2002, Bischetti et al., 2009*) by digging 7 soil profiles at 2.5 and 1.5 m at different angles downslope from 2 representative chestnuts. A frame with known dimensions was leant on the profile and a picture was shot; in addition, 4 soil samples were collected.

Fig. 3: Diameter of the falling rocks. (Ph: Arrigoni F.)

Fig. 4: Evidence of rockfall on a sweet chestnut. (Ph: Acrami P.).

Adopted models

A first tool adopted for the evaluation and description of the role of protection forests is a form developed by *Regione autonoma Valle d'Aosta* and *Regione Piemonte* (2006), which allows evaluating the actual protective capacity of the forest against rockfall hazard. The form also provides, by data comparison, a short and mid-term forecast of the forest development that contributes to establishing whether a human intervention shall be necessary.

A second tool is RockForNet, which estimates the level of protection against rockfall given the defined conditions; furthermore, it creates an ideal and minimum diameter class distribution for rockfall protection, given those forest conditions. The level of protection is the percentage of stones stopped by trees (*Berger & Dorren, 2007*).

To evaluate the role of forest in shallow landsliding process, the PRIMULA (PRobabilistic Multidimensional shallow Landslide Analysis) model has been adopted. In the PRIMULA a 3D limit equilibrium model and Monte Carlo Simulation model interact with other sub-models as shown in

the flowchart in Fig. 5. It, then, provides a distribution function of each input and output parameter. PRIMULA provides a landslide hazard map as output (*Cislaghi, 2017*).

PRIMULA requires a root distribution model (RDM) and root reinforcement model. In this case study it has been used the RDM developed by Schwarz et al. (*2010*), which uses the strong correlation existing between the stem diameter of the trees and the number of roots of different diameters with distance from the stem (*Ammer and Wagner,2005; Bauhus and Bartsch,1996; Brockway and Outcalt,1998; Drexhage and Colin, 2001*). For the root reinforcement, it has been adopted the Root Bundle Model Weibull (RBMw; *Schwarz, 2013*), which estimates it as the sum of the maximum tensile force of each root divided by the soil profile area. The model considers root distribution and maximum resisting force in addition to mechanical and geometrical properties. The pull-out force is calculated as a function of diameters and displacement.

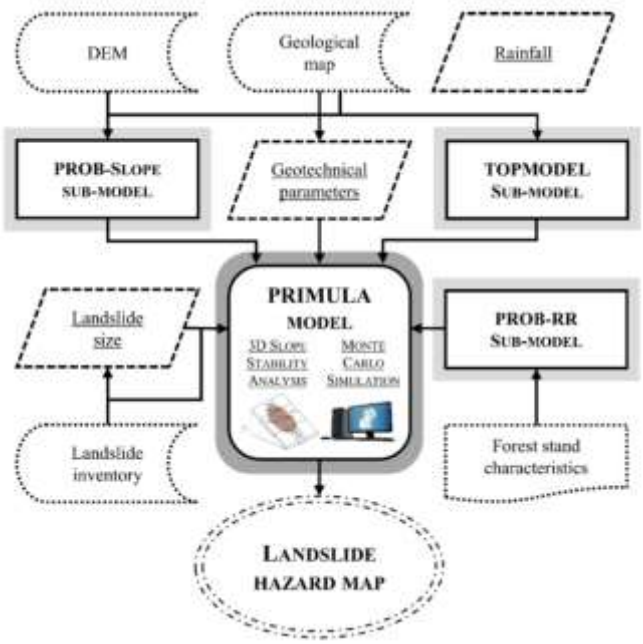

Fig. 5: *The PRIMULA (PRobabilistic Multidimensional shallow Landslide Analysis) model*.

Laboratory analyses

Rockfall analysis

The age of the 35 representative trees amongst the dominant tree species at stand scale was obtained by coring the trees with a Pressler borer. The cores were then examined with a microscope for the rings count. The age of each other tree was then estimated using diameter-age linear and non-linear regression models (*Rozas, 2003; Favillier et al., 2015*) for chestnut, manna ash, hop-hornbeam. The same steps were followed to estimate the height of each tree, by using diameter-height regression models built with the data collected from the 35 representative trees.

In dendrogeomorphic studies, the recurrence intervals represent the average time period between two successive rock impacts at a specific point (*Šilhán et al., 2013; Trappmann et al., 2014*). Accordingly, observed recurrence intervals (*Ri*) were calculated for each of the three subplots as following:

$$Ri = \frac{(a_{mean} \times CIP)}{\sum S}$$

Where a_{mean} is the mean age of trees, $\sum S$ represents the sum of the rockfall collisions, and *CIP* is the conditional impact probability (*Favillier at al., 2017*):

$$CIP = \frac{L_{IC}}{L_{plot}}$$

The cumulative length of the projections of the circles of impact on the downslope side of the cell is identified by L_{ic}, and L_{plot} is the length of the downslope side of the cell.

The frequency is calculated as the inverse of return period (Ri).

The datasets of the forest survey were positioned as geo-objects in a geographical information system (GIS) and were also drawn on a graph paper. In the graph paper, trees' position, diameters, species and gaps were drawn, allowing to calculate the CIP parameter.

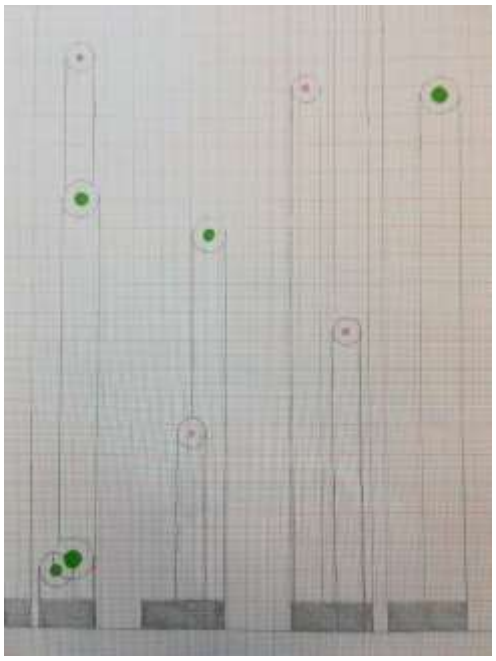

Fig. 6: Section of graph paper illustrating trees distribution. (Ph: Castelli L.)

PRIMULA application

RBMw model (Schwarz et al., *2010b*) needs as input parameters the maximum tensile force Fmax (in N), the Young's modulus E (in MPa), and the root length L (in mm) as a function of root diameter φ. Equations of F and E are estimated by the tensile tests, whereas equations of L is evaluated by direct field measurements. The tensile tests were conducted on 64 roots with diameters that ranged from 0.86 mm to 6.61 mm picked up from all the trenches, with an average value of 2.58 and a SD of 1.24.

PRIMULA model requires some input, which recovers from shapefiles. First of all, the hydrologic basin of Re creek has been designed and overlayered on the DTM, as shown in Fig. 8, and the land use, taken from DUSAF (*Regione Lombardia 2015*). The study area is located in a fruity chestnuts forest (Fig.9). Other inputs are the slope map, and the soil texture defined as sandy-loam according to the pedological map of Regione Lombardia.

Fig. 7: Universal testing machine. (Ph: Castelli L.)

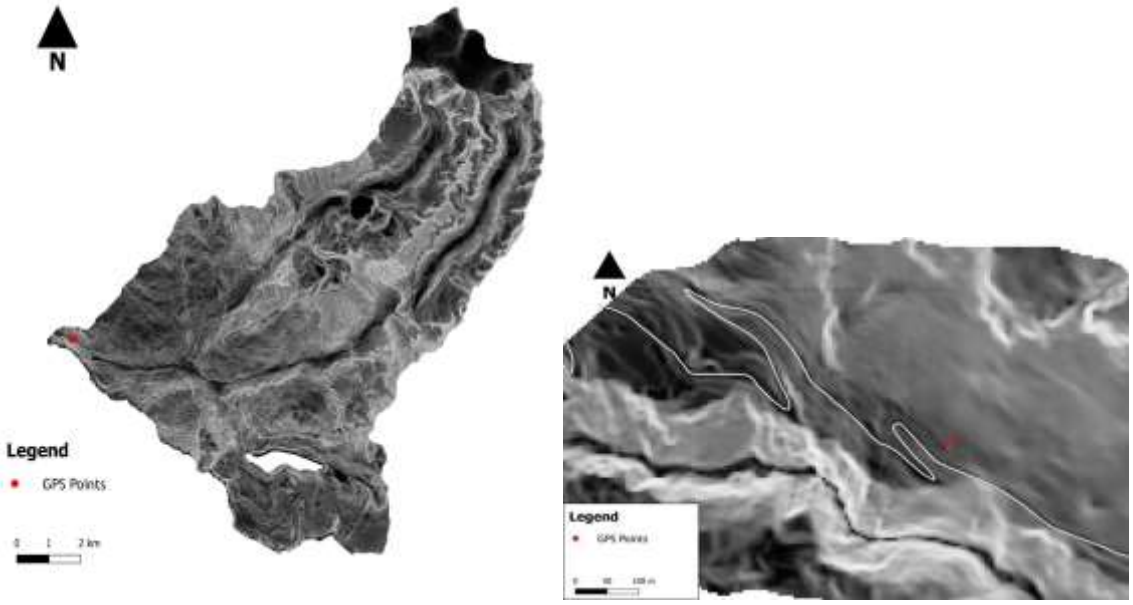

Fig. 8: Re creek basin. The red dot identifies the study area.

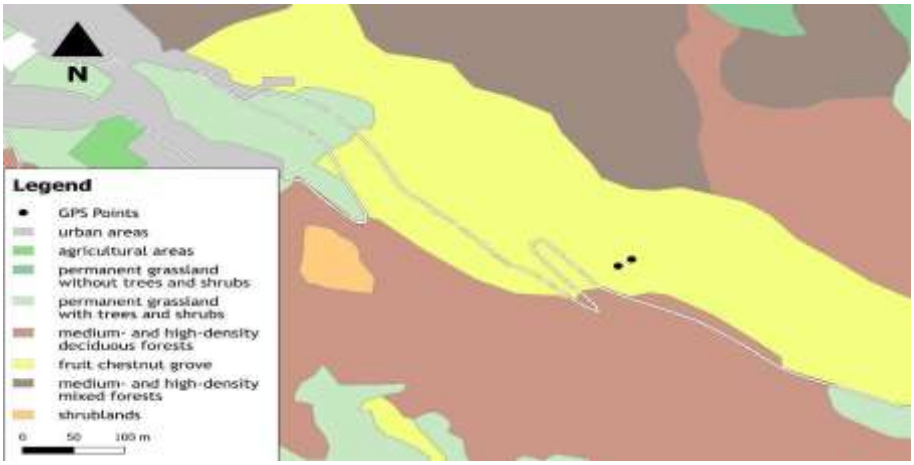

Fig. 9: Land use map.

Results and Discussion

Rockfall and forest characteristics

The data collected in the transect plot were used to:

1. build regression equations to estimate the age and height of all trees, draw trees distribution maps and estimate the recurrence interval and CIP;
2. run the RockForNet model;
3. fill in the evaluation and description form for the role of protection forests (*Regione Piemonte e Valle d'Aosta, 2006*).

The diameter-age relationship shows regressions with good R-squared values (Fig.10, Fig.11 and Fig. 12). Diameter-height regressions were less satisfactory, especially for *Ostrya carpinifolia* and *Fraxinus ornus* (Fig. 14, Fig. 15, and Fig. 16).

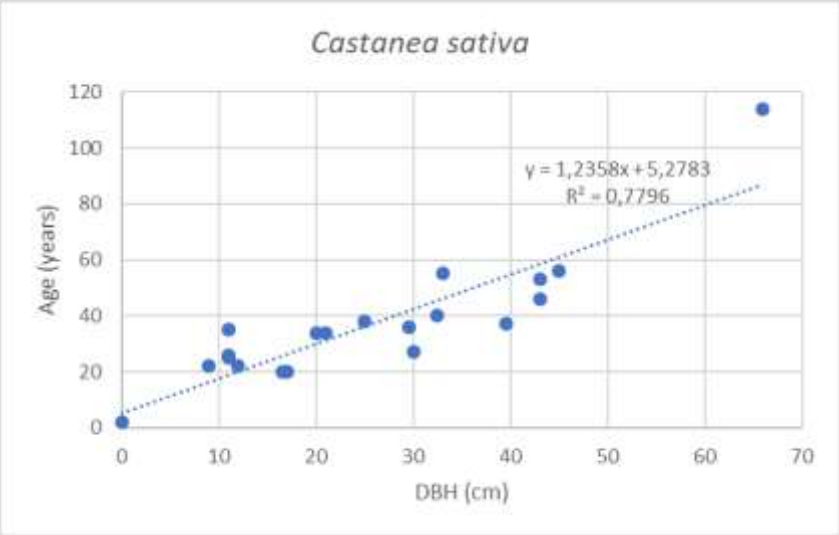

Fig.10: DBH age Linear regression for Castanea sativa.

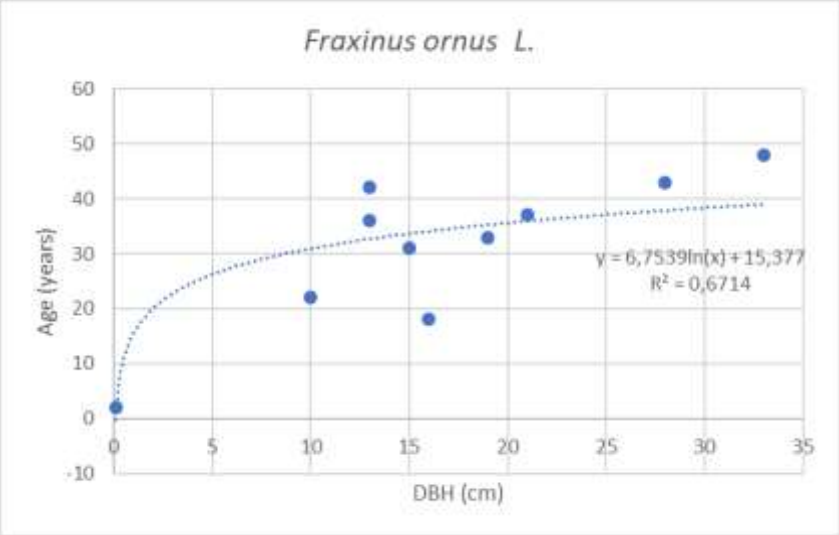

Fig. 11: DBH-age linear regression for Fraxinus ornus.

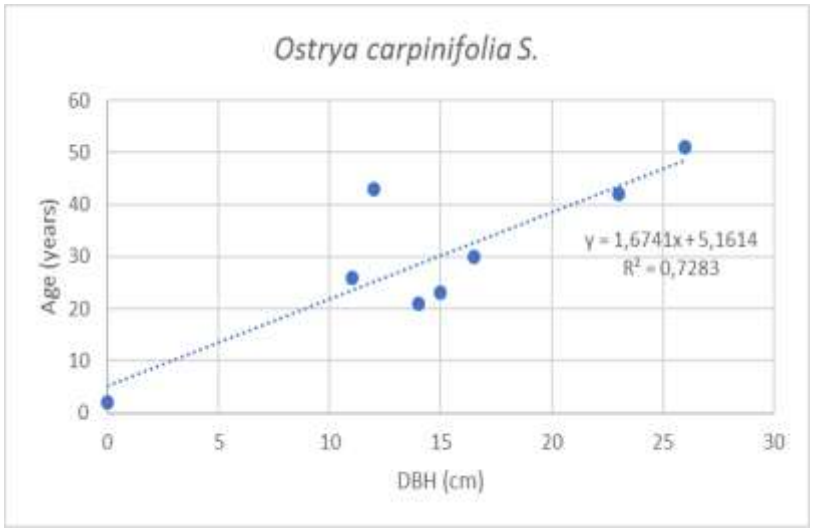

Fig. 12: DBH linear regression for Ostrya carpinifolia.

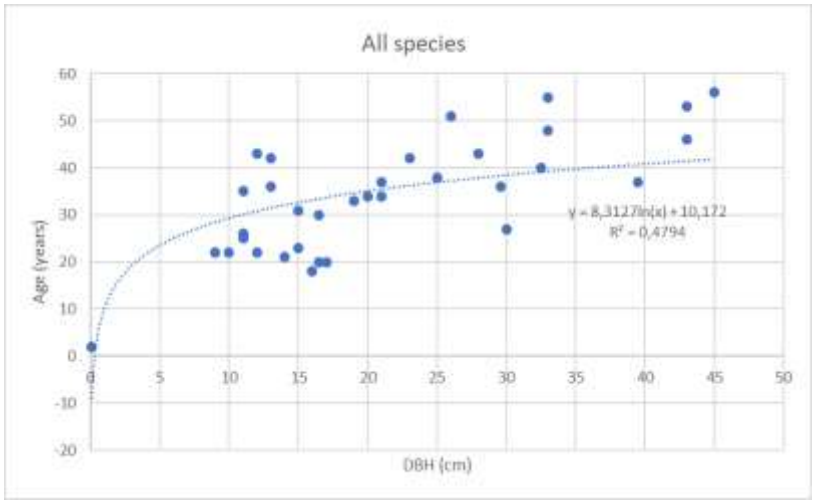

Fig. 13: DBH-age linear regression for all other species.

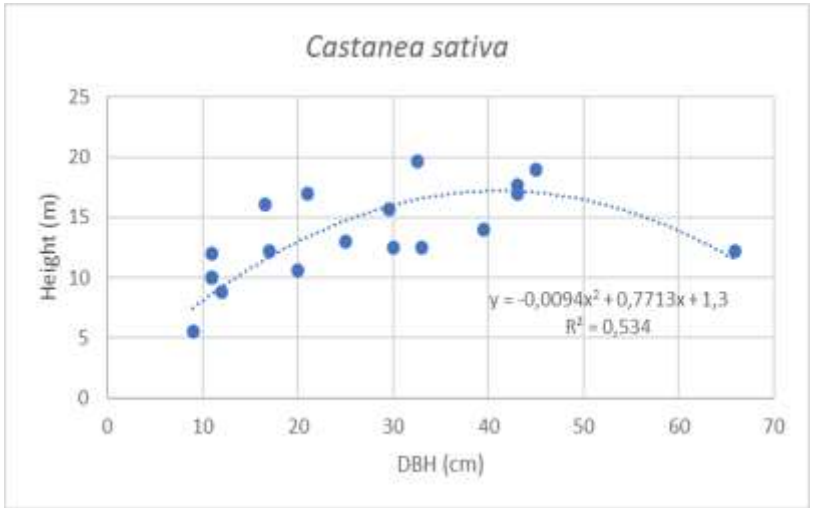

Fig. 14: Linear regression DBH-height of Castanea Sativa Mill.

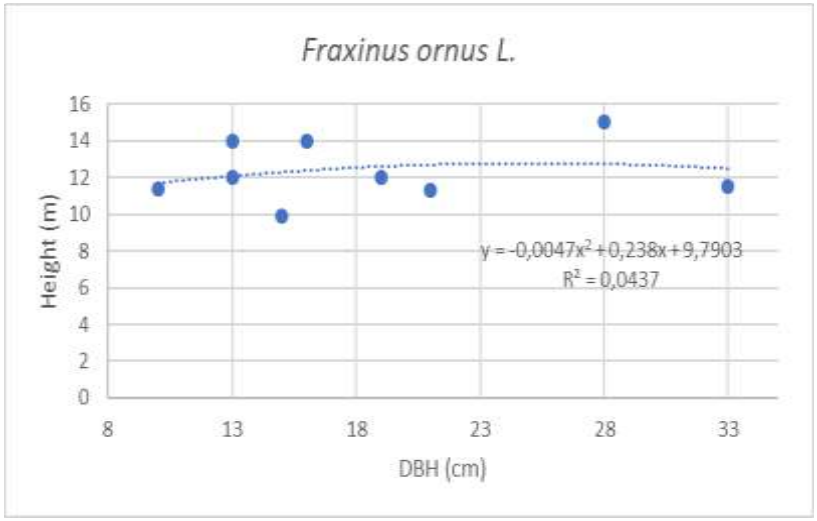

Fig. 15: Linear regression DBH-height of Fraxinus ornus.

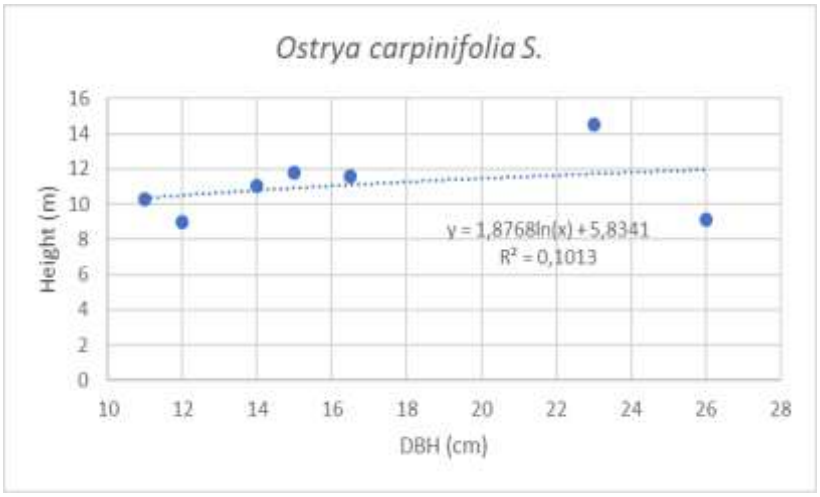

Fig. 16: Linear regression DBH-height of Ostrya carpinifolia.

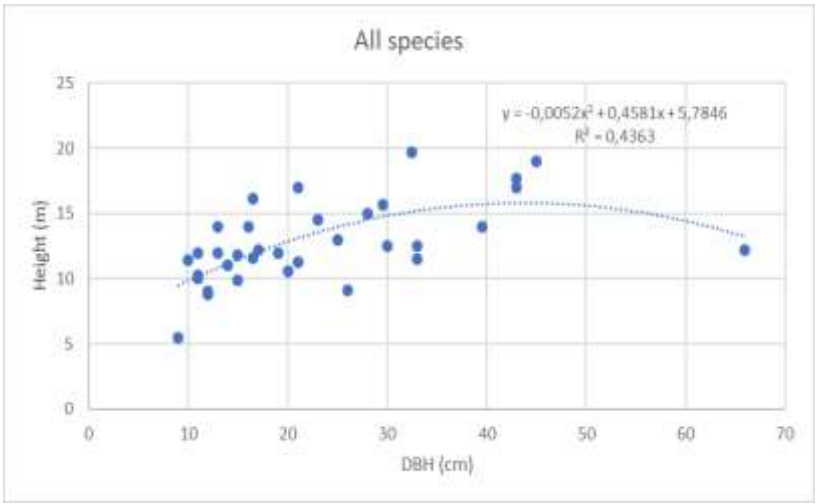

Fig. 17: Linear regression DBH-height of all species.

RockForNet model

The trees distribution is sufficiently uniform among the subplots. The species distribution shows that *Castanea sativa* is the dominant tree species (48,5%), followed by *Fraxinus ornus* (24,8%) and *Ostrya carpinofolia* (17%) (Fig.18).

The estimated rockfall events occur every 58,4 days (Ri=0,16 year) and the trees intercept 67% of total falling rocks (Tab. 1).

The forest protection level estimated by the RockForNet is in a range of 50-75% in every subplot. The model also provides an ideal diameter distribution for rockfall protection that can be compared to the current forest diameter distribution profile, as shown in Fig. 20.

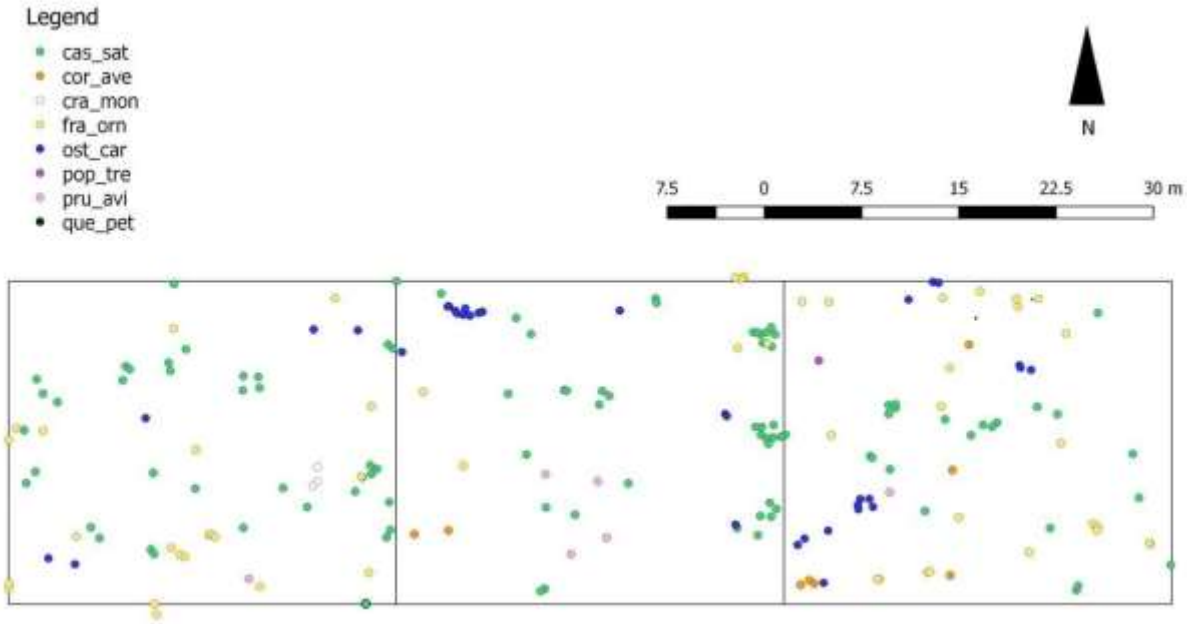

Fig. 18: Species distribution used for RockForNet model.

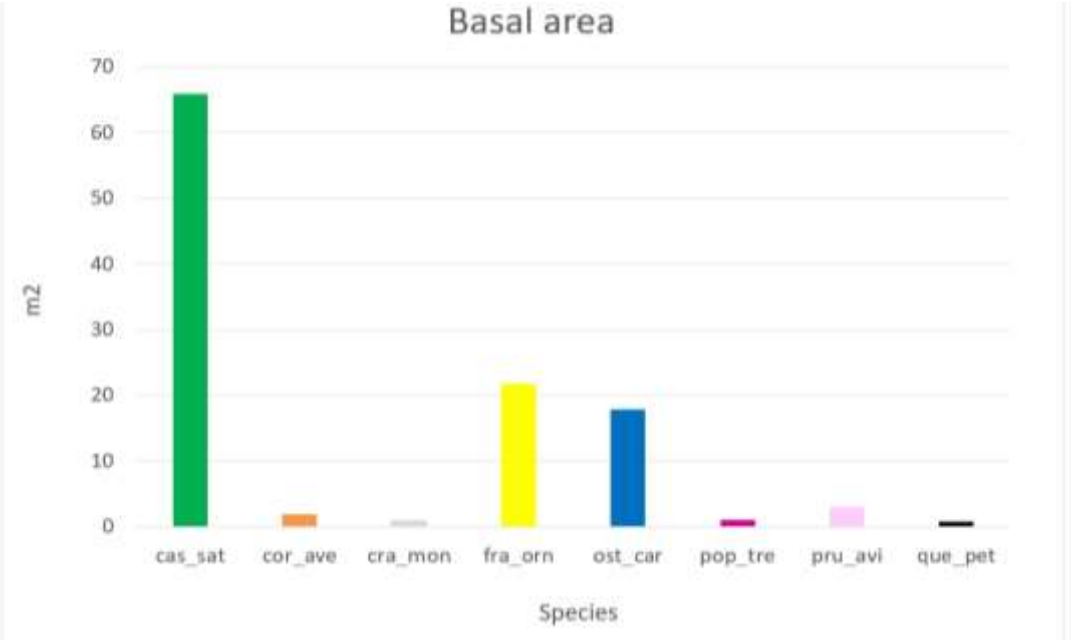

Fig. 19: Basal area of the trees in the whole plot.

Tab. 1: Ri and CIP of the three subplots and the whole plot

Coefficients	Subplot 1	Subplot 2	Subplot 3	Plot
Ri (year)	0,11	0,20	0,18	0,16
CIP (%)	65	60	75	67

Fig. 20: Diameter forest profiles for Subplot 1, 2 and 3.

Role of protection forest in rockfall hazard evaluation

The evaluation and description form highlights that the forest satisfies the minimum requirements for effective protection against rockfall hazard. Accordingly, the forest holds a great protection capacity, and forestry interventions are regarded as having low priority: it shall be required, within 10 to 15 years, to monitor the health status of the stools and the presence of regeneration, limited by animals' browsing, and to intervene where required. As the chestnut trees, growing old, get structurally weaker and, therefore, threaten forest stability, it is advisable to plan to cut old stumps to facilitate the regeneration from stools and the growth of seedlings. Furthermore, the dead stumps would continue to dissipate or exhaust the kinetic energy of falling rocks until decayed.

The three methods provided consistent results, with estimates all within the 50-75% range. Nevertheless, both RockForNet and the form highlighted that the forest regeneration and stability shall be ensured in order to achieve the ideal forest profile, while the trees distribution map and the form highlighted the need to intervene in case of long downslope clearings. The forest management strategy shall then provide for:

- the cutting of mature chestnut trees (older than 100 years), arranging the logs on the ground transversally to the maximum slope;
- pest monitoring and control;
- restrictions/limitation to animals' browsing;
- structural measures or hydraulic forest management for long downslope clearings.

Root reinforcement

The results of root counting and distribution along with the profiles, ranked in four different categories (0.5-1 mm, 1-2 mm, 2-5 mm and >5 mm) show that there is substantial variability of density among the profiles: it varies from 234 roots/m^2 to 552 roots/m^2 (Fig. 21). In general, there are more roots near the trunk, and the spatial distribution is more homogeneous at 1.5 m than 2.5 m. Furthermore, there was a higher number of small-diameter roots near the trunk, whereas the structural ones (>5 cm) are located farther from the trunk.

RDM, using root distribution data collected, provides, as output, a simulated spatial distribution of diameters, to track a probabilistic 3D map. It was detected a well-fitting between observed and RDM simulated data. Once, RDM calibration was completed, then it was possible to run the RBMw (Fig. 22).

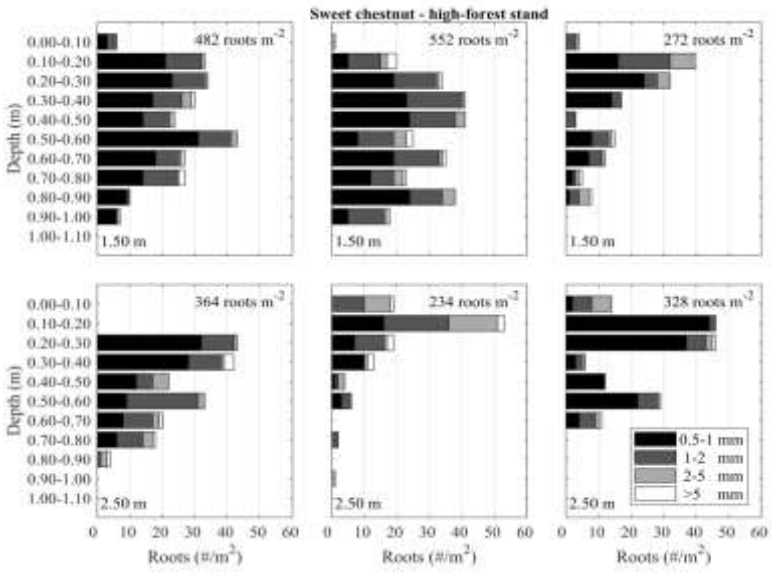

Fig. 21: Average root density classified in four diameter classes (0.5-1 mm, 1-2 mm, 2-5 mm and >5 mm) at two different distances from the chestnut trunk (1.50 m, 2.00 m).

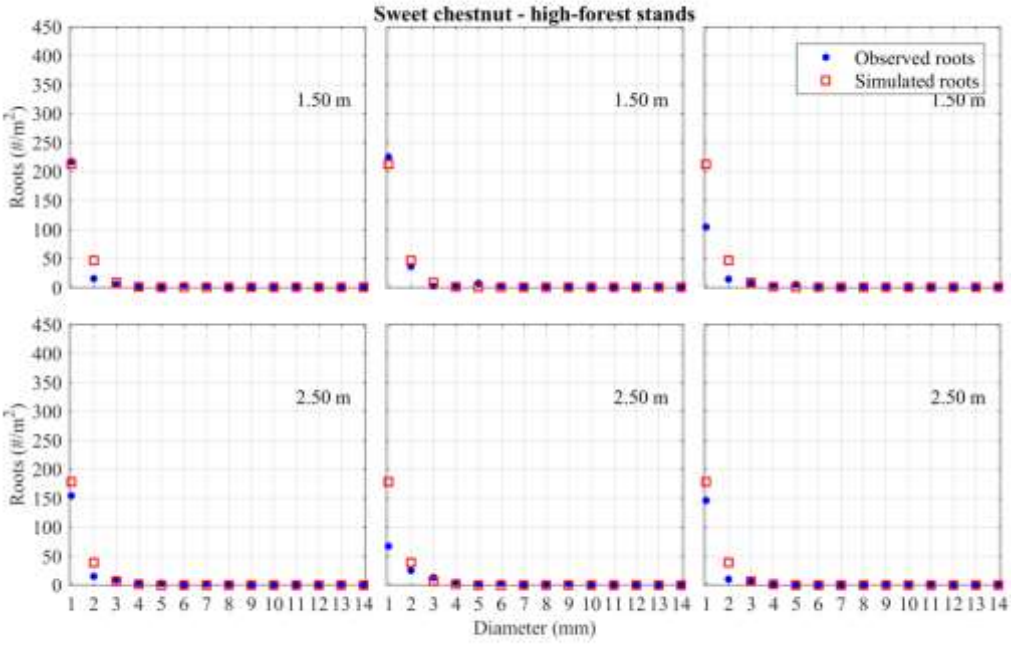

Fig.22: Discrepancies between observed and RDM simulated number of roots divided into diameter classes at two distances from the chestnut trunk (1.50 m, 2.50 m).

RBMw was calibrated using field-measured data, and a quite strong correlation was obtained (Fig. 22). The resistance of roots at 1.5 m from the trunk increases and reaches a peak at 7 mm of displacement, and reinforcing at this point varies from 9 kN to 14.5 kN, then decreases to 0 near 13 mm of displacement; the line in these profiles and the simulated curve is between observed data curves. Whereas at 2.5 m the simulated curve is over than observed curves data, the peak is around 7 mm of displacement, and the reinforcing varies from 9 kN to 11.5 kN then decrease as the graphs of 1.5 m (Fig. 25).

PRIMULA results

The PRIMULA model results show that the majority of the high-risk zones correspond to the areas near the streamlines and the steepest areas, as expected. With the current conditions, the safety is guaranteed for the infrastructures: indeed the road is entirely in the safe zone (Fig. 26a). Whereas, if PRIMULA simulates without root reinforcement, the high-risk areas increase, reaching the main road and the village, situated in the upper-left part of the maps (Fig. 26b).

It is possible to state that PRIMULA worked well; indeed, the high-risk zone corresponds to landslides regional maps. PRIMULA, with root reinforcement equal to 0, highlights some areas close to the main infrastructures that are not covered by landslide maps.

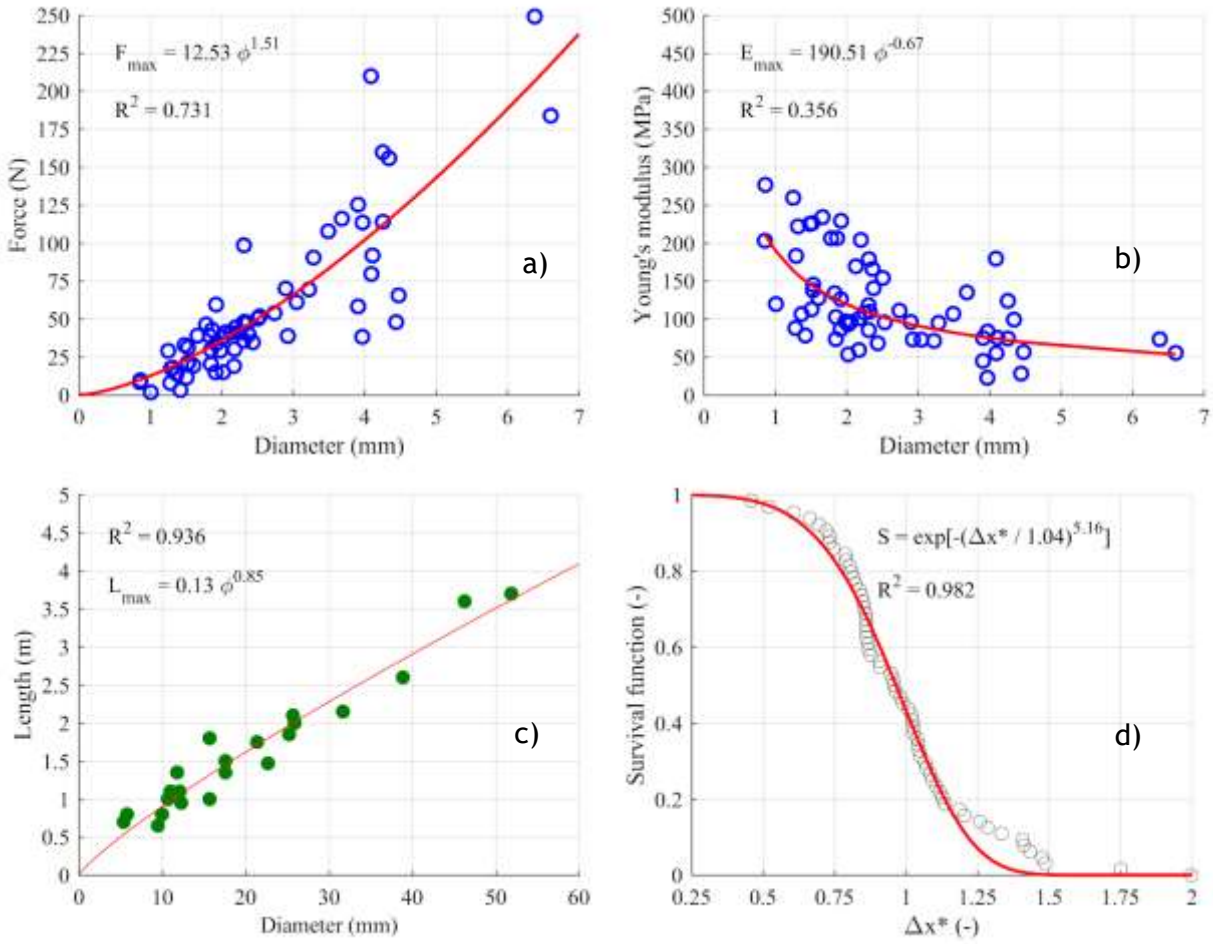

Fig.24: a) maximum tensile force vs root diameter relationship, b) Young's modulus of elasticity vs diameter relationship, c) root length vs diameter measured in field, d) survival function.

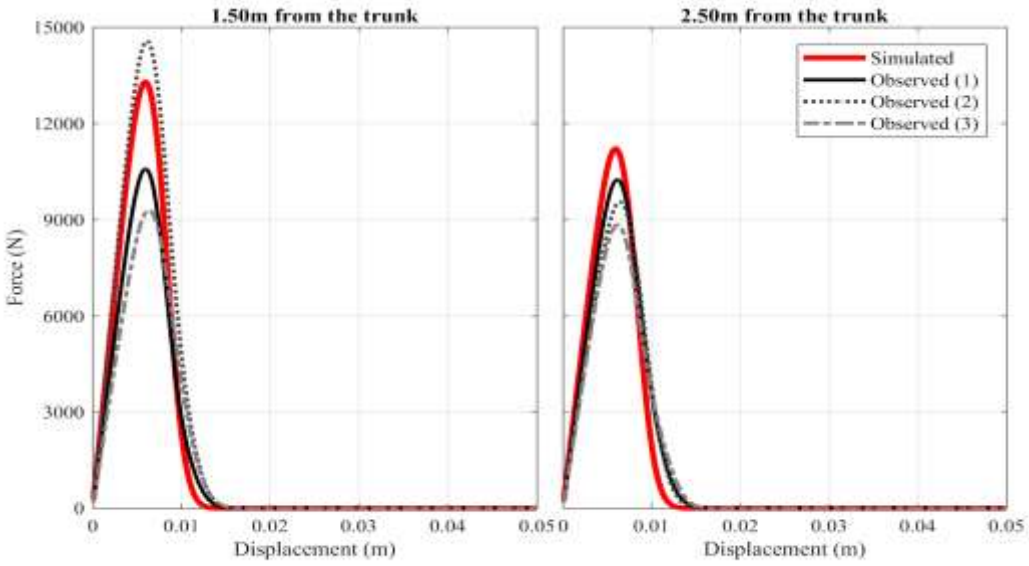

Fig. 25: RBMw output as function of the two distances from the trunk.

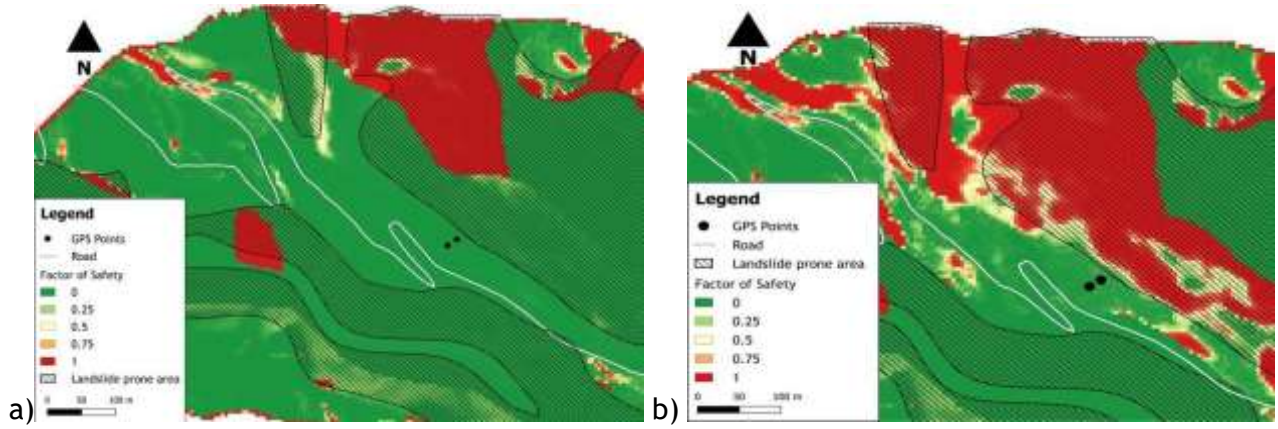

Fig. 26: Hazard map provided by PRIMULA a) with current root reinforcement; b) without root reinforcement (dashed areas are landslide areas as napped by Regione Lombardia).

Conclusions

In this case study, current knowledge and novel tools regarding forest models and slope stability were used to assess the protective role of trees, against rockfalls and landslides, for a road.

RockForNet and the evaluation and description form represent two excellent instruments to analyse the protection role of a forest and to plan silvicultural interventions. These actions, along with hydraulic forestry management could increase the safety factor up to around 100%.

The root reinforcement calculated for chestnut (9-14 kN) is consistent with that found in the literature (e.g., 15 kN; *Bischetti et al. 2009*).

PRIMULA provides different scenarios changing the vegetational or land use parameters and, thereby, it could be used to identify areas most susceptible to landslides in intermediate and large-scale projects.

Finally, regarding rockfalls, these tools are less expensive than conventional geotechnical manufactures; indeed, the first paragraph of the Mountain Forests Protocol of the Alpine Convention, states: "The mountain forests offer the most effective, economical and suitable for landscape protection, against natural risks" (*Dorren, Berger, and Putters 2006; Alpine Conv. 2013*)

Concerning the landslides, PRIMULA should be used to verify the areas under hydrological constraint and simulate how safety factor change with the evolution, or modification, of the forest stand.

References

Alpine Convention, 2013. 'Vademecum per l'applicazione della Convenzione delle Alpi, per la buona amministrazione del territorio montano e per la qualità della vita della popolazione'. In Convenzione delle Alpi e buone pratiche nei comuni italiani. Linea Grafica, Castelfranco Veneto, Italia: Segretariato permanente della Convenzione delle Alpi.

Ammer, C., Wagner, S., 2005. An approach for modelling the mean fine-root biomass of Norway spruce stands. Trees 19: 145-153. https://doi.org/10.1007/s00468-004-0373-4

Bauhus, J., Bartsch, N., 1996. Fine-root growth in beech (*Fagus sylvatica*) forest gaps. Canadian Journal of Forest Research, 26: 2153-2159.

Berger, F., Dorren, L., 2007. Principles of the tool Rockfor.net for quantifying the rockfall hazard below a protection forest. Schweiz Z Forstwes 158: 157–165.

Berger, F., Rey, F., 2004. Mountain Protection Forests against Natural Hazards and Risks: New French Developments by Integrating Forests in Risk Zoning. Natural Hazards 33: 395–404.

Brockway, D.G., Outcalt, K.W., 1998. Gap-phase regeneration in longleaf pine wiregrass ecosystems. For. Ecol. Manag. 106,125-139.

Cislaghi, A., 2017. Assessing shallow landslide susceptibility of vegetated hillslopes through a physically-based spatially-distributed model. PhD Thesis, Università degli Studi di Milano, Milan.

Dorren, L., Berger, F., Imeson, A.C., Maier, B., Rey, F., 2004. Integrity, stability and management of protection forests in the European Alps. Forest Ecology and Management 195: 165–176.

Dorren, L., Berger, F., Putters, U.S., 2006. Real-size experiments and 3-D simulation of rockfall on forested and non-forested slopes, Nat. Hazards Earth Syst. Sci., 6: 145–153, doi.org/10.5194/nhess-6-145-2006.

Drexhage, M., Colin, F., 2001. Estimating root system biomass from breast - height diameters. Forestry 74: 491 - 497.

Favillier, A., Mainieri, R., Lopez Saez, J., Berger, F., Stoffel, M., Corona, C., 2017. Dendrogeomorphic assessment of rockfall recurrence intervals at Saint Paul de Varces, Western French Alps. Géomorphologie: relief, processus, environnement 23, 2: Varia.

Meloni, F., Lingua, E., Motta, R., 2006. Analisi della funzione protettiva delle foreste: l'esempio della "Carta delle foreste di protezione diretta della Valle d'Aosta". Forest@ 3: 420-425.

Moos, C., Bebi, P., Schwarz, M., Stoffel, M., Sudmeier-Rieux, K., Dorren, L., 2018. Ecosystem-based disaster risk reduction in mountains. Earth-Science Reviews 177: 497–513. doi.org/10.1016/j.earscirev.2017.12.011

Regione Autonoma Valle d'Aosta, Regione Piemonte, 2006. Selvicoltura nelle foreste di protezione - Esperienze e indirizzi gestionali in Piemonte e in Valle d'Aosta. Compagnia delle Foreste, Arezzo, pp. 224.

Regione Lombardia. Direzione Generale Agricoltura, 2010. Sistemazioni Idraulico Forestali: Indirizzi per gli interventi. Quaderni della Ricerca 116.

Schmid I. and Kazda M., 2002. Root distribution of Norway spruce in monospecific and mixed stands on different soils. For. Ecol. Manage. 159: 37–47

Schwarz, M., Giadrossich, F., and Cohen, D.: Modeling root reinforcement using a root-failure Weibull survival function, Hydrol. Earth Syst. Sci., 17, 4367–4377, https://doi.org/10.5194/hess-17-4367-2013, 201

Schwarz, M., Lehmann, P. and Or, D. (2010), Quantifying lateral root reinforcement in steep slopes – from a bundle of roots to tree stands. Earth Surf. Process. Landforms 35: 354-367. doi:10.1002/esp.1927

Trappmann D., Stoffel M., Corona C., 2014 – Achieving a more realistic assessment of rockfall hazards by coupling three-dimensional process models and field-based tree-ring data. Earth Surface Processes and Landforms, 39, 1866-1875. DOI : 10.1002/esp.3580

Wilford, D. J., Innes, J. L. & Hogan, D. L. (2006) Protection forests: recognizing and maintaining the forest influence with regard to hydrogeomorphic processes. Forest Snow and Landscape Research 80, 7–10.

Xu, Y.J., Röhrig, E., Fölster, H., 1997. Reaction of root systems of grand fir (*Abies grandis* Lindl.)

Acknowledgments

The authors would like to thank for the support: G. Bischetti, G. Vacchiano, T. Campagnaro, A. Cislaghi, E. Morotti, P. Sala

SMARTCOW

Precision livestock farming tools to study factors affecting milk production and animal welfare in early lactation dairy cows

Bianchi C., Bonizzi S., Comparelli A., Galli G., Lazzari A., Pavesi M., Massimini E., Piffari P., Tanchella M.

Abstract

The timely and constantly updated information of the herd are valuable for the farmer: they allow the increase of farm profitability, the elimination of inefficiencies, preserving the health and welfare of the cows. The aim of the study was to focus on the factors that influence animal production and welfare in cows at the beginning of lactation. The trial took place at the A. Menozzi farm in Landriano and the data were collected with the help of innovative methods. In particular, activity sensors (Moomonitor and Hobo pendant) and temperature-humidity-brightness sensors (environmental Hobo) were used; moreover, the Herd navigator milk sampling system, that automatically analyses milk betahydroxybutyrate, the somatic cell counting instrument. Some parameters were manually gathered: Locomotion score, Body condition, Teat Apex, Hygiene and Hoof score. From the collected data it emerged that the hygienic conditions are optimal (Hygiene score = 1) and milking parameters and procedures are well calibrated (Teat apex score = 1); the locomotion score is good for more than 60% of the animals (Locomotion Score = 2), the environmental parameters are below the critical value (Temperature Humidity Index = 67), the average body condition of the animals is ideal (Body Conditon Score = 3.36). There is correspondence between the somatic cells measured in the two ways DeLaval™ Cell Count and Somatic Cell Count (R^2 = 0.783). On the contrary there is no relationship between somatic cell value and lactation days (R^2 = 0.034), number of lactations (R^2 = 0.004), milk production (R^2 = 0.2286), differential cells (R^2 = 0.2471). The relationship is also low between the Locomotion Score and milk production, the BHBA, the linear score, the BCS. Thanks to the Moomonitor and the Hobo pendant the behavior of the cows in the 4 days of experimentation was observed: on average they were lying down for half the time (51%), excluding the hours of milking.

Key words: Precision farming, Animal welfare, Dairy cows, Early lactation

Introduction

All the sectors of animal husbandry, including dairy cow husbandry, aim to obtain good productions, reproductive efficiency and respect of animal welfare.

The first period of lactation is particularly delicate for the cows because they have to face hormonal, environmental and feeding stress, so is essential to properly manage this phase. The main problems concern udder health, lameness, metabolic disorders and heat stress.

To avoid as much as possible any udder problems is necessary to manage the cleaning of the bedding area and the barn environment; the cubicles must be large enough to prevent that animals lie down in dirty areas, the litter must also be managed very well to create a comfortable environment and to avoid the proliferation of pathogens. Another important aspect is the cleaning of the teat and milking machine to avoid cross contamination among cows.

Over time, these management aspects are very important because manage them correctly can reduce the incidence of mastitis and consequently the use of antibiotics, especially in the first stage of lactation.

Another important problem is lameness because it represents the third cause of culling. Lameness have in fact several consequences on animal welfare and health, farm productivity and costs.

The average costs of lameness can reach about 320 €, including loss in milk yield indicatively of 360 kg in a standardized lactation of 305 days. Moreover, if the lameness occurs before 120 days of lactation, the cost is about 67€/head (Casellato et al., 2007).

In addition, lameness seems to be underestimated by farmers. An U.S. study estimates the extent of lameness at 20-25% (Calderon et Cook, 2011) but other studies report that farmers believe the percentage of cattle with lameness in their herd is about 5-10% (Blokhuis, 2018).

Therefore, helping farmers in analysing and monitoring their herds in terms of locomotion becomes important to realize farm problems and optimize animal performances. Because lameness is closely influenced by other management and environmental factors and by cow's health and comfort, even more important is to be able to analyse all these factors and explore how they are connected.

The metabolic diseases at the beginning of lactation are very important because they can compromise the whole lactation. To identify risk, indicators such as Body Condition Score (BCS) are used. BCS is a visual assessment of the animal's body that allows to evaluate animal fat reserves. According to the Edmonson system a score from 1 (very thin) to 5 (very fat) is attrubuted to eight different anatomical points of the animal. It must not exceed 3.5 because higher values can compromise calving and can induce rapid decrease of fat reverves in the *post partum* period associated with lower fertility and metabolic disorders as for example ketosis.

The evaluation of BHBA (betahydroxybutyrate) in milk can help to detect ketosis in dairy cows. Subclinical ketosis can cause reduction of the reproductive efficiency and to the the productivity too. A study (Duffield et al., 2009) estimates that high BHBA concentration in first or second week of lactation (first week> 1,000 mol / L; second week> 1,400 mol / L) can lead to a decrease in fertility up to 20%; high BHBA levels in both first weeks can cause a fertility reduction up to 50%.

Dairy cattle in many subtropical, tropical and semi-arid regions are subject to high environmental temperatures (Ta), relative humidity (RH) and high solar radiation for prolonged periods. This compromises the ability of the dairy cow to dissipate heat, causing heat stress (Bouraoui, 2002). Unfortunately, heat stress compromises animal welfare, causing less milk production: an important economic loss for the farmer. Another aspect that affects business costs is reproduction: two key moments that lead to the emergence of a pregnancy are heat and fertilization.

Since animals in heat move much more than their average, a technique can be used is a special collar or a pedometer or ruminometer that have inside an activometer that identifies the increase in physical activity (walking, climbing, getting up and lying down).

Unfortunately, all the factors that limit the movement of animals also limit heat detection; measurement of the reproductive concentration of hormones is the key for identifying many reproductive problems and heat. Progesterone is one of the hormones that regulates the estrous cycle, so if it is measured in milk or blood, it can be used to detect the state of heat. The measurement can be done manually with kits, or with Herd navigator, an automatic milk collection and analysis system during milking. Progesterone monitoring throughout the cycle allows to create a curve and accurately identify the start of heat. The conception rate can vary from 18% if the concentration of progesterone to fertilization is greater than 10 ng / ml, to 60% if this value is less than 1 ng / ml (Dairy zoom, 2016).

Aim

The purpose of this paper is to analyze the factors that influence production and animal welfare in primiparous and multiparous cows at the beginning of lactation with the use of precision livestock farming techniques.

Materials and Methods

The farm in which studies and analysis were conducted is an experimental dairy farm of the University of Milan. The data were monitored during a week, between September 9th and September 13th. At the time of study, there were about 100 cows in lactation, among which about 22 animals in early lactation (<100d). During the test period, several aspects were assessed: Hygiene Score, Teat Apex Score, Somatic Cells Count and Differential Cells, Locomotion Score and Hoof Score, BCS, Temperature Humidity Index, daily activity and resting time and betahydroxybutyrate in milk.

Individual Somatic Cells Count have been measured both daily from September 10th to September 13th using the DeLaval™ cell count) and by monthly controls by the Italian Breeder's Association. Besides total cell count, individual milk controls have always evaluated the Differential Cells (the percentage of Polymorhponuclear neutrophilis plus lymphocytes compared to macrophages)that give an important index of the stage of infection allowing to prevent serious situations, data collected by individual controls are shown in Figure 1.

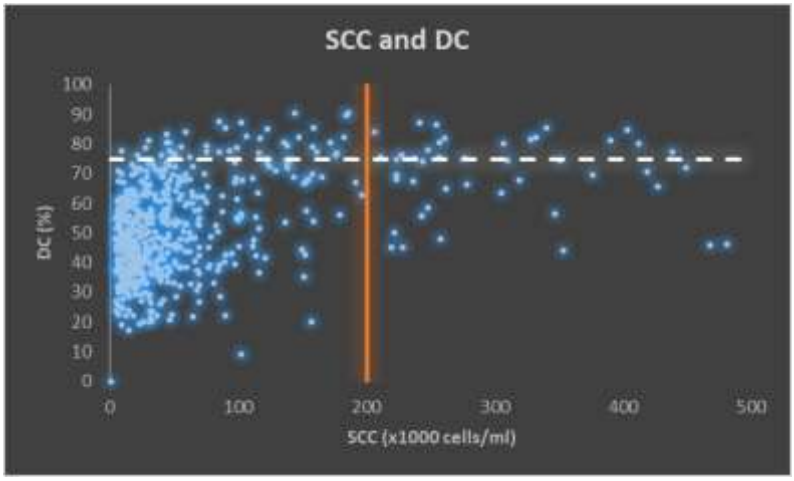

Fig. 1: Somatic Cell Count and Differential Cell Count correlation

The Teat Apex Score and the Hygiene Score were assessed on a sample basis during the 4-day milking test using specific scoring tables (Fig. 2-3).

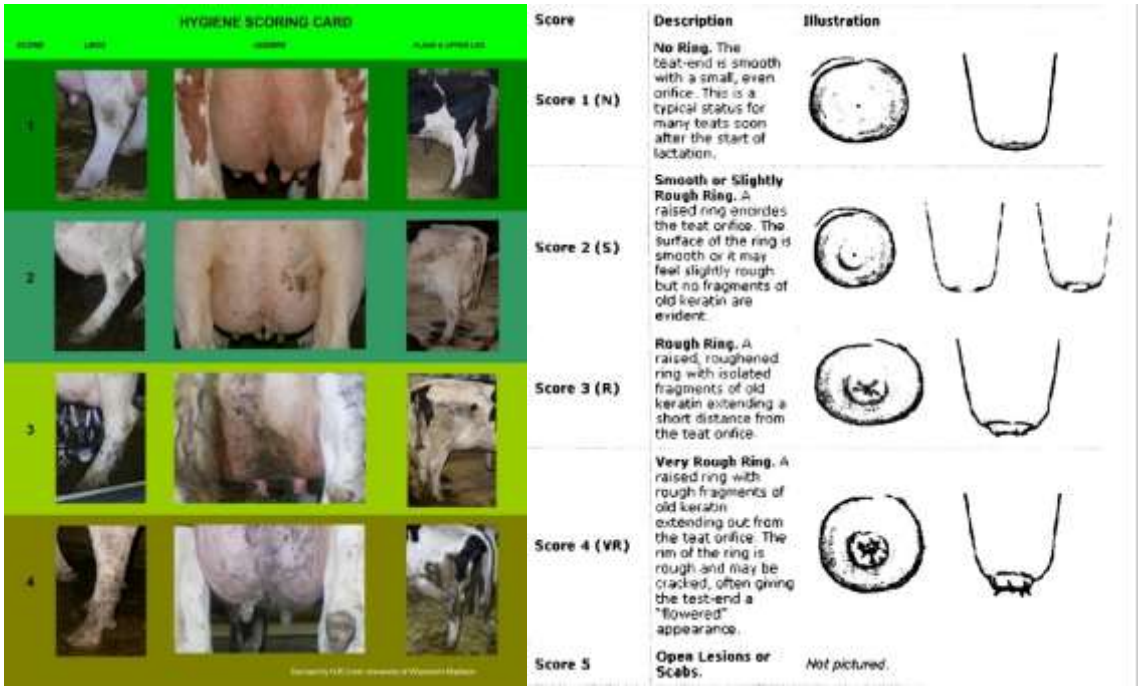

Fig. 2-3: *Hygiene score chart used during experiment (on the right), Teat apex scoring chart used during experiment (on the left).*

To estimate the extent of lameness in the farm it was adopted a scoring method called locomotion score; the evaluation of locomotion score has been done with visual detection. For each cow a score between 1 (normal) and 5 (severely lame) has been attributed (Cardelli, 2017). The observations were made outside the milking parlour (figures 4 to 7). It has been considered a place where cows could walk normally and quietly without other stress factors. It is considered optimal if 10% of the herd have a score equal or above 3 (De Vecchis, 2008).

Fig. 4,5,6,7: Evaluation of Locomotion Score.

Either a hoof scoring has been conducted, thanks to pictures taken during milking. For assess a score a 5-point score has been proposed, where score 3 represents the ideal condition. The other values (1-2 and 4-5) have been considered non-optimal (fig.8). The evaluation has been conducted both lateral and front side (fig. 9, 10)

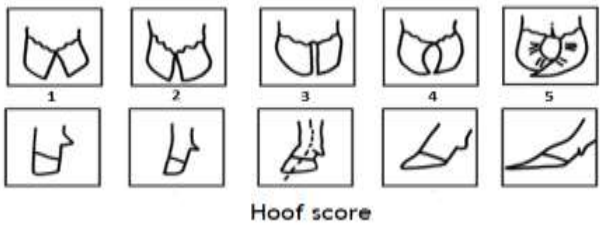

Fig. 8: Hoof Score Chart.

Fig. 9: Examples of Front Hoof Score.

Fig. 10: Examples of Lateral Hoof Score.

To define BCS a scoring chart had been used (Fig.11). In this experiment 33 dairy cows in different stage of lactation were observed. The observations were made by different operators for each cow. The method of judgment is based on Edmonson's chart.

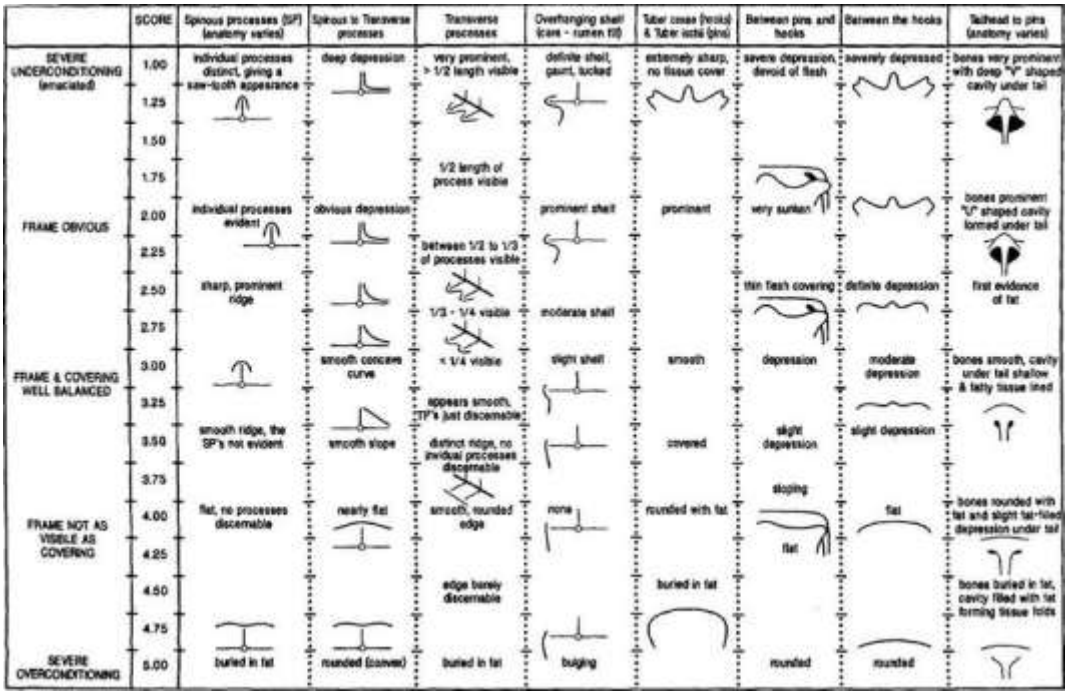

Fig. 11: Edmonson's chart used for evaluating BCS.

Temperature Humidity Index (THI) is an index that includes temperature and humidity and it is related to welfare of cows (fig. 12). Data for the calculation of THI was obtained with HOBO® devices capable of recording temperature, relative humidity and light intensity. The THI values were subsequently calculated using the formula (Bohmanova et al.,2007):

$$THI = \left\{1{,}8\,Ta - \left[\left(1 - \frac{Ur}{100}\right) \times (Ta - 14{,}3)\right]\right\} + 32$$

(where Ta= ambient temperature; Ur= relative humidity)

Temp		Relative Humidity (%)															
F	C	25	30	35	40	45	50	55	60	65	70	75	80	85	90	95	100	
77	25.0						72	72	73	73	74	74	75	75	76	76	77	MILD
78	25.6		NO STRESS			72	73	73	74	74	75	75	76	76	77	77	77	STRESS
79	26.1				72	76	73	74	74	75	76	76	77	77	78	78	79	
80	26.7		72	72	73	76	74	74	75	76	76	77	78	78	79	79	80	
81	27.2	72	72	73	73	74	75	75	76	77	77	78	78	79	80	80	81	
82	27.8	72	73	73	74	75	75	76	77	77	78	79	79	80	81	81	82	
83	28.3	73	73	74	74	75	76	77	78	78	79	80	80	81	82	82	83	SEVERE
84	28.9	73	74	75	75	76	77	78	78	79	80	80	81	82	83	83	84	STRESS
85	29.4	74	75	75	76	77	78	79	79	80	81	81	82	83	84	84	85	
86	30.0	74	75	76	77	78	78	79	80	81	81	82	83	84	84	85	86	
87	30.6	75	76	77	77	78	79	80	81	81	82	83	86	85	85	86	87	
88	31.1	75	76	77	78	79	80	81	81	82	83	84	85	86	86	87	88	
89	31.7	76	77	78	79	80	81	82	83	84	85	86	86	87	88	89	89	
90	32.2	77	78	79	79	80	81	82	83	84	85	86	86	87	88	89	90	
91	32.8	77	78	79	80	81	82	83	84	85	86	86	87	88	89	90	91	
92	33.3	78	79	80	81	82	83	84	85	85	86	87	88	89	90	91	92	
93	33.9	79	80	80	81	82	83	84	85	86	87	88	89	90	91	92	93	VERY
94	34.4	79	80	81	82	83	84	85	86	87	88	89	90	91	92	93	94	SEVERE
95	35.0	80	81	82	83	84	85	86	87	88	89	90	91	92	93	94	95	STRESS
96	35.6	80	81	82	83	85	86	87	88	89	90	91	92	93	94	95	96	
97	36.1	81	82	83	84	85	86	87	88	89	91	92	93	94	95	96	97	
98	36.7	82	83	84	85	86	87	88	89	90	91	93	94	95	96	97	98	
99	37.2	82	83	84	85	87	88	89	90	91	92	93	94	96	97	98	99	
100	37.8	83	84	85	86	87	88	90	91	92	93	94	95	97	98	99	100	
101	38.3	83	86	86	87	88	89	90	92	93	96	95	96	97	99	100	101	
102	38.9	86	85	86	87	89	90	91	92	96	95	96	97	96	99	101	102	
103	39.4	86	86	87	88	89	91	92	94	95	96	97	98	100	101	102	103	
104	40.0	85	86	88	88	90	91	93	94	95	96	97	99	100	101	103	104	
105	40.6	86	87	88	89	91	92	93	96	96	97	98	99	100	101	104	105	DEAD
106	41.1	86	88	89	90	91	93	94	95	97	98	99	101	102	103	105	106	CATTLE
107	41.7	87	88	89	91	92	94	95	96	98	99	101	102	103	105	106	107	
108	42.2	87	89	90	92	93	94	96	97	98	100	101	102	104	105	106	108	
109	42.8	88	89	91	92	94	95	96	98	99	101	102	103	105	106	107	109	
110	43.3	88	90	91	92	94	96	97	98	100	101	102	104	105	106	108	110	
111	43.9	89	91	93	94	95	96	98	99	101	102	103	105	106	107	109	111	

Fig.12: Temperature Humidity Index chart

In the farm, three HOBO® environmental devices were placed in the waiting area before parlor, in the manger and in the barn. The data from HOBO® were useful to find correlation between animal behavior and environment.

MooMonitor+® were installed on cows to monitor cow neck movements 24h×7d for heat related activity, rumination, resting, feeding, head position and restlessness. This system improves reproductive performance and minimize losses due to missed heats (www.dairymaster.com).
The device is based on an accelerometer capable of recording the movement along the three axes (x, y and z). The Moomonitor+® is therefore able to record and distinguish the acts of feeding, rumination and rest and, through an antenna, every 15 minutes the data are sent via wireless network to the Cloud system.
Animal behavior was observed thanks to HOBO pendant (pedometer): with these activometers it was possible to detect heat and control cow activity, the first parameter to check for the health of the animal. The instrument detects the movements and records the frequency with which the cow rises and lies down, it also integrates the recording function, 24 hours a day, of the cow's resting habits and times.

As a measurement tool for betahydroxybutyrate it has been used Herd navigator®. Herd navigator® is a milk monitoring and analysis tool with an adaptive sampling plan for each cow. Herd navigator® detects heat by measuring progesterone, identifies cases of mastitis in the initial phase by measuring lactate dehydrogenase, finds cases of ketosis by measuring betahydroxybutyrate, measures urea underlining cases of unbalanced protein feeding.
Herd navigator® samples 80 ml of milk per single cow and sends it to the analysis device. The software, consulting data of animals, decides for each one when to sample and what analyses to perform. It also alerts the farmer about the condition of the cows.

Results and Discussion

Results showed that animal's teat apex score and hygiene score are low. This is positive because it means that the animal and his udder are optimally managed to reduce infections (Fig. 13).

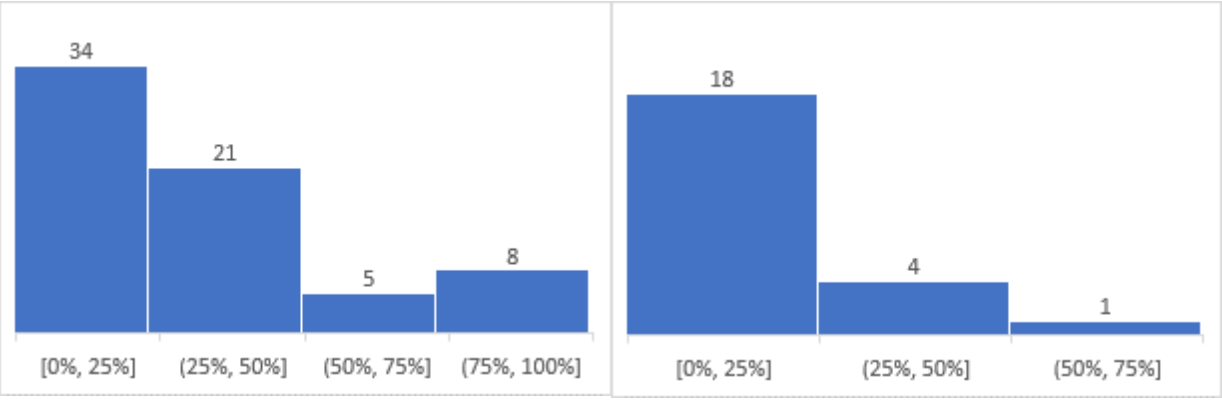

Figure 12: Number of animals with % teats evaluated > 3 Teat Apex Score (left: whole herd; right: 22 early lactation cows)

From the other analysis it is possible to highlight the relationship between DeLavalCellCount somatic cells and Somatic Cells Count from monthly controls (Figure 13). Both for organisational reasons and for mastitis that appears to be more at risk, in this analysis only early lactation dairy cow group is involved. The Figure 13 shows that the relationship between DeLaval Cell Count and monthly SCC is excellent.

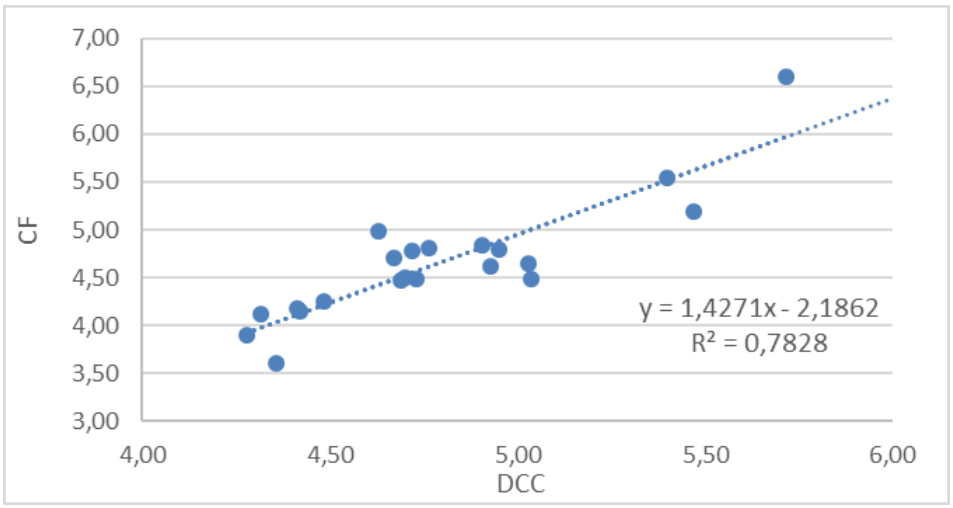

Fig. 13: Relationship between somatic cells measured with DeLaval Cell Count and Monthly measured SCC

In Figures 14, 15 and 176 the relationships between somatic cells, differential cells, milk production, number of lactations and lactation days in the herd and in early lactation dairy cows are shown.
SCC appears to slightly increase with the days of lactation in the whole herd, but the relationship is not strong enough. In the early lactation cows the trend appear to be opposite, but again the R2 is too low.
Milk production seems to be negatively related with increasing in SCC, both in early lactation cows than in whole herd.
Differential Cells does not appear to be related with days of lactation.

a

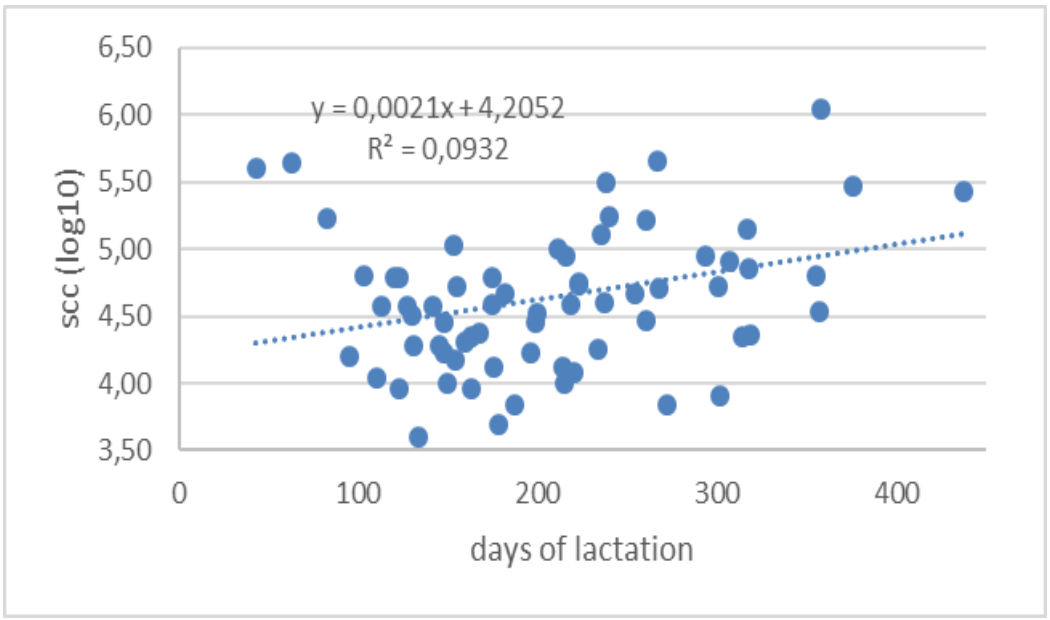

b

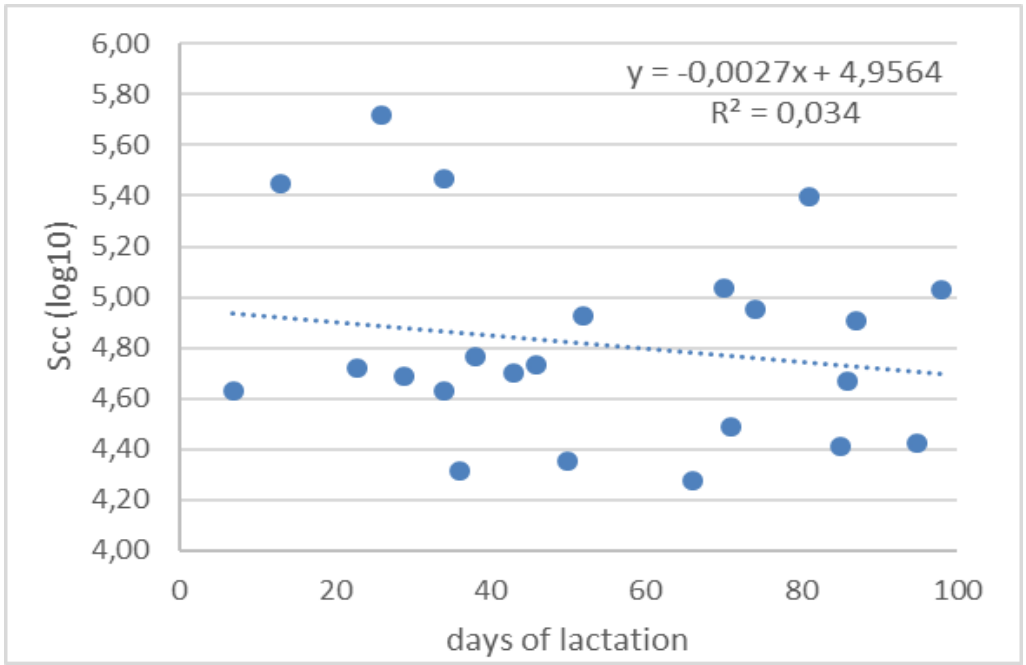

Fig. 14: Relationship between lactation days and somatic cell values (a: whole herd; b: early lactation cows).

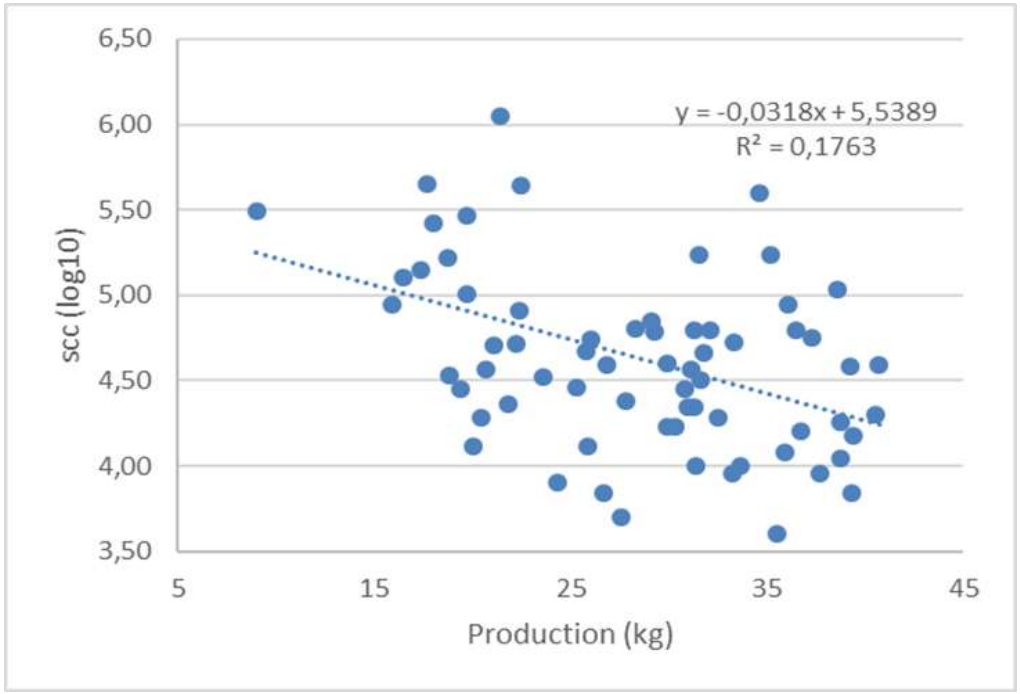

a

b

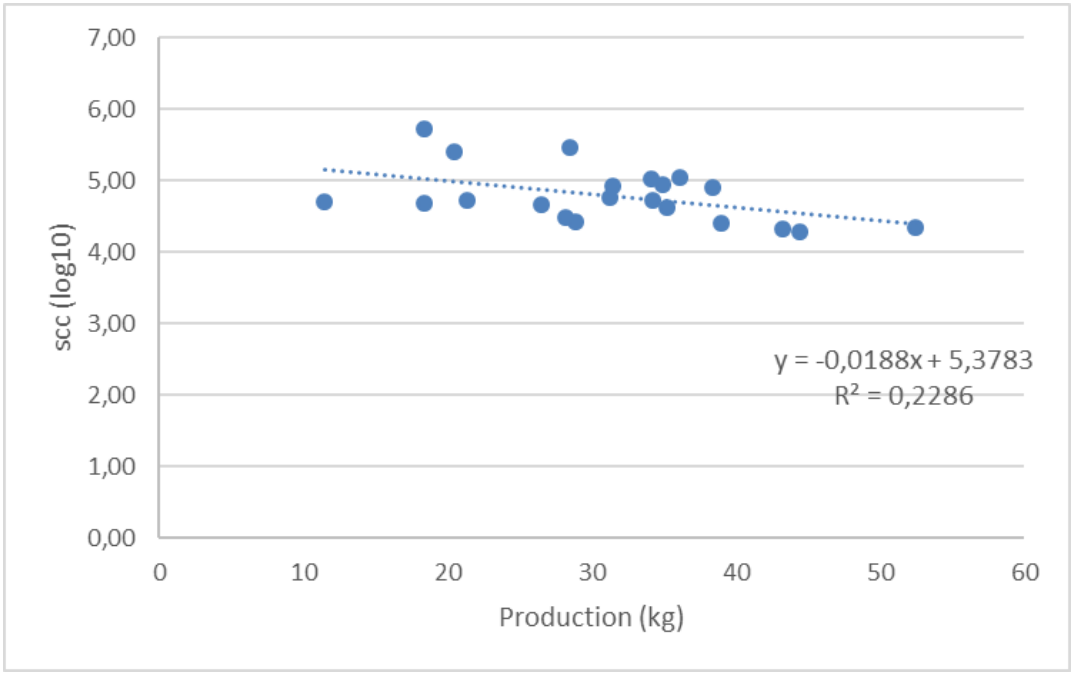

Fig. 15: Relationship between milk production and somatic cell value (a: whole herd; b: early lactation cows).

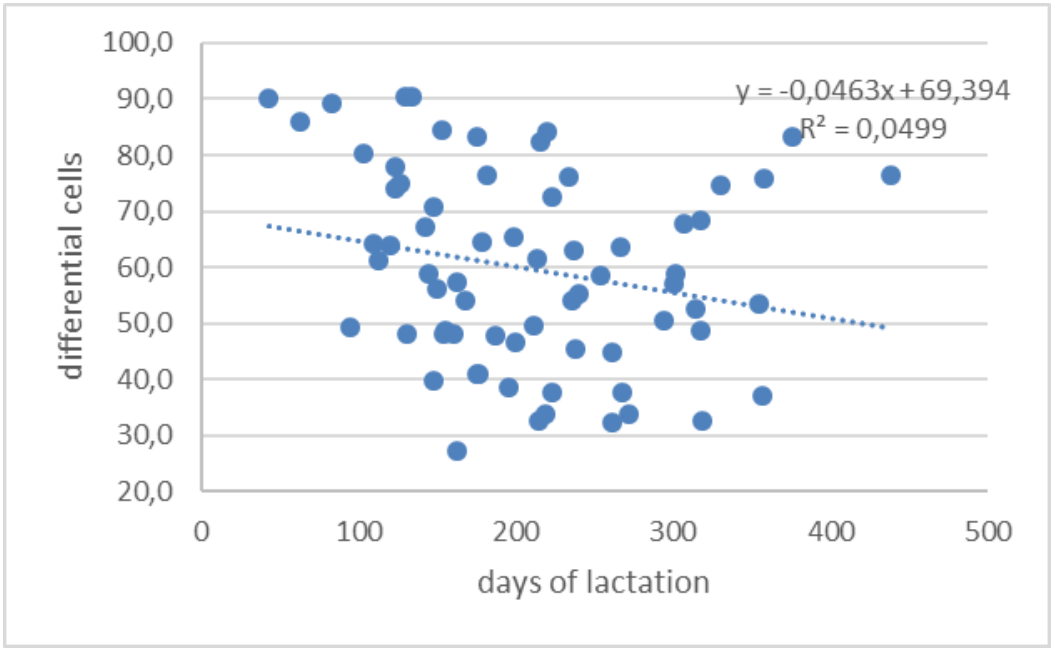

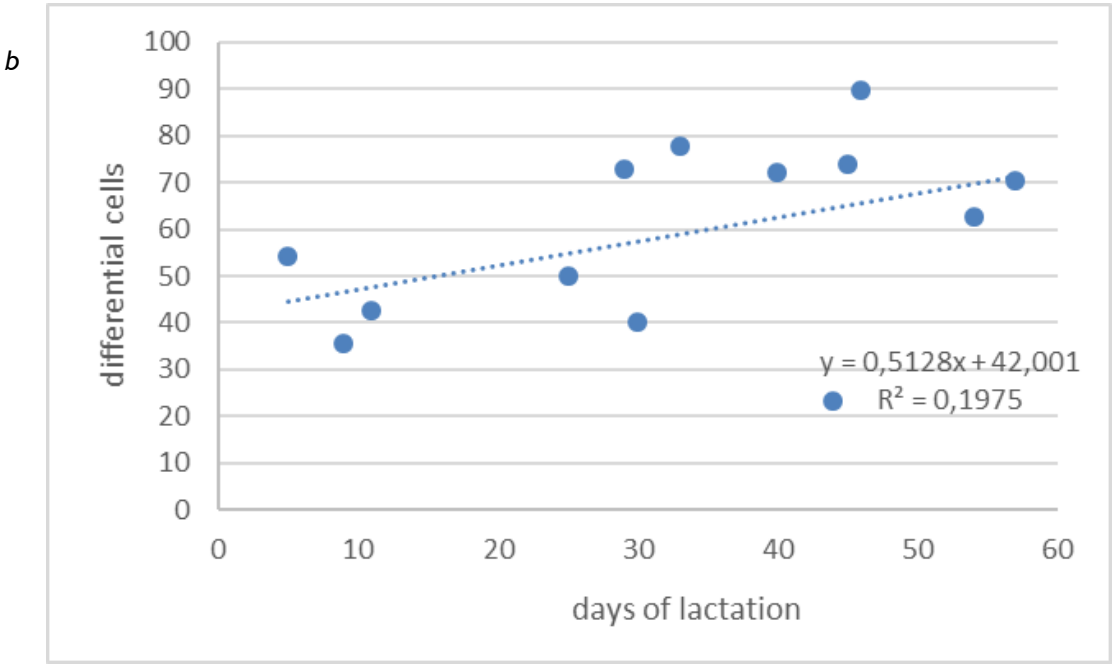

Fig. 16: Relationship between lactation days and differential cells (a: whole herd; b: early lactation cows).

Locomotion score (LS) visual tests are also conduced. Fig. 17 shows the variability of judgment of different operators. The total deviation was of 11% but each operator has its own deviation.

The variability in judgment is probably due to the lack of training of the observer.

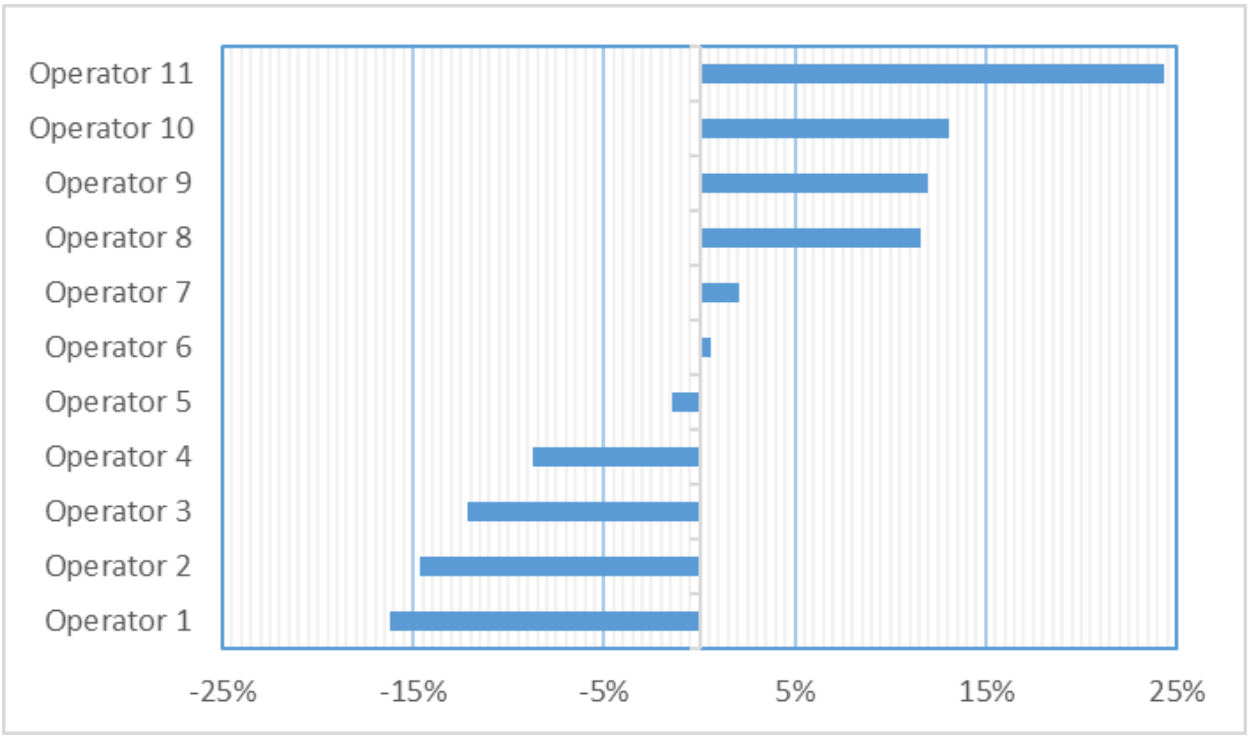

Fig.17: Variability of judgment of Locomotion Score by operators.

Figures 18, 19, 20, 21 compare the average values of Locomotion Score with milk production. Cows have been divided in lactation stage. In early lactation dairy cows, the level of production decreases with higher average values in locomotion score. The same is not for advanced lactation dairy cows. This could probably be explained by the fact that early lactation cows are more vulnerable. The samples were different: 9 cows in lactation < 50 d, 11 in 51-100 d, 21 in 101 -200 d and 43 in > 200 d.

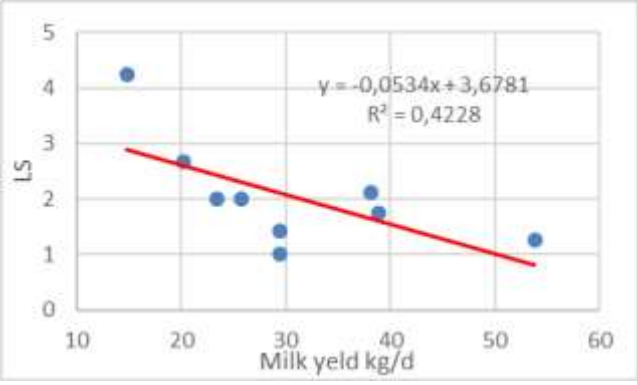

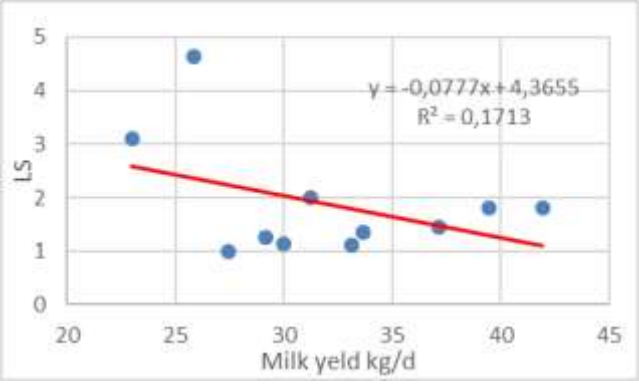

Fig. 18: Milk Yield and Locomotion Score <50 DIM. *Fig.19: Milk Yield and Locomotion Score 50 - 100 DIM.*

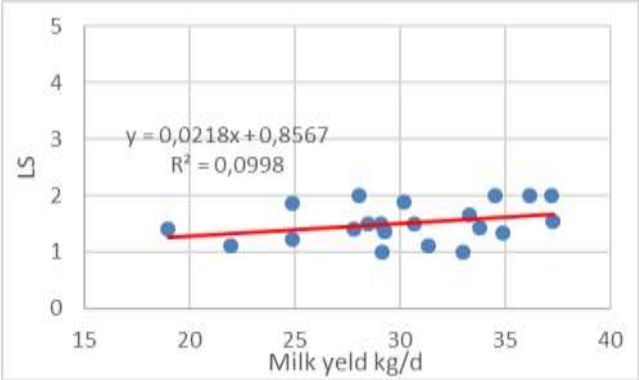

Fig. 20: Milk Yield and Locomotion Score 100 - 200DIM.

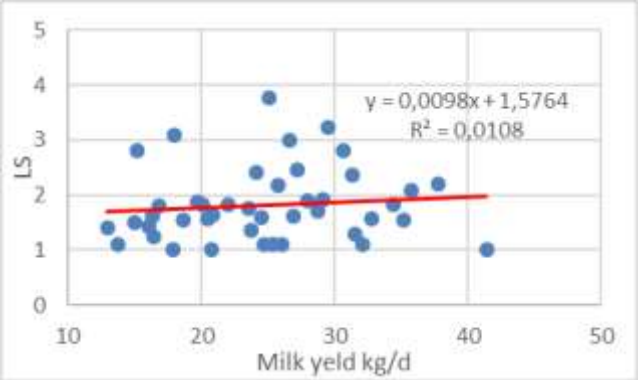

Fig. 21: Milk Yield and Locomotion Score >200 DIM

Figure 22 shows relationship between LS and BCS. High LS appears to be positively related with BCS, but relationship is very low: anyway, lameness could result worse due to greater body weight.

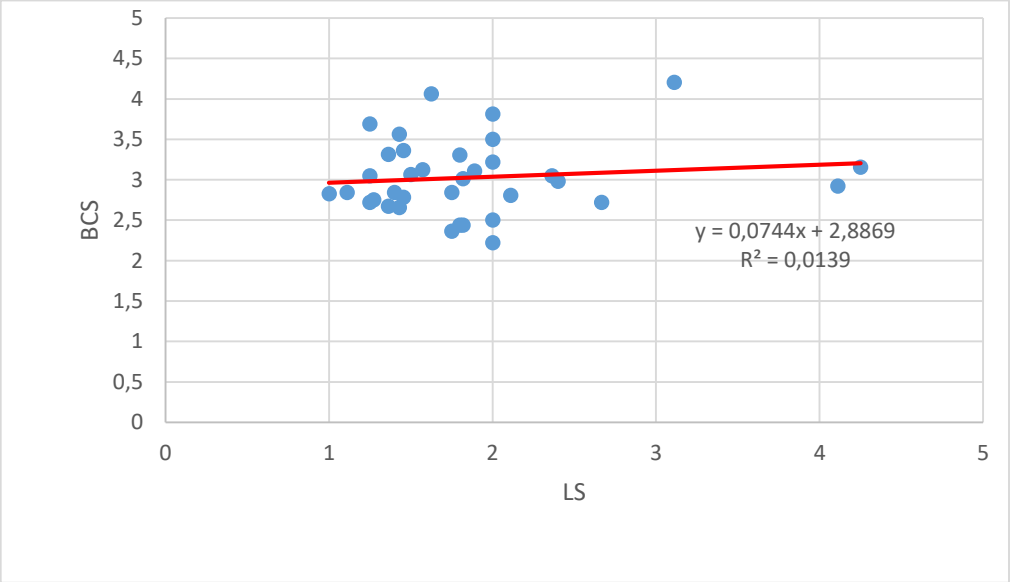

Fig. 22: Locomotion Score and Body Condition Score.

THI was calculated, also. THI obtained from the measurements of the sensors inside the barn was compared with THI obtained from the data of the Weather station of Landriano. It can be noted (fig. 23) that in the waiting area before milking there is the least variation of the THI, however in all the three areas of the stable monitored the THI variation during the day is lower than that recorded by the weather station, and this positively affects the animal welfare.

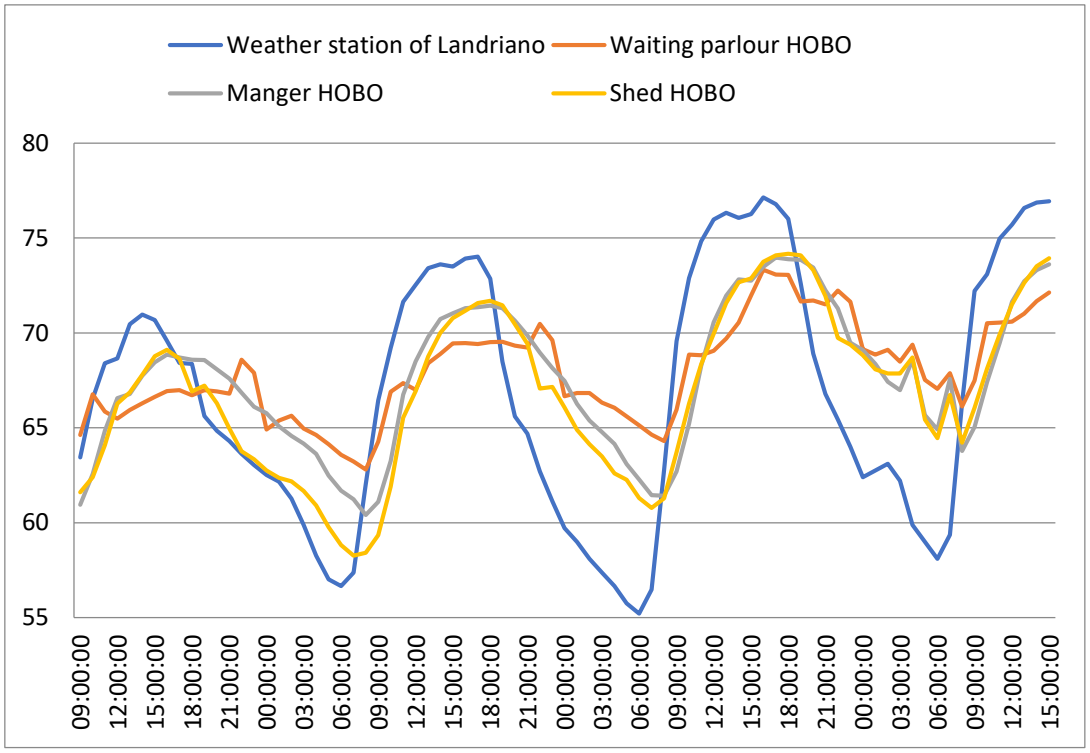

Fig. 23: Comparison Temperature Humidity Index calculated from Hobo and Weather station of Landriano data

Through Hobo Pendant and Moomonitor® devices it is possible to estimate the activity and the rumination of dairy cows. According to some studies (Petrera, 2019), in correspondence of the heat, the cows show an increase in locomotion activity with a drop of rumination (Figure 24).

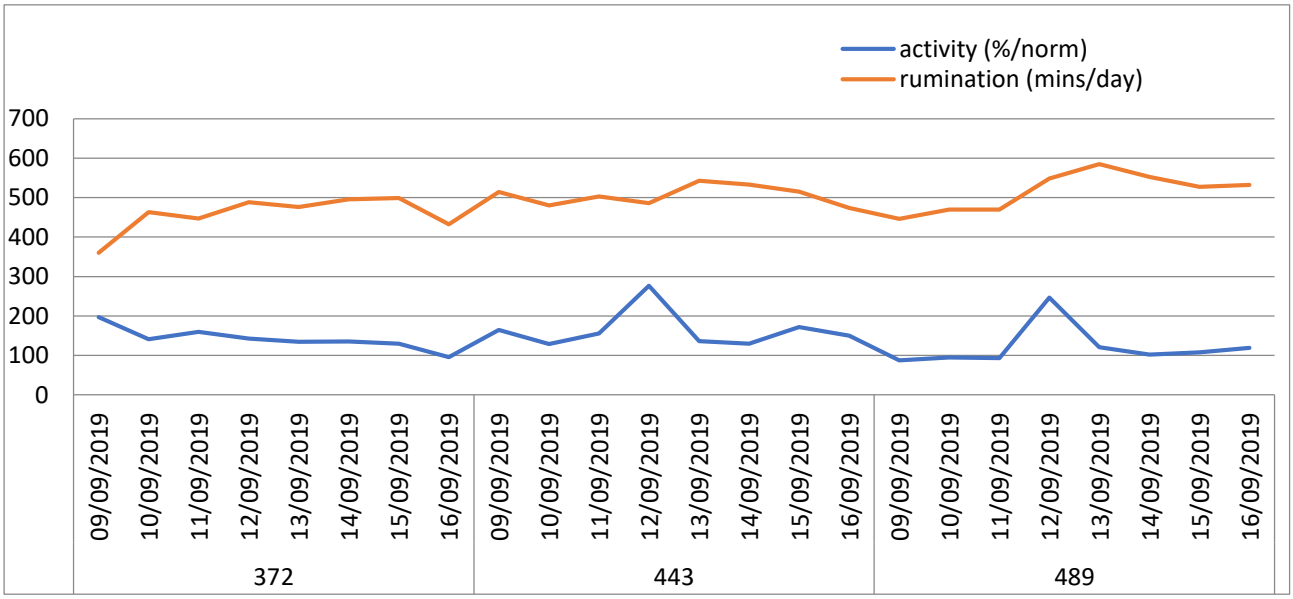

Fig. 24: Trends of weekly activity and rumination of 3 cows

Figure 25 shows herd's behavior during the day. The average of lying is 51% of total daytime. This data agrees with a study, which verified that a healthy cow lies between 12 and 14 hours sleeping, ruminating and resting. Lying hours are fundamental on milk production.

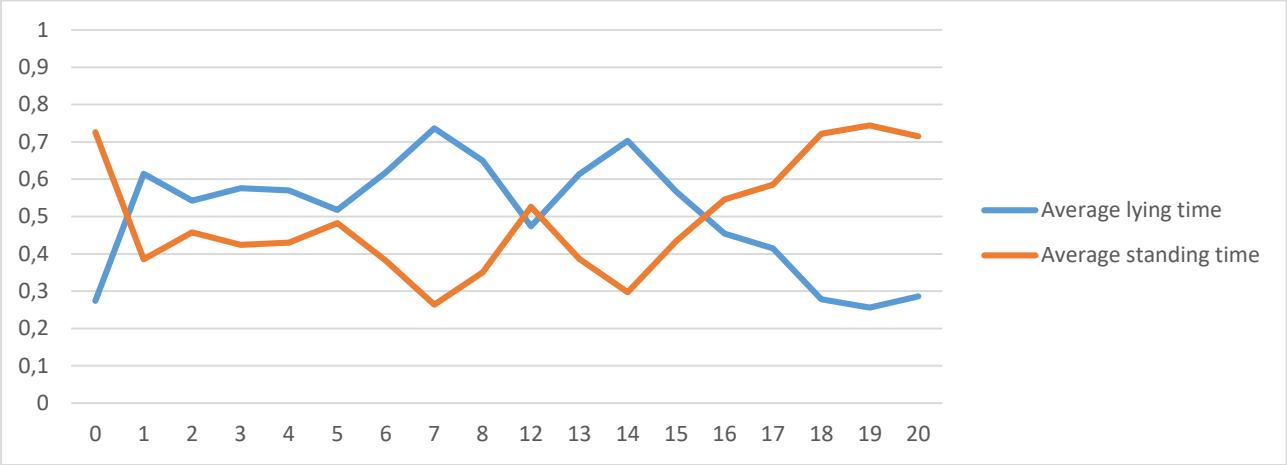

Fig. 25: Lying and standing behaviors by Hobo pendant.

In Tab. 1 BCS and BHB at different stages lactation (DIM) are shown. It is interesting to notice that the highest BCS values are in dairy cows <20 DIM. On the contrary the highest concentration of BHB are in samples milk of 101-200 DIM.

Table 1: Days in milk, Body Condition Score, Betahydroxybutyrate in milk

Days of lactation	BCS Average	± DS BCS	BHBA Average	± DS BHBA
< 20d	*3.36*	0.20	0.06	0.02
21 – 50d	2.95	0.40	0.05	0.01
51 – 75d	3.23	0.71	0.07	0.02
76 – 100d	2.57	0.29	0.05	0.01
101 – 200d	3.04	0.49	*0.09*	0.03
> 200d	3.13	0.44	0.06	0.02

In figures 26 and 27 the relationships between BCS, BHB and milk production in dairy cows <50 DIM are shown. Figure 26 shows that high production level corresponds to lower BCS level in early

lactation stage. Figure 27 shows that high level of BHBA may decrease production level in dairy cows <50 DIM.

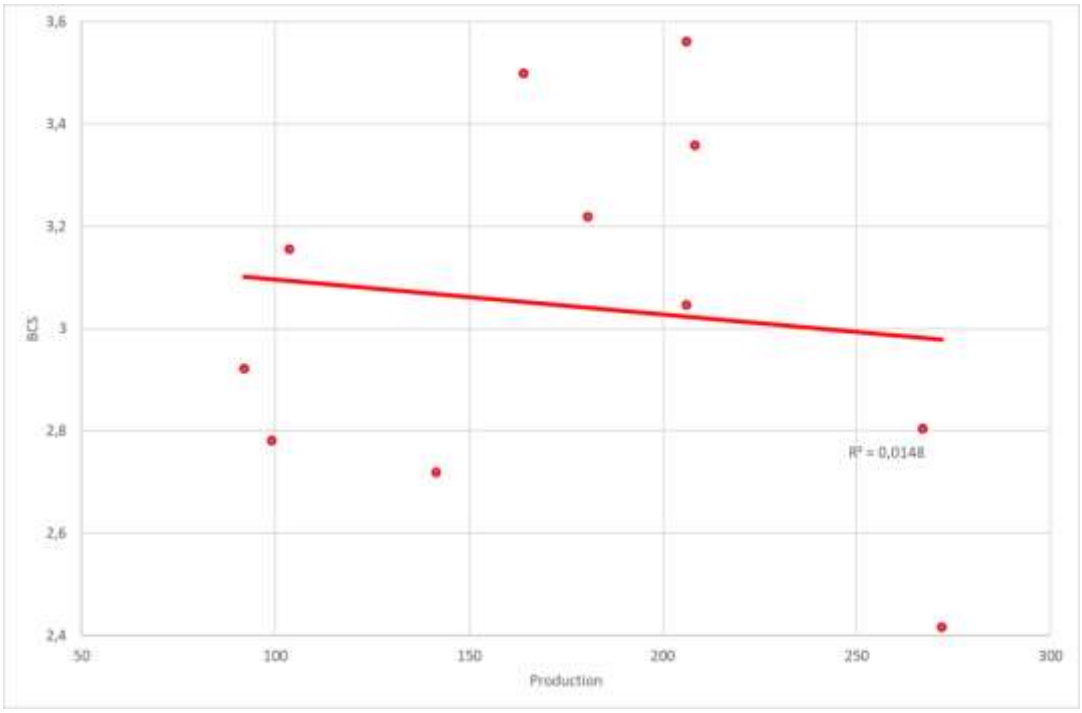

Fig. 26: BCS and production (kg) in dairy cows <50 DIM.

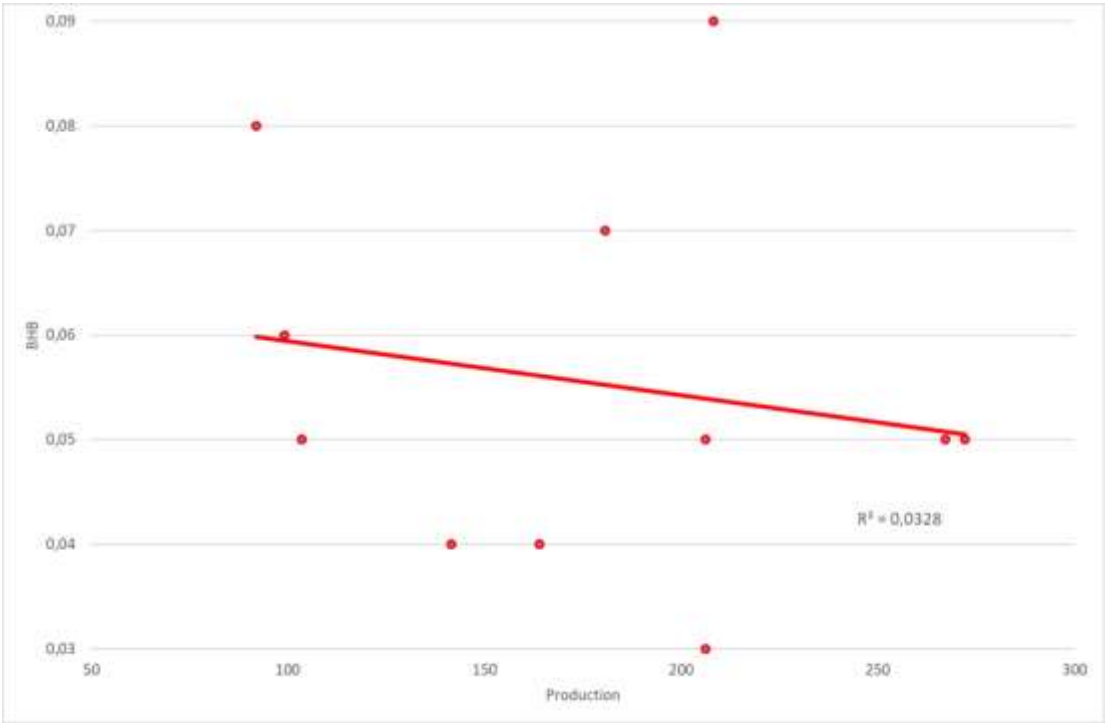

Fig. 27: BHB and production (kg) in dairy cows <50DIM.

The relationship between BCS and BHB (Fig. 28) seems very interesting. It seems that high level of BCS are correlated with high level of BHB. This can lower the production in early lactation dairy cows <50 DIM.

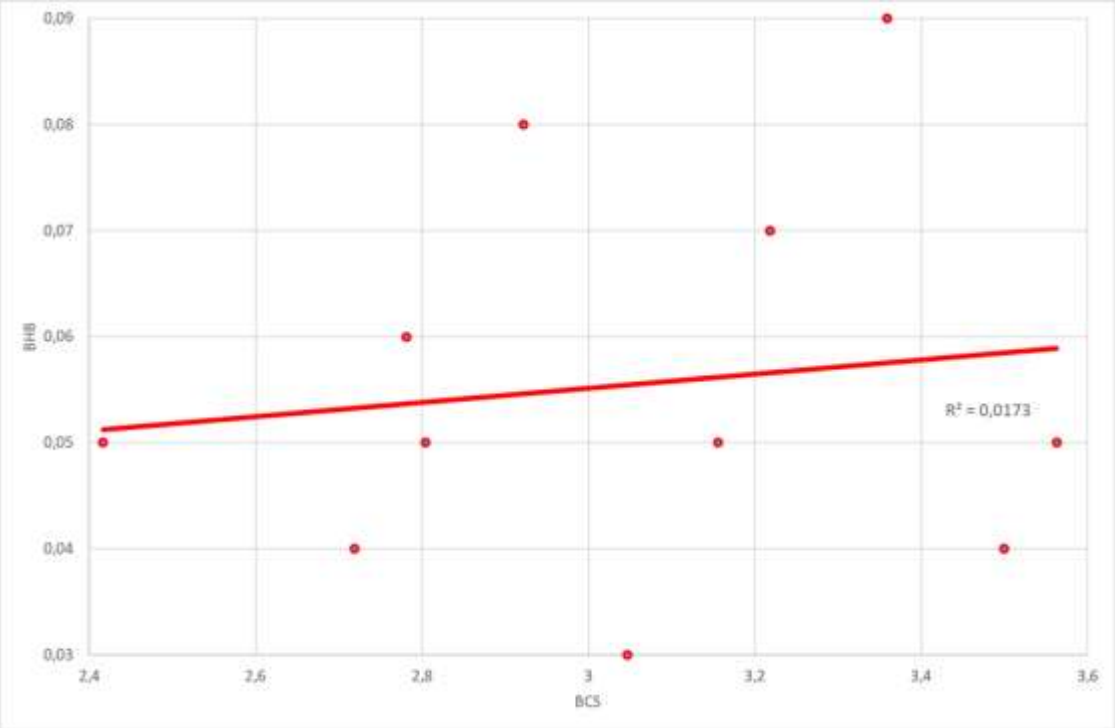

Fig. 28: BHB and BCS in dairy cows <50 DIM.

Conclusions

Most animals have a low Teat score and Hygiene score, which indicates a good management of the stable: positive for mastitis prevention. An excellent correlation between the cells calculated with DeLaval Cell Count and those detected by the monthly controls is highlighted. It should be noted that with increasing lactation days, somatic cells increase; this can be due to the milking that stresses the teat, favouring the entry of bacteria from the nipple orifice and triggering the animal's reaction. This phenomenon is confirmed by the fact that fresh cows has often lower somatic cell count. The variability in the evaluation of locomotion can be noted, due to lack in training of the operator. 28% of cows have a locomotion score equal to or greater than 3, it is not optimal because is greater than 10%. In the first 100 days of lactation appears to be a reduction in milk production associated with high locomotion score., but the relationship does not seem to be strong enough. So also the relations between Locomotion Score and betahydroxybutyrate in milk, Somatic Cell Count and Body Condition Score are very weak. There is a great variability in the evaluation of the body condition, due to the subjectivity of the method and the lack of training of the operators. High level of Body Condition Score can be seen in cows with Days In Milk <50. The betahydroxybutyrate value is higher in cows with Days In Milk > 100. It can be seen that a high level of betahydroxybutyrate and a high level of Body Condition Score cause production losses in dairy cows with Days In Milk <20. This is supported by a higher incidence of subclinical ketosis. Looking at the recorded data: the Temperature Humidity Index is below the critical value of 72, therefore the cows should not suffer from heat stress, which could influence production, animal behaviour and welfare. As for the activity and the rumination measured with the Moomonitor, does not appear to be any sort of relationship, the correlation is very low (R2 = 0.000935). All the data collected are essential to follow the right nutritional, pharmacological and managerial measures in order to have a healthy and productive herd. Knowing all of them is essential in good management practice. The variety of instrument and measures represent a huge problem for manager, that need integrated data to correctly manage the farm. More researches are needed

to identify and integrate all the different measures in a few integrated and explicative parameters.

References

Bohmanova J., Misztal I., Cole J.B; Temperature-Humidity Indices as Indicators of Milk Production Losses due to Heat Stress; Journal of Dairy Science 90: 1947–1956; 2007

Blokhuis H.J., Ridurre la percentuale di zoppie nelle vacche da latte; Welfare quality project®.

Bouraoui R., Lahmar M., Majdoub A., Djemali M., Belyea R.; The relationship of temperature-humidity index with milk production of dairy cows in a Mediterranean climate; Anim. Res. 51: 479-491;2002

Calderon and Cook N. B., The effect of lameness on the resting behaviour and metabolic status of dairy cattle during the transition period in a freestall-housed dairy herd, J Dairy Sci. 94: 2883-94; 2011

Cardelli M., Zoppie in continuo aumento, cosa fare in stalla, supplemento informatore agrario, supplemento a l'Informatore Agrario 4: 16; 2017

Casellato A., Braga P., Pecile A., Greppi G.F., Ripercussioni delle zoppie sulle performances riproduttive nella bovina da latte, Large Animal Review 13: 153-158; 2007

Dairy master; https://www.dairymaster.com/

DAIRY ZOOM (2016), Il progesterone nella vacca da latte, https://www.ruminantia.it

Duffield T.F., Lissemore K.D., McBride B.W., Leslie K.E.; Impact of hyperketonemia in early lactation dairy cows on health and production, Journal of Dairy Science 92:571-580; 2009

Petrera F. ; Attività e ruminazione, monitoriamole così; Allevatori top-Agronotizie; 2019

Acknowledgments

The authors would like to thank for the support: A. Sandrucci, A. Tamburini, L. Bava, M. Zucali, G. Provolo, A. Calcante, R. Oberti, G. Gislon, S. Celozzi, D. Lovarelli, P. Roveda, D. Reginelli, M. Colnago